NTNU

Norwegian University of Science and Technology

Master's degree thesis

IP501909 MSc thesis, discipline oriented master

SPH simulation of cylinder and wedge water entries

1120 / Zhaonan Zhong

Number of pages including this page: 98

Aalesund, 3rd June 2016

Mandatory statement

Each student is responsible for complying with rules and regulations that relate to examinations and to academic work in general. The purpose of the mandatory statement is to make students aware of their responsibility and the consequences of cheating. **Failure to complete the statement does not excuse students from their responsibility.**

*Please complete the mandatory statement by placing a mark **in each box** for statements 1-6 below.*		
1.	**I/we herby declare that my/our paper/assignment is my/our own work, and that I/we have not used other sources or received other help than is mentioned in the paper/assignment.**	☒
2.	**I/we herby declare that this paper** 1. Has not been used in any other exam at another department/university/university college 2. Is not referring to the work of others without acknowledgement 3. Is not referring to my/our previous work without acknowledgement 4. Has acknowledged all sources of literature in the text and in the list of references 5. Is not a copy, duplicate or transcript of other work	Mark each box: 1. ☒ 2. ☒ 3. ☒ 4. ☒ 5. ☒
3.	**I am/we are aware that any breach of the above will be considered as cheating, and may result in annulment of the examination and exclusion from all universities and university colleges in Norway for up to one year, according to the Act relating to Norwegian Universities and University Colleges, section 4-7 and 4-8 and Examination regulations .**	☒
4.	**I am/we are aware that all papers/assignments may be checked for plagiarism by a software assisted plagiarism check**	☒
5.	**I am/we are aware that NTNU will handle all cases of suspected cheating according to prevailing guidelines.**	☒
6.	**I/we are aware of the NTNU's rules and regulation for using sources.**	☒

Publication agreement

ECTS credits: 30

Supervisor: Karl Henning Halse

Agreement on electronic publication of master thesis

Author(s) have copyright to the thesis, including the exclusive right to publish the document (The Copyright Act §2).
All theses fulfilling the requirements will be registered and published in Brage, with the approval of the author(s).
Theses with a confidentiality agreement will not be published.

I/we hereby give NTNU the right to, free of charge, make the thesis available for electronic publication: ☒**yes** ☐**no**

Is there an agreement of confidentiality? ☐**yes** ☒**no**
(A supplementary confidentiality agreement must be filled in and included in this document)
- If yes: **Can the thesis be online published when the period of confidentiality is expired?** ☐**yes** ☐**no**

This master's thesis has been completed and approved as part of a master's degree programme at NTNU Ålesund. The thesis is the student's own independent work according to section 6 of Regulations concerning requirements for master's degrees of December 1st, 2005.

Date: 3rd June 2016

NTNU

MASTER THESIS 2016
FOR
STUD.TECHN. Zhaonan Zhong

SPH simulation of cylinder and wedge water entries

The water impact problem, i.e. moving a rigid object enters into or exits from the calm water with a velocity value, has been paid great of attentions on the field of fluid mechanics research. Various aspects have been studied in the water impact process, e.g. slamming force and slamming coefficient, the deformation of free surface, the water splash, the elevation of jets, cavitation phenomenon, etc. These researches offered great efforts to the marine industry, including sub-sea operation, offshore structures behaviors in waves, ship design, marine operations, etc.

In the thesis, it attempts to apply the smoothed particle hydrodynamics (SPH) method to simulate and calculate the fluid flow effects, and then the parameters setting in numerical program DualSPHysics will be discussed, the computation results of study will be compared with previous theoretical analyses and experiments.

The objective of this thesis is to test the characteristics of SPH simulation with DualSPHysics through computing the forces and relevant coefficients related to the water impact on cylinders and wedges in slamming process.

- Pre-study:
  - Slamming theory – vertical forces, slamming coefficients.
  - Previous theoretical analyses and experiments.
  - SPH theory – benefits and drawbacks.

- Simulation in the numerical method:
  - DualSPHysics program simulation test
  - Definition of water entry cases
  - Various cylinders and wedges models with different variables
  - Parameters of SPH method

- Comparison with previous results and discussion.

The work scope may prove to be larger than initially anticipated. Subject to approval from the supervisor, topics may be deleted from the list above or reduce in extent.

The thesis shall be written as a research report with summary, conclusion, literature references, table of contents, etc. During preparation of the text, the candidate should make efforts to create a well-arranged and well-written report. To ease the evaluation of the thesis, it is important to cross-reference text, tables and figures. For evaluation of the work a thorough discussion of results is needed. Discussion of research method, validation and generalization of results is also appreciated. Further references to thesis requirements are found in the course description website (www.ntnu.no) and Fronter, with special attention to the section "evaluation".

In addition to the thesis, a research paper for publication shall be prepared.

Three weeks after start of the thesis work, a pre-study has to be delivered. The pre-study has to include:

- Research method to be used
- Literature and sources to be studied
- A list of work tasks to be performed
- An A3 sheet illustrating the work to be handed in.

A template and instructions for thesis documents and A3-poster are available on the Fronter website under MSc-thesis. Please follow the instructions closely, and ask your supervisor or program coordinator if needed.

The thesis shall be submitted in electronic version according to standard procedures. Instructions are found on the college website and on Fronter. In addition one paper copy of the full thesis with a CD including all relevant documents and files shall be submitted to your supervisor.

Supervision at NTNU.: Karl Henning Halse

Finish: 3rd June 2016 Signature candidate: Zhaonan Zhong.

Abstract

Smoothed particle hydrodynamics (SPH) is a numerical approach applied meshless Lagrangian method in the fluid study, which is different from the common computational fluid dynamics (CFD) on the basis of the Eulerian description. Compared with the traditional experiment studies, the numerical approaches provide much simpler way in simulating fluid behaviors, and the results are also considered to be reliable and accurate. Therefore, the numerical approaches are playing a more and more important role with the support of the fast developing computer technology nowadays.

In this thesis, the water impact simulations are made in the DualSPHysics, which is a numerical program based on the SPH method. Four cases are simulated: water entries of both two- and three-dimensional horizontal cylinders with the constant velocities, free falling of two-dimensional cylinders, and water entries of two-dimensional wedges with various deadrise angles. The results of simulations in DualSPHysics are evaluated through the comparison with previous theoretical analyses, experiments and other similar numerical simulations, also the influences of the parameter settings in the program are discussed. The emphasis is on the vertical hydrodynamic forces and slamming coefficients at the slamming moments.

Most of the results are encouraging, with good agreement with the previous works, but the computing accuracy is limited by the capability of the computer. It is believed that more appropriate parameters can be applied in powerful computers, and better results can be expected as well.

Acknowledgements

I would first like to express my appreciation to my supervisor Prof. Karl Henning Halse and co-supervisor Jiafeng Xu for the professional guidance and valuable suggestions during the process of my master thesis. I am also grateful to my friend Yue Li for providing related data that are greatly helpful.

Special thanks to my friend Xu Zhuge for letting me use his desktop computer to do all the computations and simulations.

In addition, I am grateful to my wife Lili Zhu for constant support and trust.

At last I would like to thank all the people who have offered help during my postgraduate study.

Contents

ABSTRACT I
ACKNOWLEDGEMENTS II
LIST OF FIGURES V
LIST OF TABLES VII
LIST OF SYMBOLS VIII

1 INTRODUCTION 1

2 LITERATURE REVIEW 5

2.1 WATER IMPACT OF CYLINDERS 5
2.1.1 Theoretical analysis 5
2.1.2 Experiments 8
2.1.3 Numerical simulations 10
2.2 WATER ENTRY OF WEDGES 13
2.2.1 Theoretical analysis 14
2.2.2 Experiments 15
2.2.3 Numerical simulation 16

3 THEORY 18

3.1 SMOOTHED PARTICLE HYDRODYNAMICS 18
3.1.1 Kernel function 18
3.1.2 Fluid equations 21
3.1.3 Particles searching 23
3.2 DUALSPHYSICS 23
3.2.1 Workflow of DualSPHysics 24
3.2.2 Algorithm of DualSPHysics 25
3.2.3 Time integration 27
3.2.4 Computation loop of SPH code 28

4 SENSITIVITY ANALYSIS 30

4.1 DOMAIN SIZE TEST 30
4.2 TIME STEP TEST 36
4.3 PARTICLE DISTANCE TEST 38

4.4 INFLUENCE OF SMOOTHING LENGTH....40
4.5 INFLUENCE OF SOUND SPEED....41
5 RESULTS....43
5.1 WATER IMPACT OF 2D HORIZONTAL CYLINDER....43
5.1.1 Parameters setting....43
5.1.2 Results and discussion....44
5.1.3 Curve fitting method....49
5.1.4 Influence of slamming velocity....50
5.1.5 Summary....51
5.2 FREE FALLING OF 2D CYLINDER INTO CALM WATER....52
5.2.1 Parameters setting....52
5.2.2 Results and discussion....52
5.2.3 Influence of particle distance....56
5.2.4 Summary....56
5.3 VERTICAL WATER ENTRY OF 2D WEDGE....58
5.3.1 Parameters setting....58
5.3.2 Domain size test....58
5.3.3 Results and discussion....61
5.3.4 Summary....64
5.4 WATER IMPACT OF 3D HORIZONTAL CYLINDER....65
5.4.1 Parameters setting....65
5.4.2 Particle distance test....65
5.4.3 Comparison of 2D and 3D simulating results....67
5.4.4 Summary....70
6 CONCLUSION AND FUTURE WORK....71
REFERENCE....73
APPENDIX (DRAFT)....- 1 -

List of figures

Figure 2-1 Theoretical water-induced loads on a cylinder penetrating the free surface by Faltinsen et al. (1977) 7

Figure 2-2 Water-induced load on model III by Faltinsen et al. (1977) 8

Figure 2-3 the shape of domain by Ghadimi et al. (2012) 11

Figure 2-4 Comparison between the results of numerical simulation with ISPH method and experiment by Bašić et al. (2014) 13

Figure 2-5 definition of Wagner's slamming model by Faltinsen (2005) 14

Figure 2-6 slamming coefficient of varied theories by Faltinsen (2005) 15

Figure 2-7 initial particles setting by Oger et al. (2005) 17

Figure 3-1 particles and smoothing length 19

Figure 3-2 smoothing kernel function example (online data) 20

Figure 3-3 workflow of DualSPHysics (DualSPHysics, 2013) 24

Figure 3-4 computation loop of SPH code 29

Figure 4-1 peak values of vertical forces for three domains 31

Figure 4-2 fluctuation of three domain sizes 32

Figure 4-3 area of involved particles of three domains 33

Figure 4-4 reflection waves at time t=0.0296 s 34

Figure 4-5 reflection waves at time t=0.0348 s 34

Figure 4-6 (a) overview and (b) details of smoothed curves of slamming coefficient for the three domain sizes 35

Figure 4-7 vertical forces curves of four time spans 37

Figure 4-8 details of vertical forces 37

Figure 4-9 original slamming coefficient curves of three particle distances 39

Figure 4-10 smoothed slamming coefficient curves of three particle distances 39

Figure 4-11 curves of slamming coefficient for different smoothing length 41

Figure 4-12 curves of slamming coefficient for different Coefsound 42

Figure 5-1 original curves of slamming coefficient for all simulations 44

Figure 5-2 peak slamming coefficient values for all simulations 45
Figure 5-3 smoothed curves of slamming coefficient for all simulations 45
Figure 5-4 comparison of slamming coefficient with previous curve 48
Figure 5-5 curve fitting methods (a) according to Campbell and Weynberg (1980); (b) according to Miao (1989).....49
Figure 5-6 slamming coefficient curves of three different velocities 51
Figure 5-7 penetration depth curves compared with previous results 53
Figure 5-8 HB cylinder free falling comparison.....54
Figure 5-9 NB cylinder free falling comparison.....55
Figure 5-10 comparison of different particle distance.....57
Figure 5-11 geometry of the wedge 58
Figure 5-12 vertical force curves of two different domains 59
Figure 5-13 particles animation at the moments when the maximum force values appear.....60
Figure 5-14 a series of reflection energy waves at t=0.06712 61
Figure 5-15 vertical force curves of simulations 63
Figure 5-16 integrated curve of vertical forces.....63
Figure 5-17 comparison of the slamming coefficients 64
Figure 5-18 initial position of the 3D animation 65
Figure 5-19 comparison of forces with different particle distances 66
Figure 5-20 comparison of slamming coefficients with different particle distances.....67
Figure 5-21 original curves of 2D and 3D simulations.....68
Figure 5-22 smoothed curves of 2D and 3D simulations 69
Figure 5-23 animations of 2D and 3D slamming moment 70

List of tables

Table 4-1 details of domain sizes and parameters 30

Table 4-2 details of time span and parameters.....36

Table 4-3 details of particle distance and parameters.....38

Table 5-1 parameters of cylinder simulations.....43

Table 5-2 slamming coefficient related to Froude number.....46

Table 5-3 parameters for different velocities test 50

Table 5-4 parameters setting of comparative simulation.....56

Table 5-5 parameters of two domain sizes 59

Table 5-6 parameters of wedges simulation 62

Table 5-7 parameters of 3D simulations.....66

List of symbols

α_D	Calculation coefficient
β	Deadrise angle of wedges
δ	Dirac delta function
ρ	Fluid density
Π	Artificial viscosity
$\mathcal{L}$	Lagrangian
A_{33}	Two-dimensional added mass
c	Sound speed
C_S	Slamming coefficient
D	Cylinder diameter
E	System energy
F_3	Vertical Hydrodynamic force
h	Submergence depth
l	Smoothing length
L	Length of the cylinder
m	Mass
p	Momentum
P	Fluid pressure
q	Relative particle distance
r	Cylinder radius
t	Time variable

u	Specific internal energy of particles
v	Velocity variable
V	Volume
W	Kernel function
z	Particle distance
Δt	Time step

1 Introduction

In the early stage, issues of fluid mechanics have been explored widely. Among the studies, the main research methods were commonly theoretical analyses and experiments. To be specific, theoretical analyses offered the prediction of the possible physical phenomenon, and experimental studies proved the theory and provided the empirical equations for practice. Owing to the limitation of experimental conditions of fluid simulation, it was difficult to obtain the appropriate results for all types of simulations.

Computational fluid dynamics (CFD) appeared with the invention of computers, and also updated rapidly with the development of computer technology after 1960s. Apart from the traditional theoretical analyses and experiments, CFD could be also viewed as an effective way to simulate the fluid behavior and to obtain the numerical results efficiently. The application of CFD may advance in some aspects compared with other methods. Unlike the theoretical research, CFD method can be used in relatively complicated problem solving, and there is no need to make great efforts to simplify the conditions, nor to define many assumptions to reduce the workload of calculation. Additionally, in the aspect of simulation, CFD method is economic without preparing instruments to design accurate experiment, and it also saves much time to repeat similar simulations.

Now CFD method has become an independent discipline in the science field, which could be seen as important as both theoretical and experimental fluid mechanics. Especially in the recent decade, with the upgrade of the computer hardware, the computing speed and storage capability have been improved by a large margin correspondingly, providing more possibilities to solve complicated problems. Besides this, the parallel computing capability of the computer significantly improves the efficiency of simulations.

From different perspectives, the concept of CFD method is varied. In a broad sense, CFD includes all the methods which utilizes the computers to make numerical simulation or calculation of fluid (or the other fields, i.e. astrophysics). However, in recent years, some other approaches as the braches of CFD have developed rapidly, and they have different advantages to solve certain problems. Therefore, in a narrow sense, CFD method represents the numerical solution approaches which utilize Eulerian method as the basic theory. On the contrary, other approaches that apply the Lagrangian method should be distinguished from CFD approaches. To eliminate the misunderstanding of the concept, in this thesis, CFD means only approaches applying Eulerian method in the following chapters.

The relatively mature method for simulation of fluid behavior in Lagrangian method is smoothed particle hydrodynamics (SPH). In CFD approaches, geometric grids are defined, and physical characteristics of the fluid within the grids are described and simulated. Differing from CFD approaches, SPH applies Lagrangian method, in which the meshless fluid particles are defined. The separated particles can be considered as small individuals that comply with Newton's second law of motion, and the entire particles as a whole are performing like a fluid flow field. Through studying the properties of the particles, the fluid behavior can be described.

When SPH method was introduced in 1970s, it was utilized to deal with astrophysical problems, and with the development of modern computer technology, it has been widely used in many fields. Owing to the meshless smoothed particles defined in SPH mothed, main emphasis is laid on the optimized algorithm, e.g. boundary description, and accuracy research. In spite of being questioned to be less accurate than CFD method on simulation of fluid flow, SPH approach is still an appropriate method for certain numerical simulation studies, especially for calculation in large scale simulation.

The water impact problem, i.e. a moving rigid object enters or exits the calm water with a certain velocity, has been paid great attentions on the field of fluid mechanics research. Various aspects have been studied in the water impact process, e.g. vertical hydrodynamic forces and slamming coefficients, the deformation of the free surface, the water splash, the elevation of jets, and cavitation phenomenon. These researches have offered great contributions to the marine industry, including sub-sea operation, the behaviors of offshore structures in waves, ship design, marine operations, etc. For instance, in the field of sub-sea operation, the research results of water impact problems provide the theoretical basis to the scenario making, which concern with the selection of crane wires, lowering speed of the crane, even the shape of the related objects. A good designed scenario based on the water impact theory can reduce the costs in sub-sea operation efficiently, and avoid the equipment being damaged by the sudden large force caused by the slamming effects.

The paper by von Karman (1929) was considered as the beginning of the research of water impact problems. After that, theoretical analyses and experiments were made by various researchers. Among these researches, the impact on calm water of rigid cylinders and wedges was widely studied, since they were close to the practical situations, i.e. ship slamming issues. In different studies, horizontal or inclined cylinders, symmetric or asymmetric wedges with a series of angles were the main research subjects. About the cases, the penetration of free surface with a forced constant velocity and the water entry of free falling objects were the main parts

of the researches. The results of researches contained the curves of slamming coefficient in the function of non-dimensional time variables, fluid pressure, and vertical force.

In terms of applying the numerical solutions, since the water impact problems are quite complicated, there are also assumptions and limiting conditions that assist the computation of the relevant variables. To improve the accuracy of the calculations, small meshed grids in CFD and tiny particle sizes in SPH are required, hence the numerical simulation needs relative long time to run the large amount of calculations. The fast development of model computer technology offers good opportunity to solve larger scale problems. Another important aspect of the numerical simulation is the selection of algorithm and relevant parameters. For the requirement of the virtual simulation, researchers have to try every possibility to make sure that the fluid behavior is close to the real world, and the results are accuracy enough.

In previous researches, numerical results were commonly compared with the theoretical and experimental results, e.g. the empirical formula presented by Campbell and Weynberg (1980) was the classic comparable object. Due to the limitation of experiment condition and effects of various factors, the results could not reach an agreement in a high level. However, with the optimization of numerical simulation, much more reliable and accurate results can be expected.

In this thesis, the SPH method is utilized to simulate the water impact problems, and DualSPHysics which is based on the SPH method is the main applied program. In chapter 2, the previous theoretical analyses and experiments are reviewed and compared, including water impact problems of cylinders and wedges. In chapter 3, the theories of both SPH method and DualSPHysics (SPHysics) are illustrated, and then some algorithms such as particle searching and time integration are introduced. After the theory part, in chapter 4 and chapter 5, the effects of parameters are analyzed, and the results of numerical simulations are presented. To be specific, in chapter 4, the sensitivities of parameter settings are analyzed through the water impact problem of two-dimensional horizontal cylinders, and the default parameters are selected according to the previous researches referred in chapter 2. Chapter 5 is divided into four parts for different cases. In section 5.1, the water entries of cylinders are simulated with a series of constant Froude numbers as the main variables, and the model is the same as that in chapter 4. Similarly, in section 5.2, the cylinder is supposed to penetrate the water surface freely, and the slamming velocity is calculated according to the initial position. Both the neutrally buoyant and half buoyant cylinders are tested in this section. After that, in section 5.3, two-dimensional wedges with various deadrise angles are simulated, and the parameter settings are the same with the default values in chapter 4. The last simulation in section 5.4 is a three-

dimensional cylinder entering into calm water with constant velocity, the result is compared with that in section 5.1, to illustrate the effects caused by the difference between simulations of two- and three-dimensional models. All the results are compared with previous researches, and the accuracy level of DualSPHysics program is discussed.

2 Literature review

The water impact study is widely considered starting from von Karman (1929) who provided a method of momentum theory. In the research of von Karman (1929), a two-dimensional wedge was assumed to enter into water with a vertical velocity, and the force between the water and the wedge was calculated through a flat-bottomed float. Wagner (1932) developed the study of von Karman, he assumed that small amount of water rose on the free surface where the wedge and water touched, hence the dimension of flat plate mentioned by von Karman (1929) should be different due to this phenomenon. The pile-up of water was considered as the actual deformation of the free surface.

After von Karman (1929) and Wagner (1932), a variety of researches and experiments were made. Since the water impact happened in a very short time for fast speed slamming, it was not easy to set up appropriate conditions to obtain relatively good experimental results, and in terms of theory research, complicated factors also influenced the results. In recent years, analyses made by computer offered numerical and visual outcomes of simulation and improved the researching efficiency.

In this chapter, typical researches and experiments are reviewed and discussed, and the previous studies could shed some light on the future research.

2.1 Water impact of cylinders

The study of water impact of cylinders can be divided into two categories, consisting of cylinder with forced constant velocity entering into calm water and free falling from certain height into the water. The former case is studied mainly by calculating the vertical forces and the slamming coefficient C_S, while the focus of the latter case is on the penetration depth with the variable of time, and also the vertical forces on the cylinder.

2.1.1 Theoretical analysis

The widely accepted theoretical analysis was presented by Faltinsen et al. (1977), and in the paper, the results of theoretical research by Faltinsen et al. (1977) and experiments by Sollied (1976) were discussed and compared. The analytical model of the case was described as a two-dimensional rigid cylinder entering into calm water with forced constant velocity. Here the water was assumed as incompressible and irrotational fluid, and effect of gravitational acceleration was remarkably small compared with large fluid acceleration caused by the

cylinder loads. Similar theoretical calculation was made by Fabula and Ruggles (1955), which was limited by the submerge depth of the cylinder entering into the water.

Faltinsen et al. (1977) mentioned that the vertical force during the water-entering process could be defined as:

$$F_3 = \frac{d}{dt}\left[A_{33}(t)v\right] \tag{2.1}$$

where $A_{33}(t)$ is the two-dimensional added mass as the function of submergence time t, v is the forced velocity of the cylinder during the process. By writing the added mass A_{33} as the function of submergence distance h (h is the distance from cylinder bottom to the initial free surface of water, shown in figure 2-1) and defining the slamming coefficient C_S, the vertical force expression could be rewritten as:

$$F_3^{(2D)} = \frac{dA_{33}^{(2D)}}{dh} \cdot v^2 = \frac{\rho}{2} C_S \cdot 2rv^2 \tag{2.2}$$

where ρ is the density of water, r is the radius of cylinder, the expression is also mentioned by Faltinsen (1990). The initial C_S value was 3.1 in the theoretical calculation, and the value reduced with the submergence of the cylinder until it rose to another peak value when the cylinder was totally submerged, the curves are shown in figure 2-1. Compared to initial C_S value $\frac{4}{3}\pi$, the result by Fabula and Ruggles (1955), Faltinsen et al. believed that the distinction was caused by the inaccuracy of Fabula and Ruggles' method. Besides, the method was only valid before $\frac{h}{r} = 1.0$, the moment when half of the cylinder was submerged in the water.

Faltinsen et al. (1977) did not explain the reason of the appearance of the peak value when $\frac{h}{r}$ was around 2.0, because in experiments there was no such a peak value existing at the moment when the cylinder was fully submerged. The peak value of slamming coefficient represented a crest value of vertical force, and the force could be due to the buoyancy changing with the increase of cylinder volume submerged in the water, which reached the maximum value when fully submerged. However, this explanation was lack of support, since the buoyancy would never change after submergence, which meant the peak value should not decline with the submerged depth, not as the figure 2-1 showed.

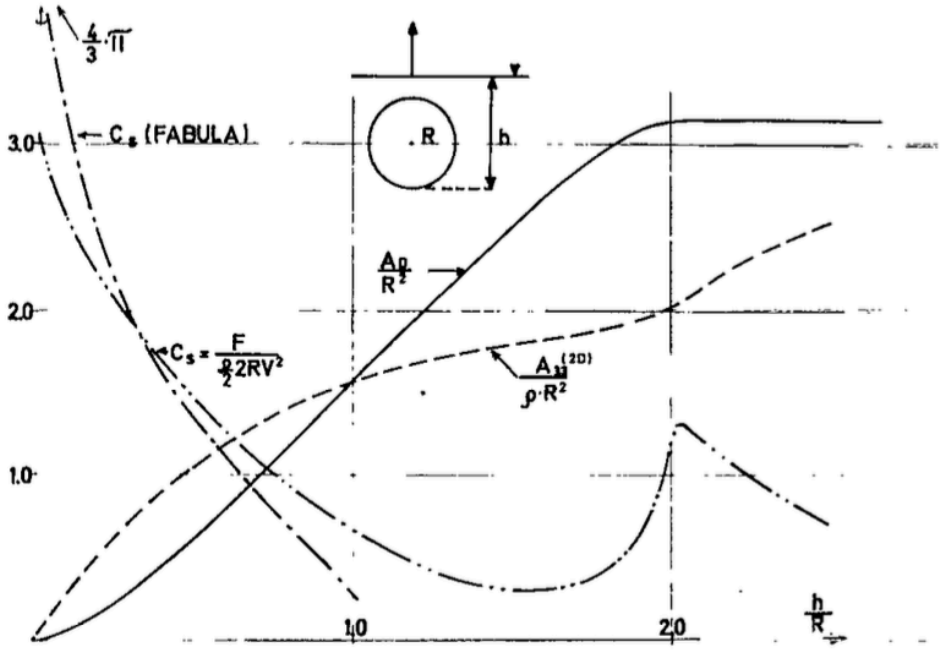

Figure 2-1 Theoretical water-induced loads on a cylinder penetrating the free surface by Faltinsen et al. (1977)

Sollied (1976) made the experiment of rigid cylinder penetrating calm water surface in Trondheim, a control unit was utilized on the model to supply a constant velocity during the experiment. The experiment was made by three different models and tested with various Froude numbers, and it was also mentioned that "*For the impact and the surface penetration it is not likely that the Reynold's number should have any great influence*" (Faltinsen et al., 1977: 120).

Although the resulting data of Sollied's experiment were not sufficient to make plots of curves, comparison curves with theoretical calculation of certain data were made by Faltinsen et al., in which the water-induced load per unit length for various submergence distance $\frac{h}{r}$ were plotted. In terms of some curves, Fabula and Ruggles' calculation seemed to agree with experiment results well, but no reasonable explanation was given in the paper. It was worth mentioning that in model III after $\frac{h}{r} > 2.0$, relatively large difference between Faltinsen et al.'s calculation and experiment result was obtained, shown in figure 2-2. Faltinsen et al. noted that it was partly because they assumed the cylinder was totally wet after submergence in their calculation. However, in Sollied's experiment, the upside of the cylinder was not wet at that moment due to the large speed, and this phenomenon was also found in the SPH simulation of this thesis.

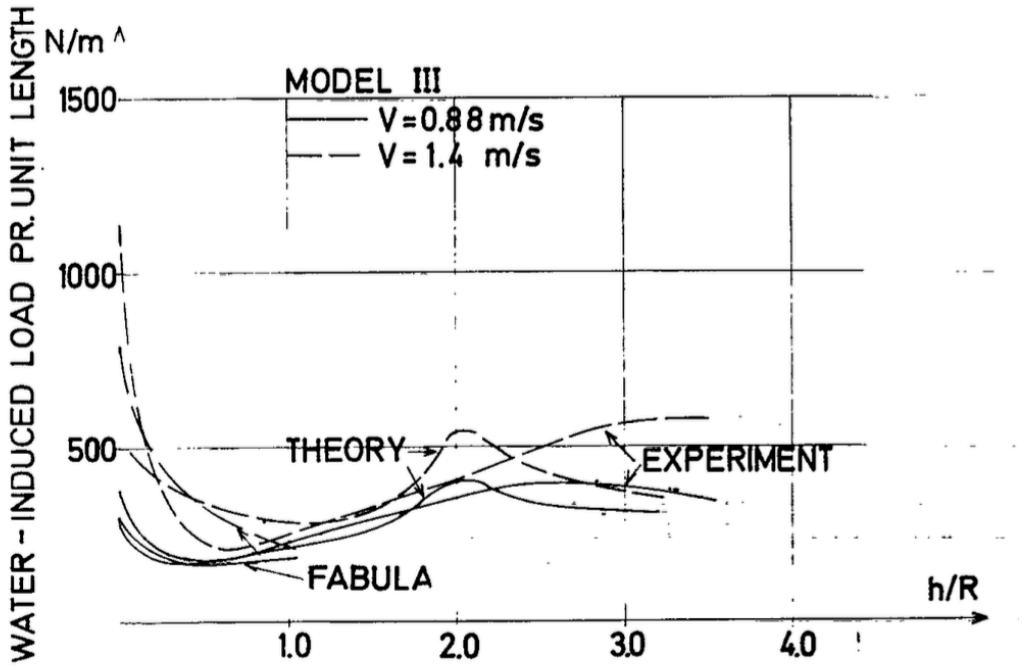

Figure 2-2 Water-induced load on model III by Faltinsen et al. (1977)

Again in figure 2-2 peak values could be obtained in the curves of theoretical result around depth function $\frac{h}{r} = 2.0$, the explanation given by Faltinsen et al. was that the buoyancy was of greater importance in the total hydrodynamic forces when the cylinder was submerged than that in the slamming moment. However, it was still not enough to explain why the curves declined after the peak value, because the buoyancy of the cylinder should keep a high value after submerged, the stably extended curves should be a reasonable result as the experiment curves showed in the figure 2-2.

2.1.2 Experiments

A series of experiments were presented by Campbell and Weynberg (1980), and the results in their experiments were widely cited in various papers and thesis. The tests were based on the experiment model made by Campbell et al. (1977) with diverse analytical approaches. In horizontal cylinder impact part of the experiment, various Froude numbers ranging from 1.9 to 5.6 were selected, and Reynolds numbers were from 0.8 to 4.4 x 10^5. It was mentioned in the paper that the slamming loads dominated in the resultant forces when Froude number was higher than 0.6 according to Miller (1977). Based on that premise, the defined Froude number was relatively large in the tests, and Campbell and Weynberg estimated that the possible contribution of the buoyancy to the slamming coefficient C_S could be from 0.05 to 0.54.

The mean velocity of experiment was constant during $\frac{h}{D} = 0.4$, and approximate 5% fluctuation was found when the penetration process went up to $\frac{h}{D} = 1$, i.e. the cylinder was fully submerged. Therefore, small error could happen during the fluctuation. To measure the forces in slamming moment, the force transducers were utilized, and the vibration of the test rig with the frequency about 550 Hz was recorded in the result plots. During the data processing the other oscillation vibration was omitted by taking the mean values. The vibration was also found in other experiments or numerical simulation, therefore, appropriate methods were needed to fit the resulting curves, including ignoring some extreme large values. Larsen (2013) mentioned this in his thesis, for the computation of vertical forces, special large values in the slamming moment were found.

The empirical equation which could describe the slam load history was defined based on the experiment by Campbell and Weynberg (1980)

$$C_S = \frac{5.15}{1 + \frac{19vt}{D}} + \frac{0.55vt}{D} \tag{2.3}$$

where D is the diameter of the cylinder, vt equals the penetration depth h, and the equation can be rewritten as C_S function of the non-dimensional time variable $\frac{Vt}{r}$

$$C_S = \frac{5.15}{1 + \frac{9.5vt}{r}} + \frac{0.275vt}{r} \tag{2.4}$$

the equation (2.4) was cited and utilized by various papers as the empirical expression in comparison. According to Campbell and Weynberg (1980) the equation was applicable to limited Froude number range, i.e. the effect of buoyancy was significantly small compared to the slamming loads.

After the experiments by Campbell and Weynberg (1980), another series of typical experiments were made by Greenhow and Lin (1983), the high speed entry of the cylinders and wedges into calm water experiments. The experiment model and parameters were not described in Greenhow and Lin's paper, but they mentioned the experiments made by Sollied (1976). More detailed pictures were taken for better fluid behavior description, so the experiment model could be considered to be similar to that defined in Sollied's experiment. The main difference between the two experiments could be the velocity of the objects, in order to test different penetration depth, the rigid bodies were needed to enter into water freely rather than the forced constant

velocity in Sollied's experiments. Due to the high speed penetration, gravity effect was considered very small and having no influence for the results. Actually, in most of the researches, no matter theoretical analyses, experiments or numerical simulations, the influence of gravity was widely considered to be of little importance in order to simplify the cases, especially when the velocity was relatively large.

The experiment was also limited in two-dimensional models, and two types of cylinders with different weight (density) that were called half buoyant and neutrally buoyant cylinders were tested. The experiment results were plotted as the penetration depth for the time variable. Distinguished with the previous theoretical study, Greenhow and Lin focused on the deformation of the free surface and the jets elevated by the interaction between cylinders and the fluid. Although there was no numerical analysis in their report, they tried to illustrate the relation between deformation of the free surface and submergence of the rigid bodies.

The pictures taken in this experiment clearly showed the penetration of the rigid bodies, and also the splash ejected by slamming interactions. These pictures were cited and compared with in various later papers, e.g. Faltinsen (1990) cited the pictures of the whole process to show the visualization of penetration process study, Larsen (2013) compared his CFD numerical simulation with the experiments and obtained similar results. The experiment results were considered to be relatively clear and accuracy data with a high practical value and through the experiments Greenhow and Lin offered referential methods for similar studies.

2.1.3 Numerical simulations

Ghadimi et al. (2012) offered both analytical and numerical solutions for the water impact of the two-dimensional horizontal cylinder problem. Specifically, as for the analytical approach, it was introduced on the basis of water entry study of rigid body with symmetric geometry, and the details of free surface condition and solutions of boundary values were discussed. In terms of the numerical program, it was called FLOW-3D, the code of which was the combination of finite volume method (FVM) and volume of fluid (VOF) method for free surface flow. Both of the methods were CFD approaches which were based on the Eulerian method.

Both the analytical and numerical results by Ghadimi et al. (2012) were compared with the previous experiments and studies made by Campbell and Weynberg (1980), Wagner (1932), etc. The comparison was made by the plot of slamming coefficient C_s as the function of the variable $\frac{h}{r}$, and it was shown that the analytical result mentioned as the linear solution agreed

with the experiment well. Nevertheless, Ghadimi et al. considered that the best agreement was the later numerical result which was not shown in the paper.

According to Ghadimi et al. (2012), the domain of the numerical model they made was not a regular shape, it was a semi-circular with a radius of eight times larger than the radius of the tested cylinder, and the top of the semi-circular was a regular rectangle with the width as same as the diameter of the lower part, and the depth was three times larger than the radius of the cylinder, as shown in figure 2-3. Ghadimi et al. did not mention the reason why they selected this unusual domain shape. However, in the figure it could be obtained that the mesh size varied due to the circular shape. Therefore, it was difficult to say what kind of effects can be made by the characteristics.

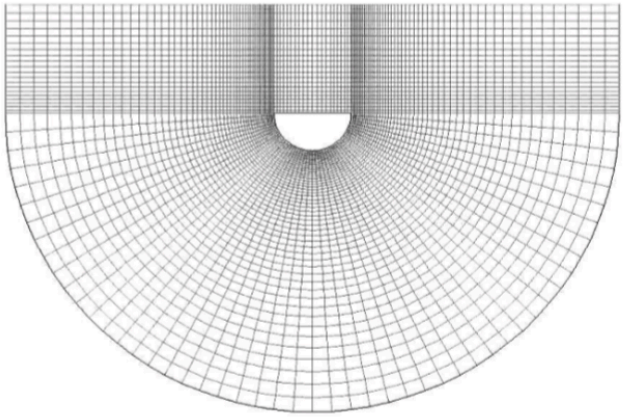

Figure 2-3 the shape of domain by Ghadimi et al. (2012)

Ghadimi et al. did not offered the specific parameters they set in the simulation, e.g. the constant velocity, and Froude number, hence this solution could be seen as a good example to test the numerical program, with little help for the later researches.

Another series of numerical simulations were made by Gu et al. (2013), both semi-cylinder and wedge models were tested in their simulation. They applied the numerical solution on the basis of Navier-Stokes equations (NSE) with fixed grids, and the results were compared with other analytical and experimental outcomes.

In their simulation, the radius of semi-cylinders was 5.5 m, with the constant vertical velocity of 10 m/s, which was a relatively large value among similar simulations. Here the Froude number was not mentioned in their paper, but it could be calculated that the Froude number was 0.963, which was a small value compared with the parameters in some other papers, e.g. Campbell and Weynberg (1980) selected the Froude number ranging from 1.9 to 5.6. The initial

position of the semi-cylinder was 1.0 m over the free water surface. The mesh sizes were defined as 0.2 m, 0.1 m and 0.05 m.

Like other numerical simulations, the slamming coefficient C_S was one of the results compared with other analyses and experiments. Gu et al. mentioned that the value in the theory of von Karman (1929) and Wagner (1932) were separately $C_S = \pi$ and $C_S = 2\pi$ in slamming moment, and the experienced value was between the two values as C_S around 5.2 according to Campbell and Weynberg (1980). The numerical result of semi-cylinder was a little higher than the experienced curve, but agreed with experimental result.

One recent numerical simulation of cylinder entering and exiting water was presented by Bašić et al. (2014). They adopted the incompressible smoothed particle hydrodynamics (ISPH) mothed to simulate the slamming process and compared the result with the experiment made by Miao (1989). In the simulation, a two-dimensional horizontal cylinder was defined and it entered into calm water with forced constant velocity ranging from 0 to 2.66 m/s, the slamming coefficient C_S was plotted as the comparable object. During the procedure, a series of parameters were considered to be related to the simulating result, e.g. Froude number, Reynold number and the roughness of cylinder surface which had influence on physical experiments. Among these parameters, they mentioned, "*The Reynolds number has little effect on the results because the major vortices are concentrated in the boundary layer of the cylinder*" (Bašić et al., 2014: 57).

Figure 2-4 showed the water entry comparative result of Bašić et al. (2014), the testing velocity of cylinder was $v = 0.5124\, m/s$. In the simulation, the ISPH spline kernel function was utilized with the smoothing length $l = 1.2\, z$, the initial particle spacing was defined as $z = 0.005\, m$, and the total number of particles was 10500. Bašić et al. mentioned that the oscillation vibration could be decreased by adjusting the ISPH parameters, e.g. smaller particle spacing and time interval. Nevertheless, it was necessary to say that there was limitation on the parameters. That was to say, if the particle spacing was beyond the size limitation, it could lead to unexpected negative effects for the simulation, and the time cost could also increase in a great extent.

In figure 2-4 it could be obtained that the ISPH curve was a little higher than the experiment curve, but the tendency basically agreed. No method was presented by Bašić et al. to deal with the vibration curve. Generally speaking, the smoothed curve could agree with the experiment result better.

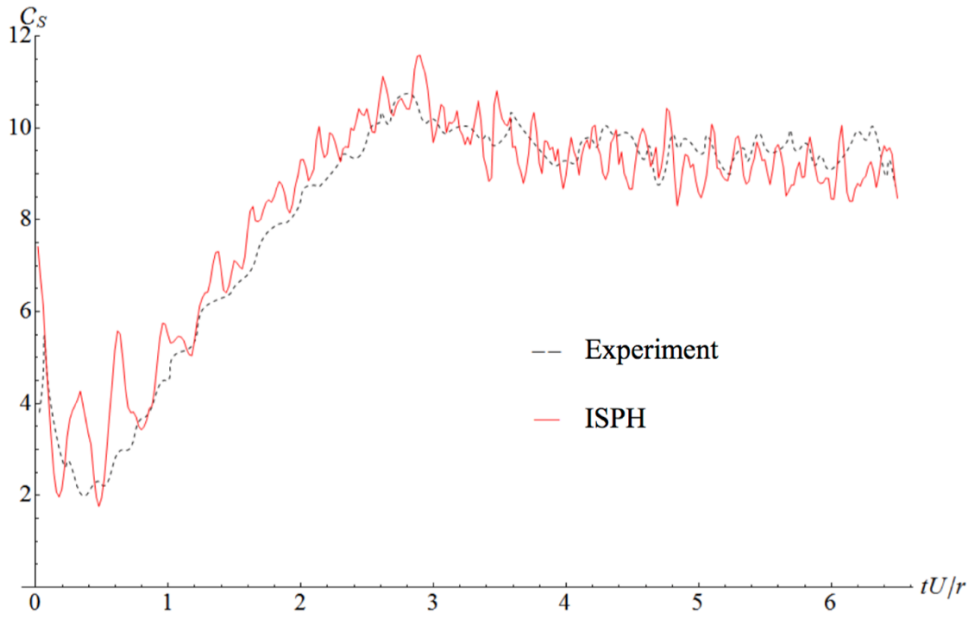

Figure 2-4 Comparison between the results of numerical simulation with ISPH method and experiment by Bašić et al. (2014)

Although the ISPH method simulating results agreed with the experiment well in the paper, the parameter selection was a difficult and important factor to obtain better outcomes. Bašić et al. simply mentioned that reducing the particle spacing and time interval, or in other words, increasing the particle numbers and the accuracy of simulation could be effective for better results. Besides, applying optimized algorithms could work better than changing the parameters, so optimization and innovation were actually the main directions to improve the stability and accuracy of numerical simulation methods.

2.2 Water entry of wedges

The study in the water entry of wedges is very typical in the researches of slamming theory and the interaction between calm water (or waves) and the moving objects that penetrates the free surface. Von Karman (1929) started the researches of water impact problems, and also indicated the research direction for the water entry study of wedges. There were diverse research methods of the water impact of wedges, e.g. symmetric and asymmetric shapes, wedges with a series of angles, vertical falling velocity, and falling along an inclined route. In this section, some typical theoretical analyses, experiments and also numerical simulations based on the wedges study are reviewed and discussed.

2.2.1 Theoretical analysis

As the widely acceptable water entry of the wedge theory, the slamming model of Wagner (1932) that developed based on the theory of von Karman (1929) was discussed and cited in many similar papers. Faltinsen (2005) introduced the theory in details in his book.

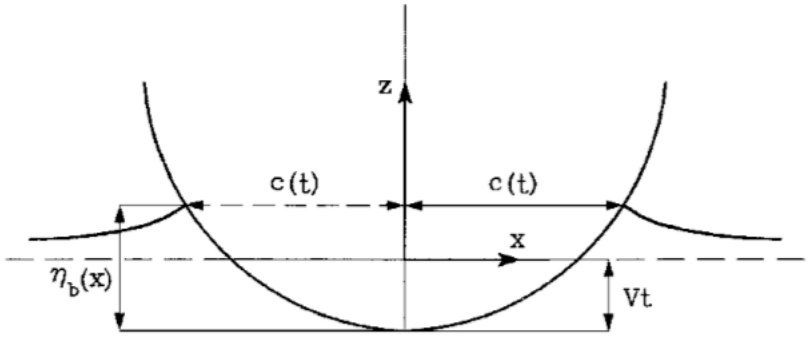

Figure 2-5 definition of Wagner's slamming model by Faltinsen (2005)

Figure 2-5 showed the parameter definition of Wagner's slamming model, the amount of upraised water was considered as the same with water displaced by the submerged object, so the wetted length was calculated according to the upraised water surface, which was the main difference between Wagner's and von Karman's theories.

The water entry of wedges was discussed briefly by Faltinsen (2005), the case was described that the wedges penetrated the calm water with a forced constant velocity, which was similar to the case of water entry of cylinders. Additionally, the slamming coefficient C_S was calculated based on various deadrise angles β, the definition of C_S was

$$C_S = \frac{F}{\rho v^3 t}(tan\beta)^2 \tag{2.5}$$

The slamming coefficient plots were plotted as shown in figure 2-6.

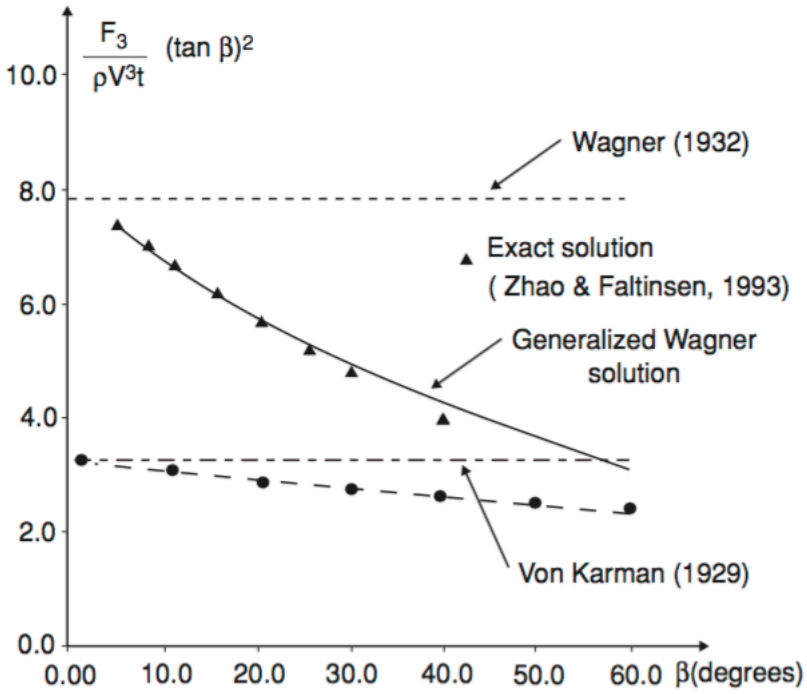

Figure 2-6 slamming coefficient of varied theories by Faltinsen (2005)

2.2.2 Experiments

As the research in the early stage, it is necessary to mention the experiments made by Greenhow and Lin (1983). As introduced in last section, they made a series of experiments including high speed water entry of wedges and cylinders. In terms of the wedge experiments part, they utilized various wedges with different angles, which were 18, 30, 60, 90 and 120 degrees. The point was that the wedge of 18 degrees was considered as a slender shape. On the contrary, the wedge of 120 degrees was predicted to act similarly as a flat plate. These tested wedges were placed on some height above the free surface, making sure that they could penetrate the water surface with an initial velocity.

The results of the experiments were compared with existing theories, Greenhow and Lin paid much attention on the deformation of the water surface. They found that under the condition of high speed water entry there was little jet elevated in their experiments, so the experiment results could not agree with some theories presented by the previous researches. However, the theory of elliptic solution offered similar prediction about the deformation of water surface to their experiments. The theory applied $\sqrt{3}$ to fit the breaking waves loop, which can describe the ejected splash quite well. Although this theory was supported by the experiment results of

Greenhow and Lin (1983), the explanation of the theory was not provided. Besides, the effects of air could be involved in the penetration process while the pile-up of water was small. However, in the experiments of Greenhow and Lin (1983), the air influence was omitted due to the large pile-up of water.

As same as the experiments of cylinders, details of the water penetration and the deformation of water surface were recorded by high speed camera, the experiments results were good comparison objects that could be utilized to compare with the later researching works, and the elliptic theory was also a good topic for researchers to study.

2.2.3 Numerical simulation

The numerical simulation of SPH method was made by Oger et al. (2005), they made a series of simulations about the water entry of two-dimensional wedges, and the results of simulations were compared with the experiment conducted by Zhao et al. (1996). In the simulation of water entry of the symmetric wedge, the angle of the wedge was 120 degrees, and the length was 0.5 m. The initial vertical velocity was 6.15 m/s, which was also the water entry velocity while the simulation started.

The smoothing length of the SPH method by Oger et al. (2005) was not all the same in the testing domain, which was different from the smoothing length setting of DualSPHysics utilized in this thesis. The smoothing length was constant in DualSPHysics program, so the computation could not be optimized by applying varied smoothing length values in different parts of the domain, which was actually a good way of reducing the time consumption of the computer. Figure 2-7 showed the varied smoothing length method, and it could be obtained that for the possible involved particles, the particle distance was quite small, which ensured the accuracy of the computation. On the contrary, the relatively large particle distance was utilized in the other area of the domain gradually.

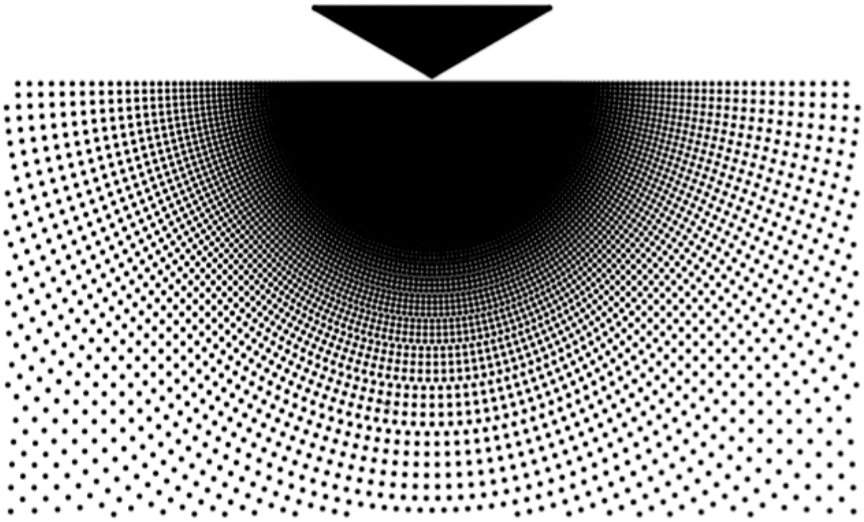

Figure 2-7 initial particles setting by Oger et al. (2005)

In terms of the results of the numerical simulation, the wedge velocity changing was plotted, and the pressure loading on the different parts of the wedge was calculated and compared with the experiment results of Zhao et al. (1996). The results agreed with the experiment well, except for the maximum load values and the fluctuation of the resulting curves. Oger et al. (2005) mentioned that the large load value could be caused by the sudden change of the status of the fluid in SPH method. In this thesis, the same situation has been found in the simulations as well, but most of the values are in the acceptable range. The fluctuation showed the instability of SPH method. Actually, both CFD and SPH methods had the problem of instability, which was the feature of numerical simulation in contrast to theoretical analyses and experiments.

For another free falling simulation of the wedge, Oger et al. (2005) obtained satisfied results. The resulting curves of vertical slamming force located between the theoretical and experiment outcomes. The numerical simulation made by Oger et al. (2005) showed quite positive results, the parameter setting was also reasonable and optimized for reducing the computer power consumption.

3 Theory

SPH method as the typical meshless simulation approach of Lagrangian method, has its own advantage by comparison with traditional CFD method, since the complicated grids utilized in CFD method can cause some problems in complex calculation. On the contrary, due to the characteristics of the SPH method, the irregular particles distribution in the fluid (or solid) can also lead to inaccurate results. Therefore, the standard SPH method is considered as lack of stability and accuracy.

To solve the problems of SPH method, various algorithms are studied. The common approaches are incompressible smoothed particle hydrodynamics (ISPH) and weakly compressible smoothed particle hydrodynamics (WCSPH). The main difference between ISPH and WCSPH is the method of calculating the particle pressure. Both the two approaches are widely utilized, and in general the optimized ISPH and WCSPH approaches are at the same level of accuracy. The program applied in this thesis is called DualSPHysics, which is on the basis of the WCSPH approach.

In this chapter, the theory of basic SPH method and DualSPHysics is introduced, and also the algorithms of simulations in this thesis is discussed.

3.1 Smoothed particle hydrodynamics

In this section, three main parts of the SPH theories, smoothing kernel function, fluid equations application, and particle searching algorithm are briefly introduced, and the emphasis is not placed on the detailed formula derivation. The same as other methods, the SPH approaches also vary for different algorithm branches. In order to solve the drawbacks of SPH method itself, e.g. continuity and boundary condition problems, various approaches are developed. Nevertheless, the common theory which is based on the Lagrangian method changes hardly, the theory adopted in this thesis is presented by Cossins (2010).

3.1.1 Kernel function

In SPH method, particles are viewed as basic elements which form the fluid. Each single particle is influenced by its neighbor ones, as shown in figure 3-1, and the interaction between particles decreased with the distance increasing, therefore, according to Cossins (2010), the kernel function W can be written as

$$\lim_{l \to 0} W(z, l) = \delta(z) \tag{3.1}$$

where z refers to the position of the particle in fluid, l is the smoothing length that describes the distance of interaction of the particles, hence it can be considered that no effect between particles can be found if their distance is beyond l, $\delta(z)$ here is called Dirac delta function (Cossins, 2010), which is featured for any function as

$$f(z) = \int_V f(z')\ \delta(z - z')dz' \tag{3.2}$$

where z' is a dummy variable (Cossins, 2010), V refers to the fluid volume.

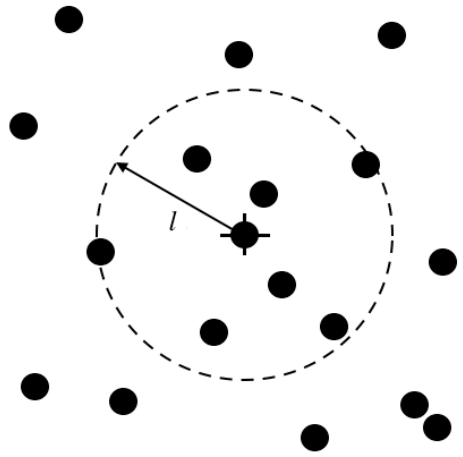

Figure 3-1 particles and smoothing length

The smoothing kernel function W should have the features mentioned as follows:

- Kernel function W is symmetric function, meaning $W(z - z', l) = W(z' - z, l)$.
- From the equation (3.1) it is known that kernel function W is also a Dirac delta function, means that $\int_V W(z - z', l)dz' = 1$. See figure 3-2.
- While the particle is out of the smooth length range, the interaction should be zero, i.e. $W(z - z', l) = 0, when\ |z - z'| > l$.
- For any position within kernel function W, the interaction should be positive, means that for any variable, $W(z - z', l) \geq 0$. (G.R. Liu and M.B. Liu, 2003).

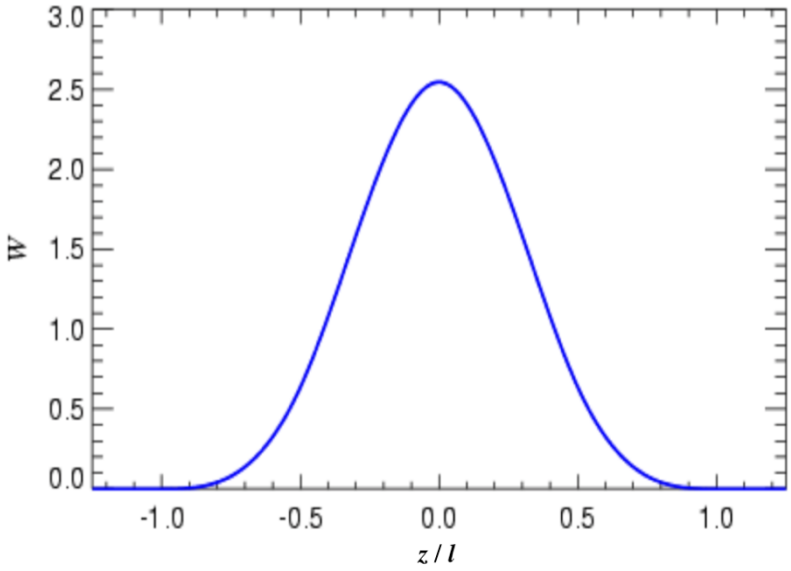

Figure 3-2 smoothing kernel function example (online data)

By writing the kernel function W as a second Taylor series expansion, and introducing the density of the particle in unit length, the approximate expression of function $f(x)$ can be rewritten as

$$f(x) \approx \sum_i \frac{m_i}{\rho_i} f(z_i)\, W(z - z_i, l) \tag{3.3}$$

where i refers to any position within the smooth length range, m is the mass of the particles, and ρ is the density at position z_i.

In the expression, $f(x)$ could be changed to the characteristics function of the fluid, therefore, the fluid properties, e.g. pressures between particles, can be calculated by accumulating the smoothing kernel function W with this method.

The researches have tried various functions that can fulfill the requirement of smoothing kernel function, an appropriate kernel function is in the form of Gaussian function, since the standard Gaussian is an uncomplicated kernel function of wide applicability,

$$W(z, l) = \alpha_D e^{-q^2} \tag{3.4}$$

where α_D is $\frac{5}{\pi l^2}$ in 2D, and $\frac{105}{16\pi l^3}$ in 3D, $q = \frac{z}{l}$ refers to the relative distance between the particles. Although the Gaussian kernel is considered as an appropriate kernel function, it is not

the best choice in numerical computation, because for any distance between two particles value z, $W(z,l) > 0$, it means that extra limitation is needed in practical computation.

3.1.2 Fluid equations

In this section, the main fluid equations, the Navier-Stokes equations, are shown in the SPH form, the smoothing kernel function is applied in the fluid equations to form the SPH formulations which are the basic expressions utilized in SPH calculation and simulation. There are three main equations used to describe the fluid behavior as follows.

- The continuity equation (conservation of mass)

$$\frac{\partial \rho}{\partial t} + \nabla \cdot (\rho \mathrm{v}) = 0 \tag{3.5}$$

where v refers to the velocity, ρ is the density as mentioned before.

Here the density ρ can be rewritten as the form of kernel function expression (3.3),

$$\rho_j = \sum_i m_i W(z_j - z_i, l) \tag{3.6}$$

take the time derivative of the equation, and rearrange the equation, finally the continuity equation becomes

$$\frac{d\rho_j}{dt} = \sum_i m_i (v_j - v_i) \nabla_j W(z_j - z_i, l) \tag{3.7}$$

that's the continuity equation in SPH form.

- The momentum equation (conservation of momentum)

$$\frac{\partial \rho v}{\partial t} + \nabla \cdot (\rho \mathrm{v} \times \mathrm{v}) + \nabla P = 0 \tag{3.8}$$

where P is the fluid pressure, the cross product means that velocity vector product includes $(\vec{x}, \vec{y}, \vec{z})$ directions, hence in this equations velocity vector (v_x, v_y, v_z) is defined. Here the Lagrangian $\mathcal{L}$ is introduced, which equals the difference between kinetic energy and potential energy in the system,

$$\mathcal{L} = \int_V \frac{1}{2} \rho v \cdot v - \rho u dr \tag{3.9}$$

where u represents the specific internal energy which is the function of density and pressure $u = u\ (\rho, P)$ (Cossins, 2010). Then the expression of density ρ (3.6) is put into the equation again, and the Euler - Lagrange equation can be applied to rearrange the expression, also with the application of the ideal gas equation of state, finally the equation becomes

$$\frac{dv_j}{dt} = -\sum_i m_i \left(\frac{P_j}{\rho_j^2} + \frac{P_i}{\rho_i^2}\right) \nabla_j W(z_j - z_i, l) \tag{3.10}$$

which is momentum equation expressed in SPH form. It should be noted that the equation is on the premise of an inviscid fluid, meaning that the viscous part of the equation is omitted. The simplification of ideal fluid could make the results of this SPH approach not accuracy in some sense. The advanced expression with viscous part will not be discussed in this thesis.

- The energy equation (conservation of energy)

$$\frac{\partial u}{\partial t} + \nabla \cdot [(u + P)v] = 0 \tag{3.11}$$

where u is the specific internal energy as mentioned above. Here the total energy of the system $E = \frac{1}{2}\rho v^2 + \rho u$ is introduced into the equation (3.3), which means that total energy equals the summation of kinetic and internal energies, so it can be obtained that

$$E = \sum_i m_i (\frac{1}{2} v_i \cdot v_i + u_i) \tag{3.12}$$

Hence, take the time derivative of the equation, and apply the energy conservation principle, the equation can be rearranged as

$$\frac{\mathrm{d}u_j}{\mathrm{dt}} = \frac{P_j}{\rho_j^2} \sum_i m_i (v_j - v_i) \cdot \nabla_i W(z_j - z_i, l) \tag{3.13}$$

which is the energy equation of SPH approach form.

The fluid equations are expressed in SPH form according to the Lagrangian description of the fluid. In these equations, kernel function plays an important role as the main feature of SPH, and for different cases, various kernel functions can be selected and make effects on the simulating results. In later sections, several applying detailed kernel functions will be mentioned. The above equations are basic principles according to Cossins (2010). In terms of

certain applied programs, more assumptions are made to obtain the optimized results, and there are also other SPH approaches which are different from these principles.

3.1.3 Particles searching

In SPH method, the distance of particles within the smoothing length can interact with each other, therefore, it is necessary to find the neighbor particles which are related to the "central" particle. The procedure of finding the concerned particles is named as nearest neighboring particle searching (NNPS).

There are several algorithms of NNPS with respective advantages. As for numerical computation, the approach called linked list algorithm is widely utilized for the efficiency in positioning the particles, especially for constant smoothing length computations. In linked list algorithm, the domain in the case is divided into several cells related to the smoothing length and domain size. For example, the $2l \times 2l$ square is usually defined as the individual cell. While the concerned particles are needed to start searching, the surrounded cells of the central particle are to be marked, i.e. nine cells altogether including the middle cell for a two-dimensional domain model, or twenty-seven cells for three-dimensional model, after that, the particles within the smoothing length are located from the marked cells.

Although the linked list algorithm is a good choice for some numerical computation programs, it is not suitable for the problems with variable smoothing length. Since the size of cells is constant, which only works efficiently for limited range of smoothing length values. However, here the other algorithms are not contained in the discussion.

3.2 DualSPHysics

SPHysics is an open-source platform based on the SPH formulation, the program was developed by researchers at the Johns Hopkins University (US), the University of Vigo (Spain), the University of Manchester (UK) and the University of Rome, La Sapienza (SPHysics, 2010). In SPHysics researchers can model various fluid problems in the Fortran code, and obtain numerical results and visual simulation.

DualSPHysics is developed on the basis of SPHysics, in which C++ and CUDA code are applied instead of Fortran code. Although it is robust and reliable, Fortran code is not considered to be the proper code for building huge simulations (DualSPHysics, 2013). In this section, workflow and algorithm of DualSPHysics, time integration, and computation loop of SPH code are introduced.

3.2.1 Workflow of DualSPHysics

In a standard case of simulation, there are several working steps as shown in figure 3-3:

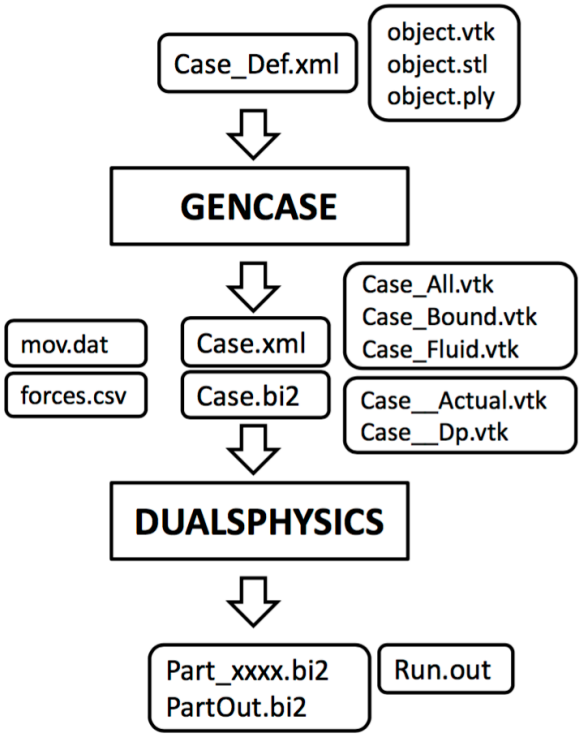

Figure 3-3 workflow of DualSPHysics (DualSPHysics, 2013)

1) Establish the model

   The simulation model is established in a .xml file, in which all the parameters are defined with the code that can be read by the program. The parameters can be divided into three parts as their functions: i) constant part, includes gravity, coefficients, fluid density, etc.; ii) geometry part, defines the distance between particles, case limitation, domain size, object shape, type of motion and other various parameters which are needed to describe the case. The size and initial position of the domain and objects are defined in a coordinate system; iii) execution part, indicates the algorithm utilized in the simulation, and the time of simulation.

2) Generate the case (Gencase)

   By running the .xml file defined in step 1), the details of the case are generated, including numbers of particles, particle mass, boundary description, initial fluid and objects models,

and so on. At the same time, initial vtk files of objects and fluid are saved, which can be read by visualization application (e.g. Paraview).

3) DualSPHysics

DualSPHysics reads the output files from Gencase, these files are rewritten in the form of .xml. During this process, as mentioned by DualSPHysics (2013), there are substeps that could be discussed in detail: i) neighbor lists of the particles are generated according to the particle distance and physical characteristics defined before; ii) particle forces are calculated based on the neighbor lists, this process may spend several hours even days depending on the model size, particle numbers and computational capability; iii) the computation results are saved as vtk and ASCII files, in which the information of the particles (e.g. position, acceleration and velocity) is stored.

4) Post-processing

This step is mainly achieved by data processing program (e.g. Matlab), in post-processing the numerical data saved in ASCII files are analyzed, in order to show the final results in plots and tables, or the vtk files can be rendered to obtain visual animation of fluid behaviors.

The DualSPHysics is able to run by both CPU and GPU. With the development of modern computer technology, GPU approach has obvious advantage in parallel computation compared with CPU. Due to the huge numbers of particles in simulation, there could be hundreds of thousands or even more than millions of particles, the simulation time is considered as an important aspect for DualSPHysics in optimization progress. In practice, the CPU and GPU approaches are usually combined in simulation. Specifically, GPU is utilized in particle interaction calculation that needs to deal with parallel computation in large scale. On the other hand, CPU approach is implemented in generating the neighbor lists and saving files. Therefore, the combination of CPU and GPU approaches can improve the efficiency significantly.

3.2.2 Algorithm of DualSPHysics

On the basis of the SPHysics, there is almost no difference between SPHysics and DualSPHysics in theory. The practical theory applied in this program refers to specifics of the SPH approach mentioned in the previous sections. However, in this section only a part of the details that are related to the parameters selection in simulation are introduced. This theory is presented by SPHysics (2010).

- Kernel function

  In SPHysics, the non-dimensional particle distance q is defined as a constant number. For a standard kernel function $W(z, l)$, where z is the distance between two neighbor particles, l represents the smooth length, so q is defined as $q = \frac{z}{l}$.

  There are two main optional kernel functions in DualSPHysics (SPHysics, 2010):

  i) Cubic spline:

$$W(z,l) = \alpha_D \begin{cases} 1 - \frac{3}{2}q^2 + \frac{3}{4}q^3 & (0 \le q \le 1) \\ \frac{1}{4}(2-q^3) & (1 \le q \le 2) \\ 0 & (q \ge 2) \end{cases} \tag{3.14}$$

  where α_D is $\frac{10}{7\pi l^2}$ in 2D and $\frac{1}{\pi l^3}$ in 3D. The cubic spline kernel is the most widely used kernel function in SPH method.

  ii) Wendland:

$$W(z,l) = \alpha_D \left(1 - \frac{q}{2}\right)^4 (2q+1) \qquad (0 \le q \le 2) \tag{3.15}$$

  where α_D is $\frac{7}{4\pi l^2}$ in 2D and $\frac{21}{16\pi l^3}$ in 3D.

  Here it should be noted that in both the above kernel functions, only particles within the distance of *2l* can interact with each other.

- Continuity equation

  SPHysics (2010) mentioned the changes in the continuity equation used in the program, actually the new equation is as the same as the expression (3.7) by G.R. Liu and M.B. Liu (2003) which is introduced in previous section

$$\frac{d\rho_j}{dt} = \sum_i m_j \vec{v}_{ji} \vec{\nabla}_j W_{ji} \tag{3.16}$$

  where $\vec{v}_{ji}$ represents $\vec{v}_j - \vec{v}_i$, and W_{ji} means $W(z_j - z_i, l)$.

- Momentum equation

  In the algorithm of DualSPHysics, an extra viscosity term is added in the momentum equation, in order to solve the problem that the particles could become discontinuous when

the properties such as velocity and density change quite fast. And then the momentum equation can be expressed as

$$\frac{dv_j}{dt} = -\sum_i m_i \left(\frac{P_j}{\rho_j^2} + \frac{P_i}{\rho_i^2} + \Pi_{ij}\right) \nabla_j W(z_j - z_i, l) \tag{3.17}$$

and the the artificial viscosity term Π_{ij} is defined as

$$\Pi_{ij} = \begin{cases} \dfrac{-\alpha c_{ij} \mu_{ij}}{\rho_{ij}} & v_{ij} \cdot z_{ij} < 0 \\ 0 & v_{ij} \cdot z_{ij} > 0 \end{cases} \tag{3.18}$$

where the coefficient α can be assigned in the parameter setting, c_{ij} is the average sound speed, and μ_{ij} is defined as

$$\mu_{ij} = \frac{l \cdot v_{ij} \cdot z_{ij}}{z_{ij}^2 + 0.01 l^2} \tag{3.19}$$

- Equation of state

  Like most the problems of fluid mechanics, the ideal gas equation of state is necessary to be added into the fluid equation. In SPHysics the equation of state is defined as

$$P = B\left[\left(\frac{\rho}{\rho_0}\right)^{\gamma} - 1\right] \tag{3.20}$$

  where $\gamma = 7$ which can be defined in constant parameters, $\rho_0 = 1000\ kg\ m^{-3}$ as the reference fluid density, $B = c_0^2 \rho_0 / \gamma$ in which c_0 is the speed of sound in the reference density. The coefficient of sound speed also can be defined in constant parameters, and the common valid range is from 10 to 30.

3.2.3 Time integration

Various time stepping algorithms can be selected in SPHysics (DualSPHysics). In this part, one common approach, the Verlet scheme algorithm is introduced and utilized in practice. First of all, the equations of momentum, density, position and internal energy are defined as

$$\frac{dp_i}{dt} = F_i\ ;\ \frac{d\rho_i}{dt} = D_i\ ;\ \frac{dz_i}{dt} = v_i\ ;\ \frac{du_i}{dt} = U_i \tag{3.21}$$

where *p* represents the momentum. In general, the time stepping variables are calculated as

$$\begin{aligned} &p_i^{n+1} = p_i^{n-1} + 2\Delta t F_i^n\ ;\ \rho_i^{n+1} = \rho_i^{n-1} + 2\Delta t D_i^n\ ; \\ &z_i^{n+1} = z_i^n + \Delta t v_i^n + 0.5\Delta t^2 F_i^n\ ;\ u_i^{n+1} = u_i^{n-1} + 2\Delta t U_i^n \end{aligned} \tag{3.22}$$

where Δt is the related time step. To prevent the time integration diverging, in every 40 time steps, the variables are calculated as

$$p_i^{n+1} = p_i^n + \Delta t F_i^n \; ; \; \rho_i^{n+1} = \rho_i^n + \Delta t D_i^n \; ; \\ z_i^{n+1} = z_i^n + \Delta t v_i^n + 0.5 \Delta t^2 F_i^n \; ; \; u_i^{n+1} = u_i^n + \Delta t U_i^n \tag{3.23}$$

3.2.4 Computation loop of SPH code

For a standard SPH simulation in SPHysics (DualSPHysics), the computation of SPH code complies with the procedure of calculating the main variables in fluid equations in one step, and shifting to next time step for the same calculation. In this computation loop, some special algorithms are needed as the addition of limited conditions or method corrections, e.g. artificial viscosity, time stepping selection, and boundary conditions. The standard computation loop of SPH code is shown as follows, also see figure 3-4.

1) Simulation model input. As the beginning of the computation, the models of domain, moving objects, fluid and wave maker (if any, depending to the cases) are generated in the program, including the particles involved and boundary types. The time steps are also defined according to the case description file.
2) The initial nearest neighboring particle searching (NNPS) is processed according to the NNPS algorithm, e.g. while applying the linked list algorithm, the domain is divided in various cells with the related size, then initial particles are positioned, and so are the concerned particles.
3) The calculation of artificial viscosity which is the extra part of the standard fluid equations, and the specific smoothing kernel functions are applied in the fluid equations to computing the variables.
4) The calculation of the main variables, particles positions and velocities, the change of momentum and internal energy, particle density, pressure, and if needed, the particle acceleration.
5) Updating the information of all the variables, and saving them as the results at the certain simulation time (depending on the simulation time steps).
6) Checking the boundary conditions.
7) The new variables are applied in next time step, computation loop continues.

8) After the whole simulation is finished, all the resulting information is stored as the indicated format, e.g. in the format of vtk and ASCII files. that can be read and utilized in other programs for post-processing.

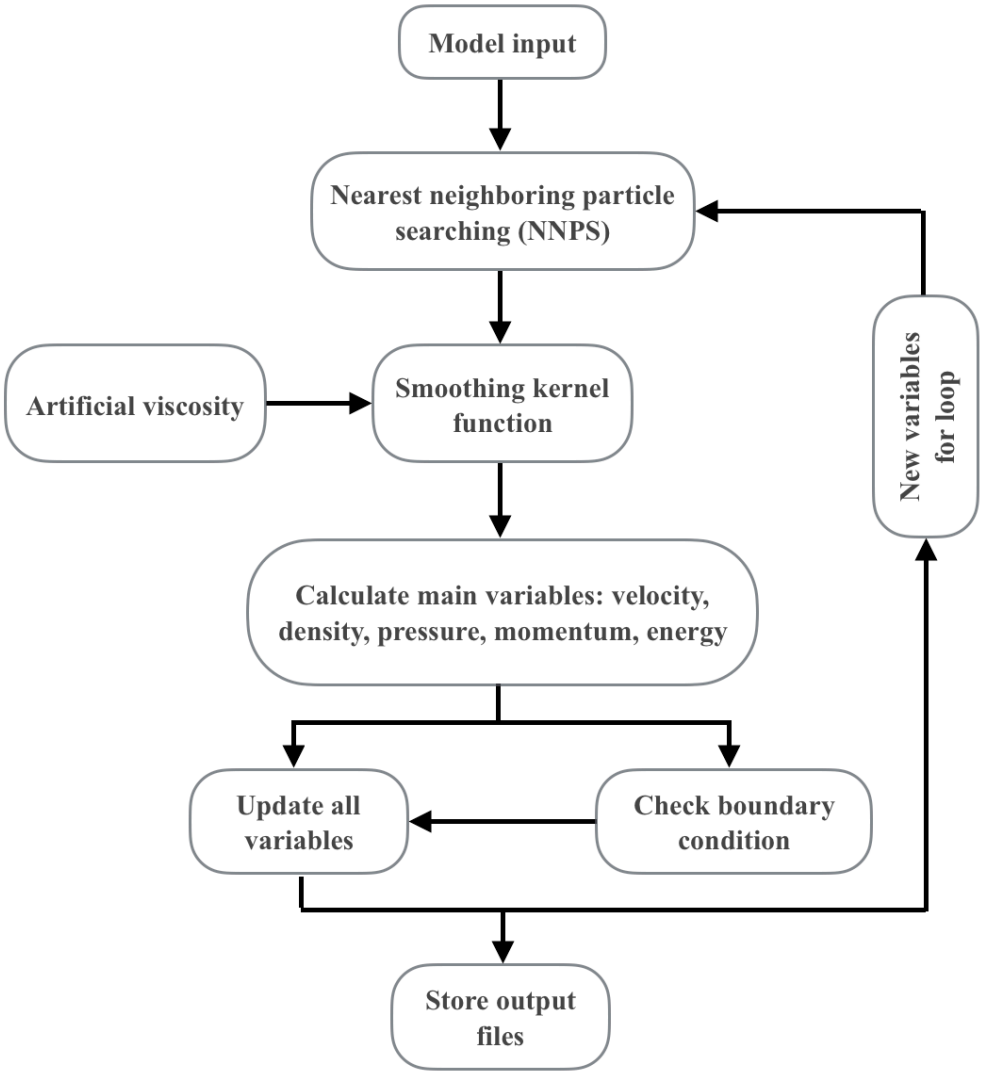

Figure 3-4 computation loop of SPH code

4 Sensitivity analysis

In this chapter, the initial simulating parameters are discussed separately, since in numerical simulation, the selection of parameters could have positive or negative impacts on the final results in various extents. The main parameters contain dimensional variables, e.g. domain size, particle distance and time steps; and system parameters which are specialized variables in SPH method, including the coefficient of sound speed, smoothing length, etc. During the analysis, the case of the water entry of a two-dimensional horizontal cylinder with a constant velocity is selected for testing, and the details of the case will be discussed in next chapter.

4.1 Domain size test

In most of the experiments and numerical simulations, the influence of the domain size should be eliminated, i.e. the boundary condition should not make effects on the structure, so the boundary condition is commonly described as in infinite distance. However, in numerical simulation, too large domain size means unnecessary power consumption in computation, as a result, an appropriate domain size should be selected.

Three different candidate domain sizes are tested with the default Froude number 3.57, which is calculated with the tested cylinder radius 0.1 m and default velocity 5 m/s. The so-called default parameters are applied according to the numerical simulation presented by Larsen (2013). Here the domain sizes are selected according to the radius, which are separately 2.0 m × 0.5 m, 4.0 m × 1.0 m and 8.0 m × 2.0 m with the shape of rectangle in the form of width × height. Among the domains, the minimum width 2.0 m is ten times larger than the diameter of the cylinder. The details of the comparison of the three sizes are listed in table 4-1.

NO.	Domain size (m × m)	Scale of width and cylinder diameter	Particle distance (m)	Particle numbers	Computing time (minutes)
D1	2.0 × 0.5	10	0.0025	166498	10
D2	4.0 × 1.0	20	0.0025	647418	42
D3	8.0 × 2.0	40	0.0025	2569418	196

Table 4-1 details of domain sizes and parameters

In terms of particle distance, the value is 0.0025 m, which is chosen according to the acceptable total particle numbers for computation. The simulation time is calculated with the depth to which the cylinder is supposed to penetrate, and the initial position of the cylinder, 0.1 m from the bottom to the water surface. Here the penetration depth is defined as three times of the cylinder radius, i.e. 0.3 m, hence the total simulation time is 0.08 s with the velocity 5 m/s. Besides, in order to avoid missing peak values, 1000 time steps are considered as default, the effect of time steps will be discussed later.

In table 4-1 it is obtained that with the increase of domain size, the total particle number rises in a similar scale, i.e. the latter domain is four times larger in volume (area) than the former one, and the increasing scale of particle number is also about four times, for the total particles include those constitute the varied domains and also the cylinders with the same size. However, the addition of computing time does not act in the same way. For NO. D3 domain, the computing time is 196 minutes, nearly five times longer than the computing time in NO. D2. The total computing time contains the time spent in pre-processing, calculations and output data saving, each procedure tends to increase the entire time consumption with the increase of particles.

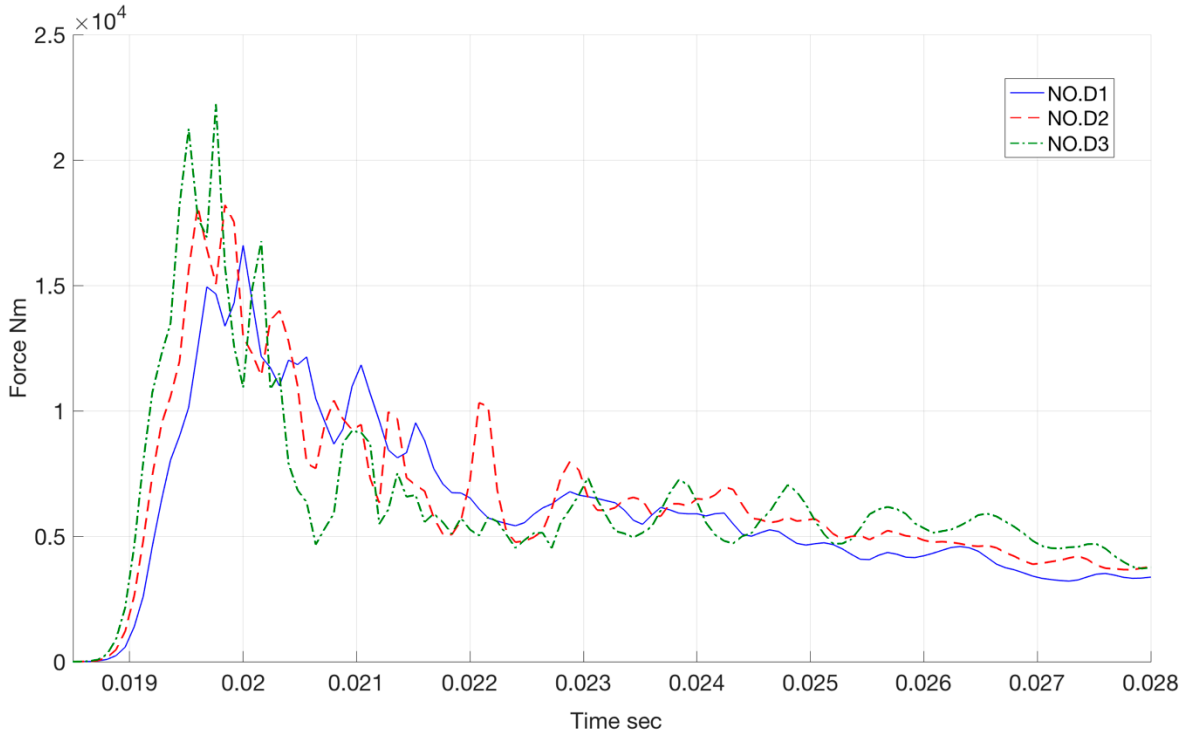

Figure 4-1 peak values of vertical forces for three domains

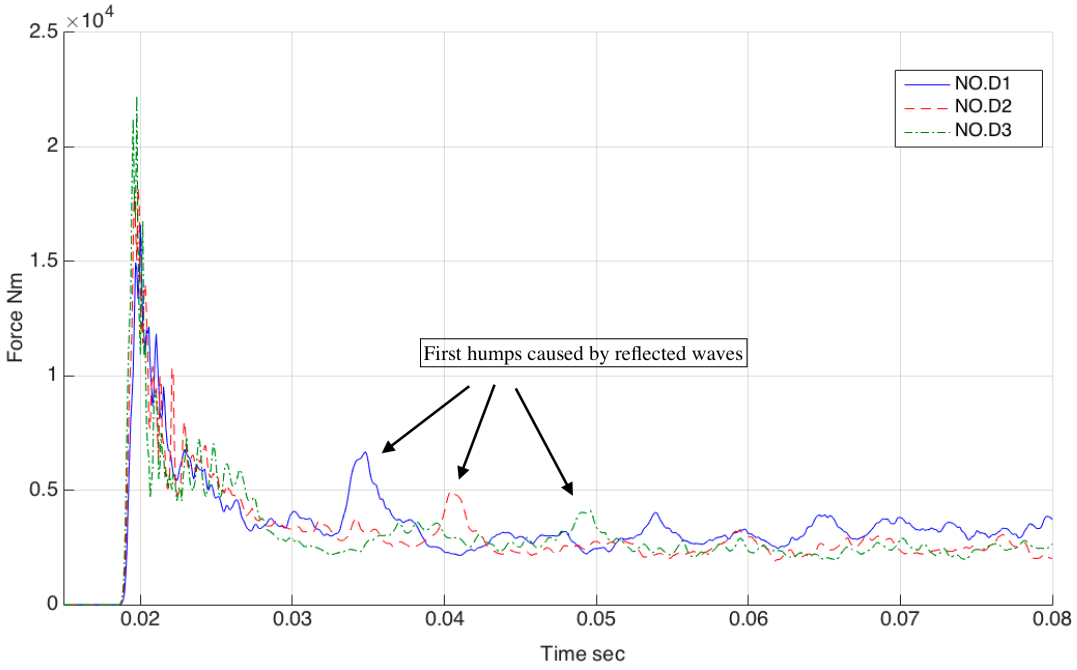

Figure 4-2 fluctuation of three domain sizes

Apart from the computing time, the simulating results are not the same in plots, figure 4-1 shows the peak vertical forces calculated individually in these three domains. With the increase of the domain size, the slamming force rises substantially. It is difficult to explain why the slamming force that happens in a very short time is influenced by the domain size, i.e. higher slamming forces could be obtained in larger domain. This could be due to the error of numerical method in DualSPHysics, because the amounts of the involved particles at the same moment are different, see figure 4-3. It is noted that larger force values do not equal better accuracy level, since more extreme values are also found in the curve of NO. D3. Another problem that is caused by the DualSPHysics program is that the slamming moment happens earlier than that in practice. The time when the tested cylinder touches the water surface should be 0.02 s theoretically, however, in figure 4-1 it can be found that the vertical force starts to increase before 0.02 s.

Furthermore, the unusual high values can be obtained in all the three curves as shown in figure 4-2, and these humps are formed due to the energy waves that reflects by the boundaries of the domain. Therefore, in smaller domain the humps exist earlier and more frequently, and with the increase of the distance the reflection waves propagate, the induced forces reduce significantly, i.e. peak values of the first humps decrease with the increase of the domain sizes. In terms of the effects caused by the domain sizes, large domain has its own advantage -- less boundary

influences. On the contrary, there are also problems of inaccurate slamming moment, noises and long computing time.

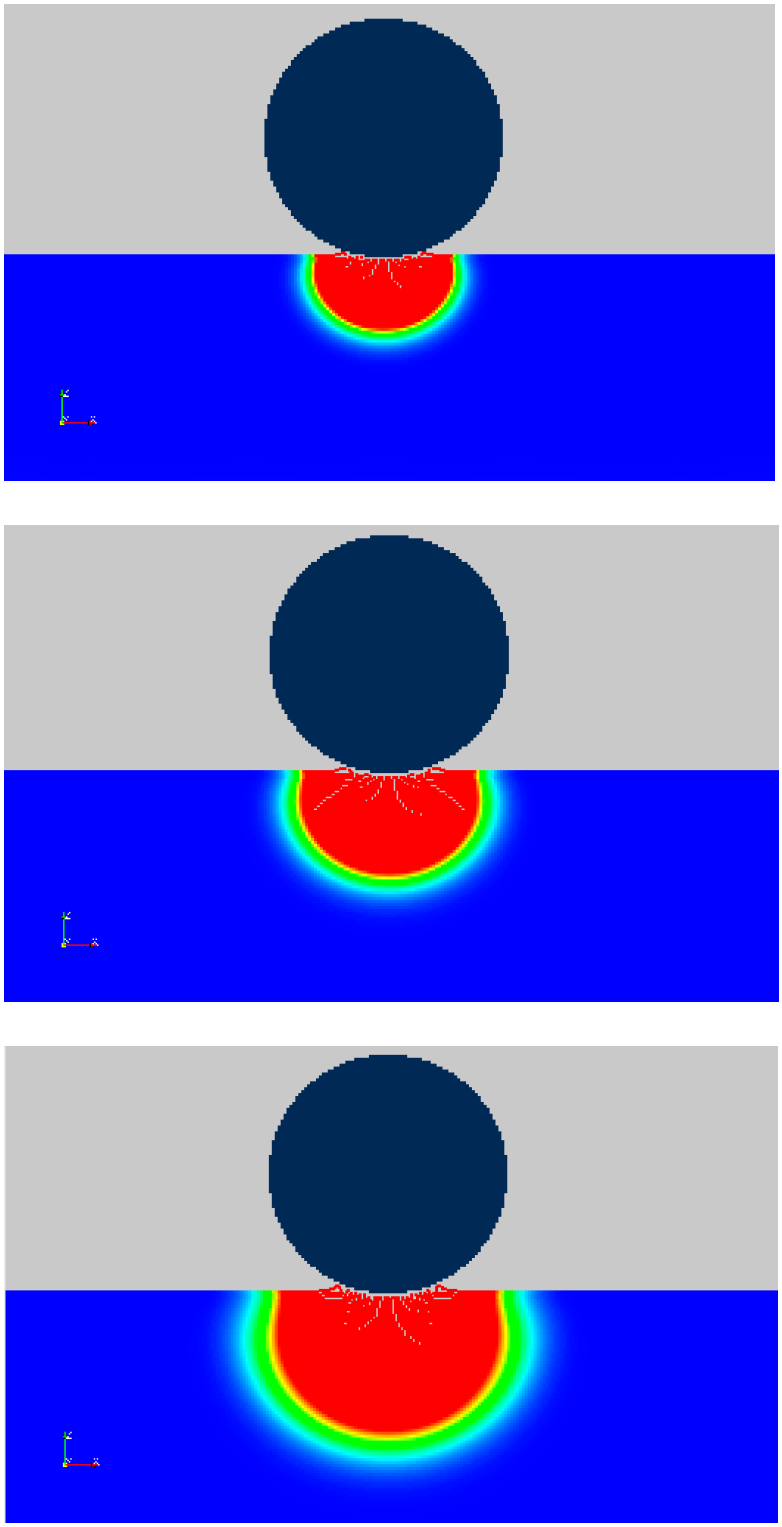

Figure 4-3 area of involved particles of three domains

Figure 4-3 shows the areas of involved particles in three domains at the same time $t = 0.02008\ s$, the three figures are arranged in the order from NO. D1 to No. D3 under the same scale. Two points can be obtained here, the first one is that the slamming moment in DualSPHysics happens earlier than theoretical calculation, which is caused by the particle distance setting in the program, as the interaction of the particles occurs before they touch each other. The second point is that the quantity of involved particles in slamming moment can be affected by the domain sizes, i.e. in larger domain more particles are influenced, so the vertical force loading on the cylinder is larger than the other two domains. This could be caused by the error of numerical method in DualSPHysics, because theoretically the domain size should not have effects on the structure in the slamming moment. Another opinion is that it is possibly caused by varied compressibility of different domain sizes in DualSPHysics. Anyway, there is no clear explanation for this problem, leading to lack of accuracy of the simulating results.

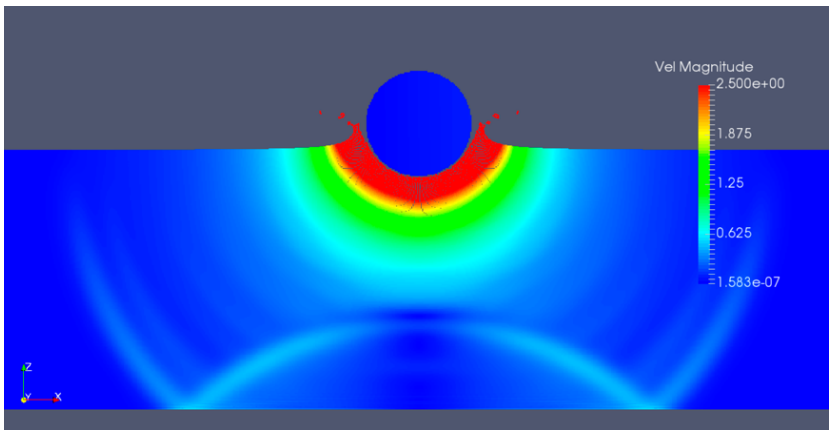

Figure 4-4 reflection waves at time t=0.0296 s

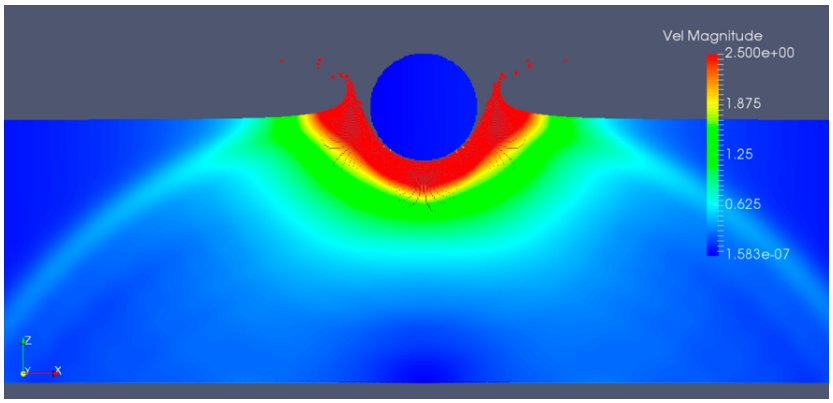

Figure 4-5 reflection waves at time t=0.0348 s

Figure 4-4 and 4-5 show the reflection wave motions in the simulation, the peak value of first hump in test NO. D1 occurs at the moment $t = 0.0348\ s$, and in the animation it is the moment when the reflection wave reaches the free surface. The propagation of energy waves is affected by the sound speed which will be discussed later.

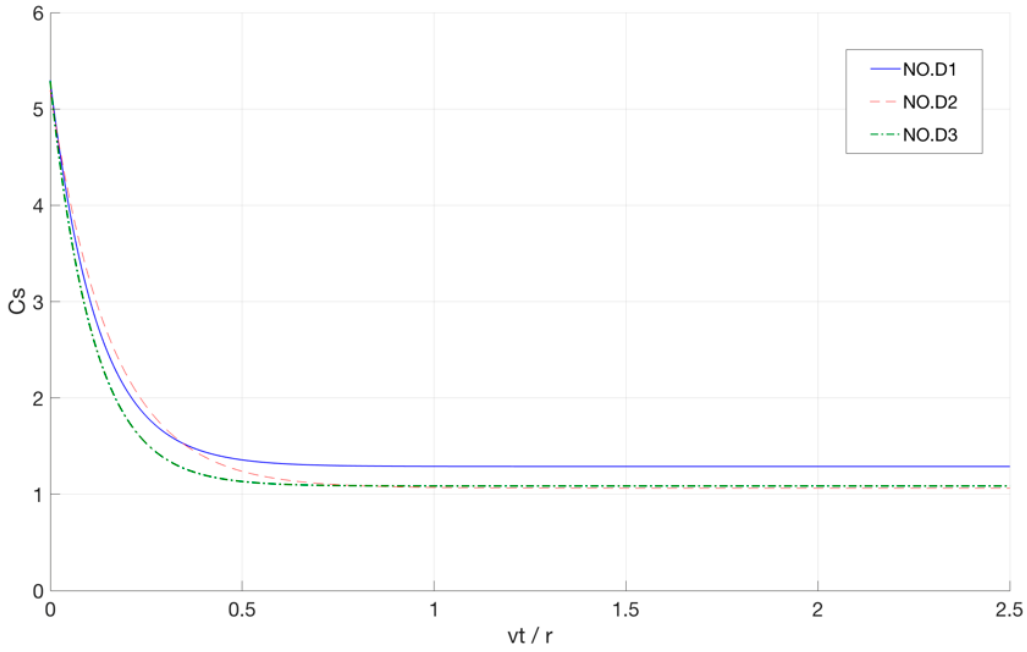

(a)

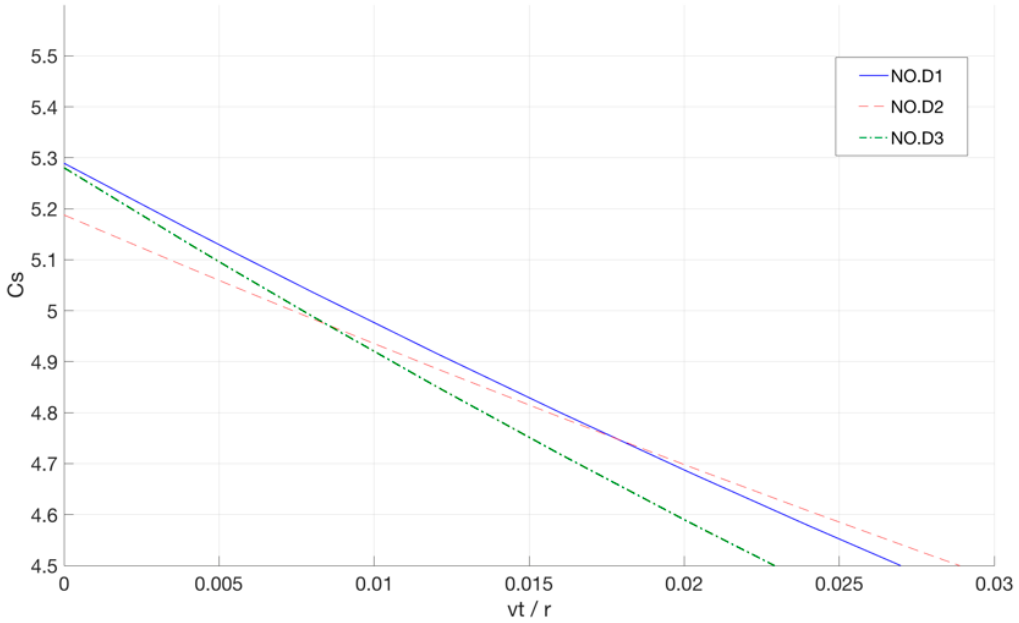

(b)

Figure 4-6 (a) overview and (b) details of smoothed curves of slamming coefficient for the three domain sizes

The smoothed slamming coefficient C_S plots are shown in figure 4-6, with omitting the extreme values and fluctuation of the computation results, the obtained peak values of all the three smoothed curves are in a small range, from 5.1 to 5.3. However, small domain is easy to be affected by the reflection of waves, so the average value of NO. D1 after 0.5 is higher than the other two domains. All the three smoothed curves are under the same fitting method, meaning that the accuracy of the maximum slamming coefficient values are almost in the same level for the three domain sizes. Therefore, NO. D2 domain is considered as the appropriate selection.

4.2 Time step test

The time step setting is related to the accuracy of the results of simulation, since large time span may lead to the missing of critical values in plotting curves. Generally speaking, all the computation results are saved in the process files, so the time step could make limited effects on the animation. However, for the plots of curves, the more time steps are applied in the computation, the better results could be expected.

In the time step test, the domain size of NO. D2 is selected as mentioned in above section. The default time step value is 1000. In order to test the effect level of the time steps on the resulting curves, four values are tested: 500, 1000, 2000, 5000 steps, the relevant time span is calculated based on the simulation time. Other parameters are consistent with the default values, as show in table 4-2.

NO.	Time span (seconds)	Simulation time (seconds)	Time steps	Storage spacing (GB)	Computation time (minutes)
TS1	1.6E-4	0.08	500	21.9	46
TS2	8.0E-5	0.08	1000	43.8	42
TS3	4.0E-5	0.08	2000	87.4	71
TS4	1.6E-5	0.08	5000	218	153

Table 4-2 details of time span and parameters

The vertical force curves are shown in figure 4-7, and there is almost no difference in the shape of the curves, hence it is quite difficult to distinguish these four curves, except for the peak values of NO. TS3 and NO. TS4, which seem a little higher than the other two. A large scale

plot of curves is shown in figure 4-8, here the details can be obtained that the NO. TS1 is not accurate enough for all the peak values, and the other three have the same level of accuracy. Therefore, 1000 time steps are considered to be a better optimized scenario for the simulations.

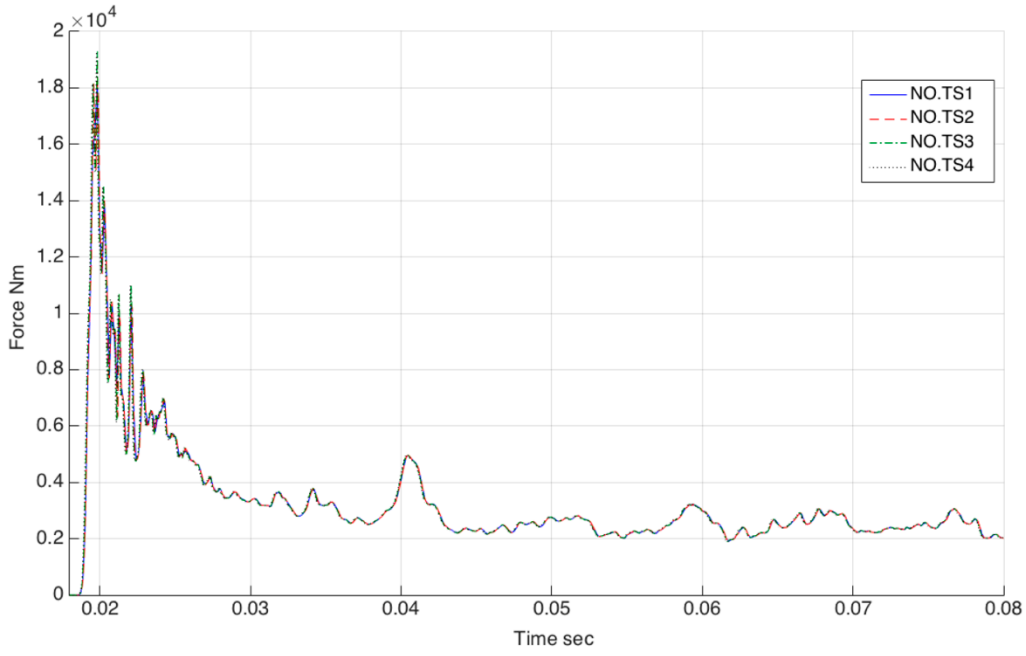

Figure 4-7 vertical forces curves of four time spans

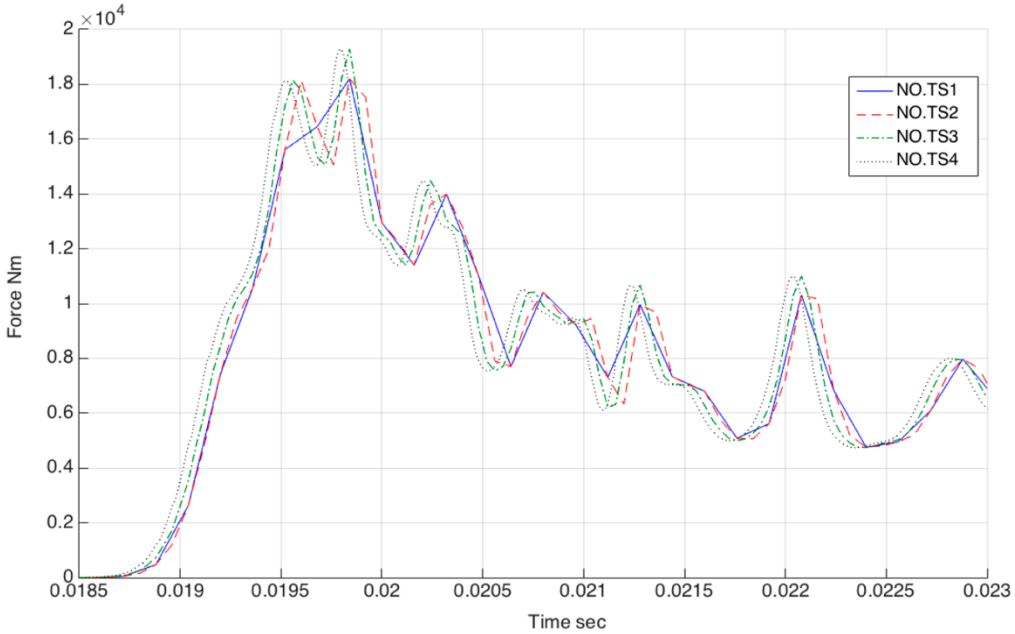

Figure 4-8 details of vertical forces

4.3 Particle distance test

As the main feature of the SPH method, particle distance is considered as an important parameter in the simulation. Single particle acts like a solid body which complies with the Newton's second law, and a great amount of particles can behave as the fluid flow does. Therefore, the number of particles should reach required order of magnitude in order to guarantee the accuracy, which means that the particle distance should be small enough in comparison to the dimensions of the domain and the cylinder. Besides, a large amount of particles affects the computing time directly, including the time cost in the neighbor particles searching, the properties of involved particles, etc. In this section, three different particle distances are tested.

NO.	Particle distance (m)	Particle numbers	Storage spacing (GB)	Computing time (minutes)
PD1	0.0025	166498	11.0	10
PD2	0.0015	460435	30.7	77
PD3	0.0008	1616175	108.0	559

Table 4-3 details of particle distance and parameters

Table 4-3 shows the details of the parameters for different particle distance settings. In order to reduce the computing time consumption, the domain size applied in this test is NO. D1, the smallest one. As the same tendency as above simulations, though the small domain is selected, the computing time increases significantly. For NO. PD3, the computing time reaches 559 minutes, in other words, nearly 10 hours, which is quite a long time for simulating one case. Simultaneously, the storage spacing is also increasing, but still in an acceptable range.

The curves of figure 4-9 and 4-10 show that the slamming coefficient could be influenced by the particle distance. Generally speaking, the more particles involved in the simulation, the more accurate result can be expected. In case NO. PD3, the slamming coefficient is about 5.0, which locates in the acceptable range, actually even the highest value that occurred in NO. PD1 is 5.3, with a little difference from the other two values, and also in the theoretical range between $C_S = \pi$ (von Karman, 1929) and $C_S = 2\pi$ (Wagner, 1932). The hump that exists at about $\frac{vt}{r} = 0.7$ is also caused by the reflection of the waves from the boundaries.

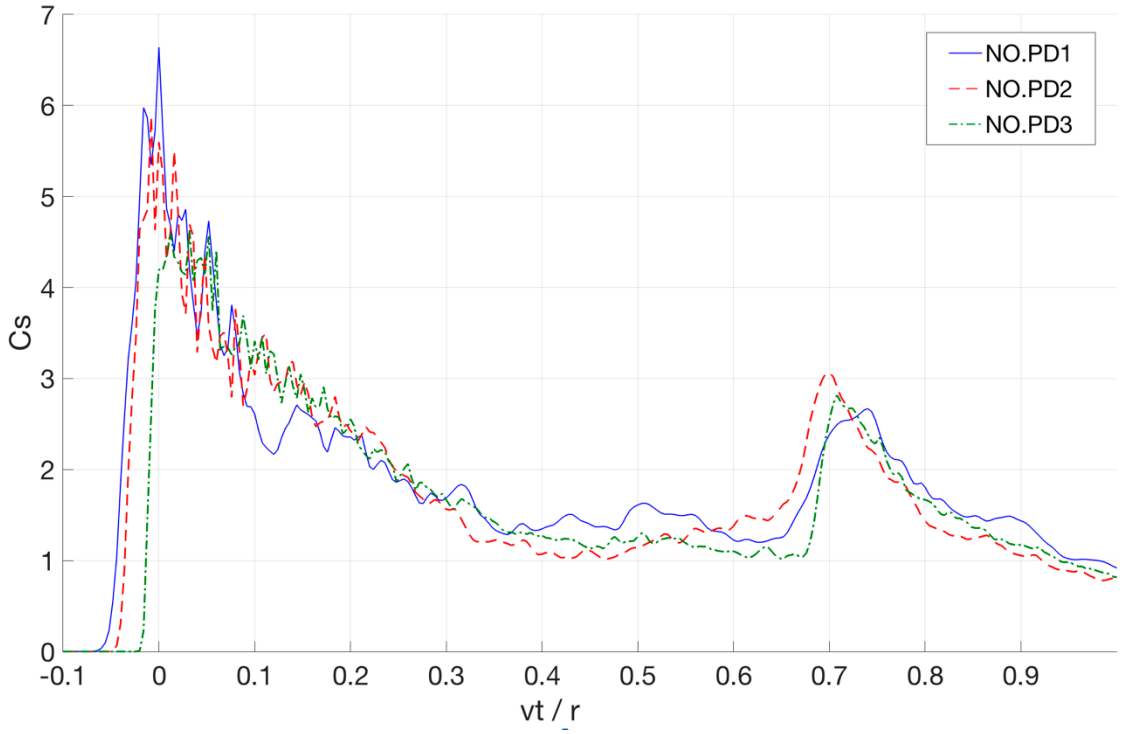

Figure 4-9 original slamming coefficient curves of three particle distances

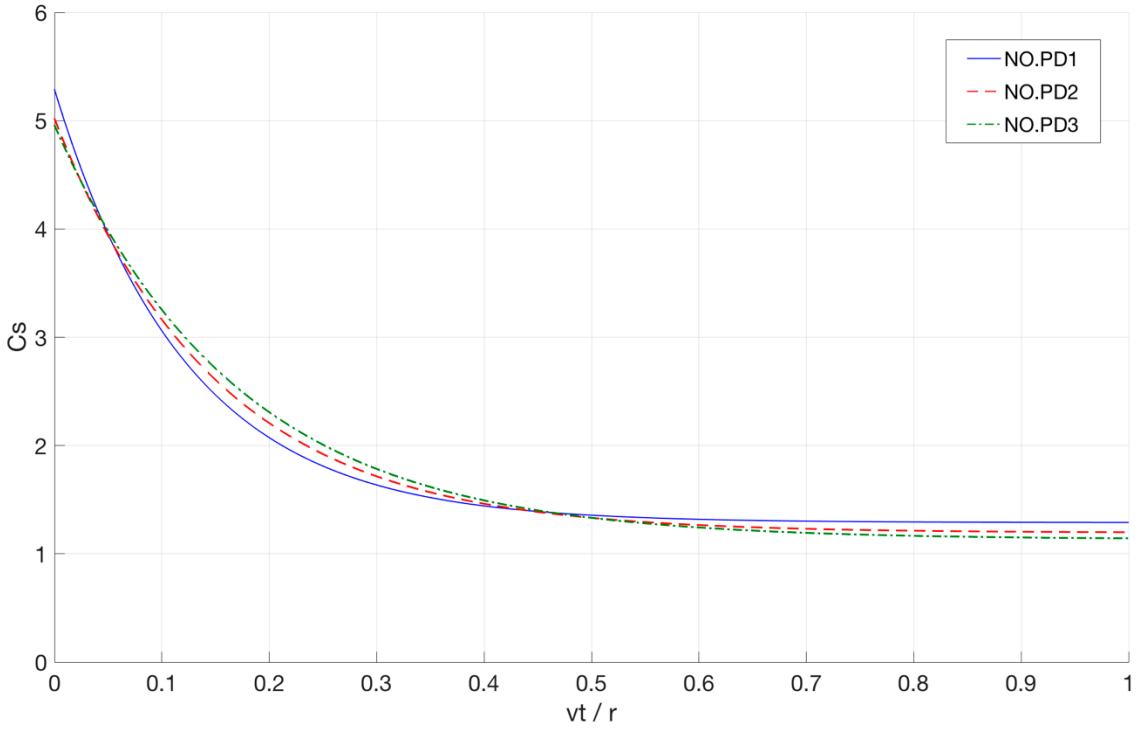

Figure 4-10 smoothed slamming coefficient curves of three particle distances

In the original curves, the difference of the peak values of the slamming coefficient can be obtained substantially, and it is noted that the slamming moments are related to the particle distances, i.e. larger particle distance makes the slamming occur much earlier than the theoretical value. In the smoothed curves the difference of peak values is weaken because the extreme values are omitted. From the viewpoint of the fitting method function, it is acceptable to eliminate the influence of the extremely large values. Especially in the numerical simulation, the noises of the resulting values make the curve relatively unstable. Furthermore, considering that the humps of the curves are mainly caused by the reflection waves, it is also reasonable to remove the fluctuations in smoothed curves.

In this section, the extreme particle distance setting is not included, which costs more that 24 hours to simulate one case, and unexpected negative influence is obtained in that simulation. Some particles that are not directly involved in slamming vibrates severely. Therefore, there is no necessity to apply the extreme parameters. In conclusion, small particle distance is preferred for the numerical simulation, in the case of selecting the reasonable value range.

4.4 Influence of smoothing length

Similar to the particle distance, the smoothing length is also a typical parameter in SPH method. In DualSPHysics, the value of smoothing length is defined by the coefficient that is defined as $coef = \frac{l}{\sqrt{2}z}$ in 2D, or $\frac{l}{\sqrt{3}z}$ in 3D, where z is the particle distance and l is the applied smoothing length, and the applied value is fixed during the computation. Particle distance parameter decides the total quantity of particles in simulation, while smoothing length parameter determines the neighbor particles that are influenced by the central particle in computation. In other words, larger smoothing length could make the fluid become more viscous, and more computing time assumption can also be predicted, because more particles interact with each other at the same time.

In this thesis, the default smoothing length coefficient is 1.2, meaning that $l \approx 1.7z$, and 9 particles are involved in the interaction area. In this section, another coefficient 0.848528 is applied to test the effects of the parameter, and according to this value, it can be calculated that $l \approx 1.2z$, hence only 5 particles are involved at the same moment.

The comparison curves are shown in figure 4-11, the fluctuation level of the dash curve with the smaller smoothing length setting is much higher than the solid curve, which proves that the relevant fluid is less viscous and easy to be influenced in the slamming process. Besides, more extreme values can be obtained in the dash curve, because the constrains of the particles become

weak under the condition that less particles involved in the interaction. In this comparison plot, the result of dash curve is unacceptable due to the fluctuation level and extreme values. In contrary, the result of the default setting $coef = 1.2$ is satisfied. Nevertheless, much larger smoothing length will not lead to better result, because it could make the fluid become too viscous and the influences could be quite negative.

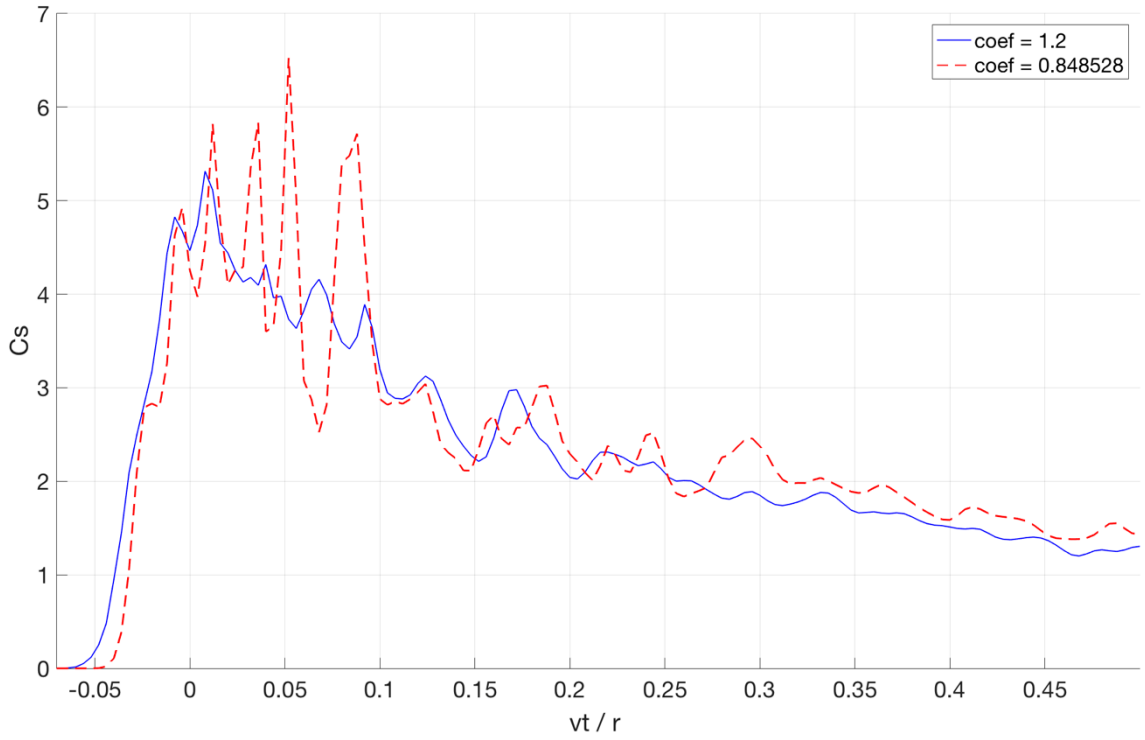

Figure 4-11 curves of slamming coefficient for different smoothing length

4.5 Influence of sound speed

In the real world, the sound speed in water is about 1482 m/s, this number is related to the computing time of DualSPHysics. However, in the program it cannot apply the real sound speed directly, since it means too much computer power consumption. Therefore, the sound speed is calculated by the sound coefficient for simplification, called Coefsound in DualSPHysics, which multiplies the maximum particle velocity resulting the applied sound speed, and this value is quite small compared with that in the real world. The default value in this thesis is 20, in this section, the comparison of another coefficient value 30 is made to analyze the influence of this parameter, both of these two are the common values utilized in DualSPHysics.

The most obvious difference of the curves is the occurrence moment of the humps, because the reflection waves moves at the sound speed, meaning that higher Coefsound value could cause

the humps to exist earlier and more frequently, which could be obtained in figure 4-12 that the fluctuation of the solid curve is much severer than the dash curve, and the first hump also occurs earlier due to larger sound speed. In terms of the peak value of the slamming coefficient, larger value can be found in the curve of higher Coefsound, because higher sound speed means that the energy wave moves faster in water, more particles will be involved in the slamming effect. Therefore, the comparison proves that Coefsound = 20 is more suitable for the water impact simulation.

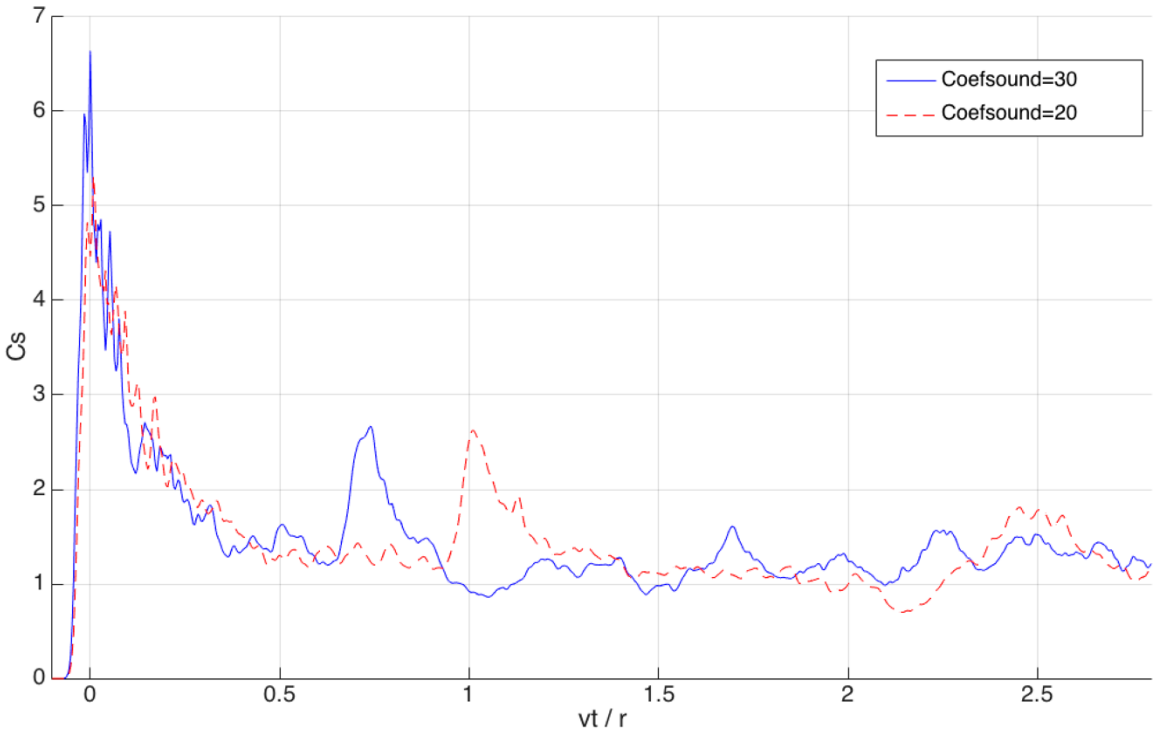

Figure 4-12 curves of slamming coefficient for different Coefsound

5 Results

5.1 Water impact of 2D horizontal cylinder

In this part, the water entry of the two-dimensional horizontal cylinder with forced constant velocity is simulated in DualSPHysics, and the main variable is the non-dimensional Froude number ranging from 1.428 to 7.139. The results are compared with previous theoretical analyses, experiments and other numerical simulations. The parameter setting is according to the sensitivity analysis in last chapter. After the simulation, an extra test with various slamming velocities will be presented.

5.1.1 Parameters setting

The initial position of the center of the cylinder is 0.2 m above the free surface, i.e. the gap between the bottom of the cylinder and the free surface was 0.1 m according to the applied radius of the cylinder. Therefore, the slamming will not happen until the bottom of the cylinder touches the water surface theoretically. The radius of the cylinder is 0.1 m as the default radius in the simulation, and the Froude number is set in a larger ranging than that defined by Campbell and Weynberg (1980). Besides, other main parameters apply the default variables mentioned in last chapter, and the detailed parameters are shown in table 5-1.

NO.	Velocity (m/s)	Froude number	Simulation time (s)	Particle distance (m)
1	2.0	1.428	0.2	0.002
2	4.0	2.856	0.1	0.002
3	5.0	3.570	0.08	0.002
4	6.0	4.284	0.067	0.002
5	8.0	5.711	0.05	0.002
6	10.0	7.139	0.04	0.002

Table 5-1 parameters of cylinder simulations

According to the parameters setting, the amount of particles is more than one million, which can fulfill the requirement of accuracy. Through the observation of the animation of slamming process, the reflection waves propagate with the shape of a semi-circle, so the waves are reflected at different moments due to the rectangular shape of the domain, making the particles vibrate irregularly. A semi-circular domain was designed by Ghadimi et al. (2012), which could reduce the effects of reflection waves.

5.1.2 Results and discussion

All the six resulting curves are plotted in figure 5-1, the fluctuation levels of them are obviously different. As discussed in previous chapter, the fluctuation is mainly caused by the reflected energy waves, which is also proved by the curves. Due to the varied penetrating velocity of the cylinders, the simulation times are different as shown in table 5-1, meaning that for NO.1 simulation, the reflection waves move around more times than other simulations during the process. As a result, the NO.1 curve seems unstable and inaccurate. In terms of the peak values shown in figure 5-2, the result of NO.1 simulation is unacceptable in the original curve, since the extreme peak value reaches more than 10.0. This could be caused by the noises of numerical simulation, for similar extreme results were also found by Larsen (2013) with CFD method, so the extreme values are omitted in smoothed curves.

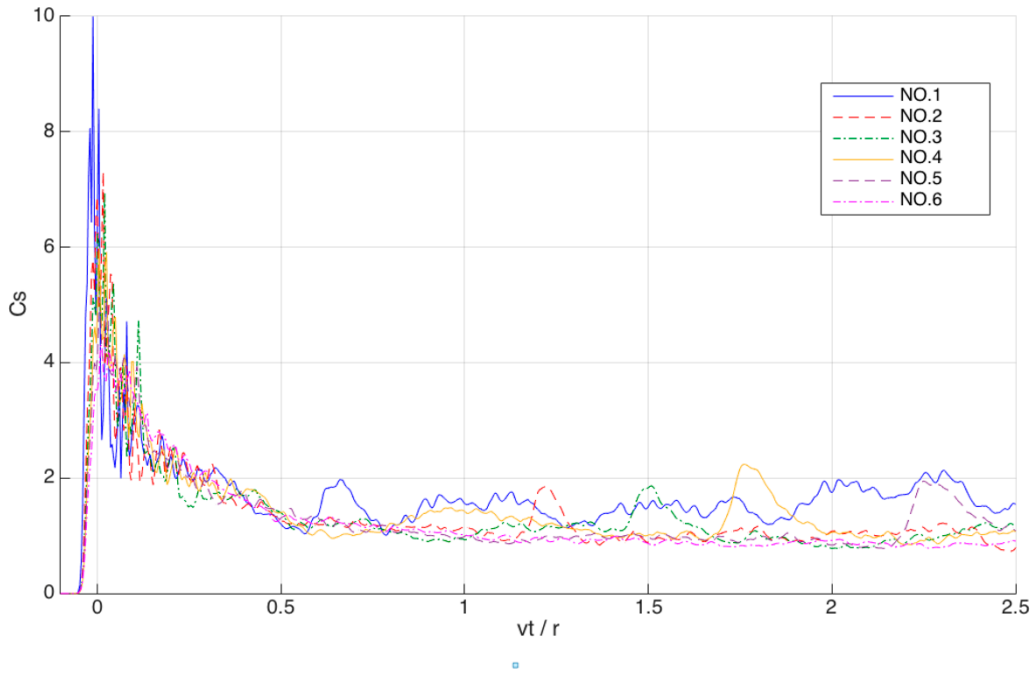

Figure 5-1 original curves of slamming coefficient for all simulations

Figure 5-2 peak slamming coefficient values for all simulations

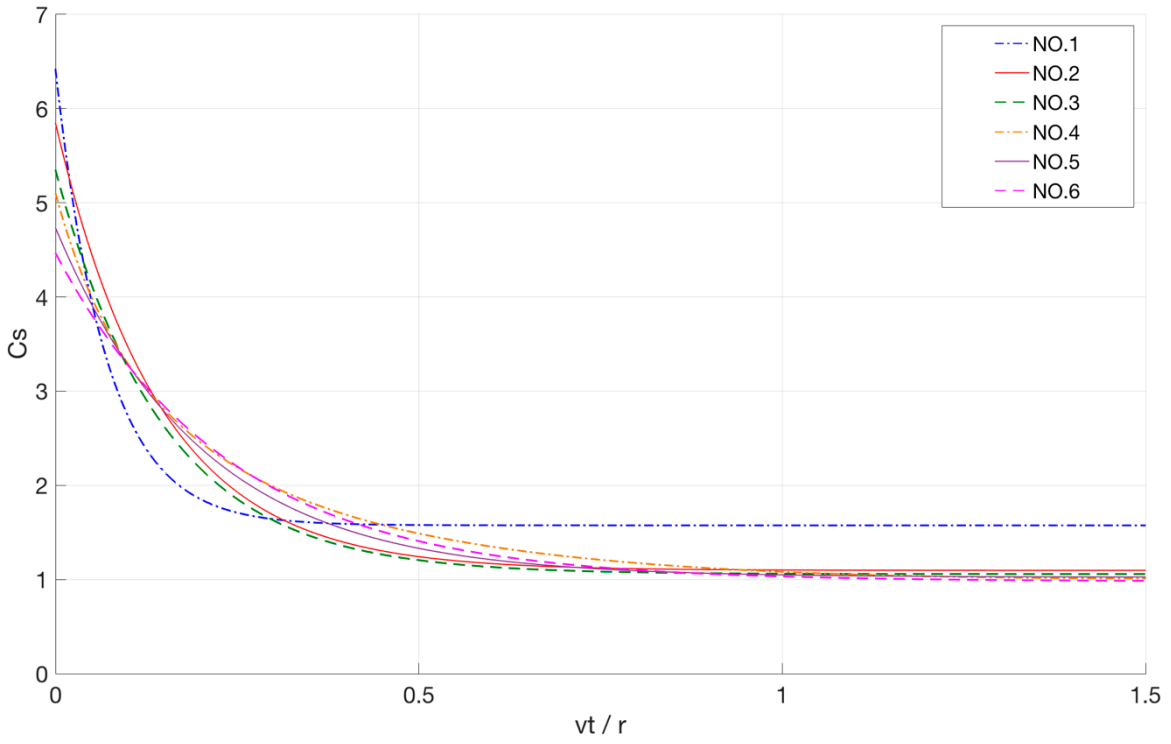

Figure 5-3 smoothed curves of slamming coefficient for all simulations

In the smoothed curve, the optimized slamming coefficient of NO.1 is 6.38, which is beyond the other values, and out of the theoretical value range, see figure 5-3. However, the average values of NO.1 after the peak are much higher than other results, this could be caused by the buoyancy effects during the simulation. When the Froude number is relatively low, the buoyancy cannot be omitted in this procedure, and according to Campbell and Weynberg (1980), the buoyancy contribution to the slamming coefficient could be from 0.05 to 0.54.

In Figure 5-3, the slamming coefficient at the beginning moment varies substantially. Most of the values are in an acceptable range, and the peak value drops down with the increase of the penetrating velocity (Froude number), as shown in table 5-2. An interesting thing that can be found in the table is that the decreasing rate of slamming coefficients reduces gradually, hence there is a limit for the minimum value, which could be $C_S = \pi$ as mentioned by von Karman (1929). The conclusion is in contradiction with the Campbell and Weynberg's theory, which is that the slamming coefficient is independent of Froude numbers, the results of the simulations present changeable slamming coefficients according to various Froude numbers. Considering that the empirical formula (2.4) has been widely accepted and applied in practice, e.g. in DNV (2014), the possibility of errors in DualSPHysics cannot be excluded, as discussed in previous chapter, different parameters setting can make results fluctuate in some extent.

NO.	1	2	3	4	5	6
Froude number	1.428	2.856	3.570	4.284	5.711	7.139
Slamming coefficient	6.38	5.85	5.35	5.07	4.73	4.47

Table 5-2 slamming coefficient related to Froude number

All the smoothed curves of the six simulations are compared with the results of previous theoretical analyses, experiments and numerical simulations, see figure 5-4. As the calculation parameters are the same as Larsen (2013) with CFD method, the curves are also plotted based on the comparison figure of his thesis. Most of the resulting curves are in the similar range of the previous works, and they actually agree with Larsen's curves best as shown in the figures, both of which are made by numerical simulations, SPH and CFD methods. Furthermore, under the condition of applying high Froude numbers, the peak values of SPH method are under the other curves. As mentioned above, the slamming coefficient seems to change with the Froude

numbers, which is not consistent with the empirical theory, hence further study is needed to obtain more supports for the conclusion.

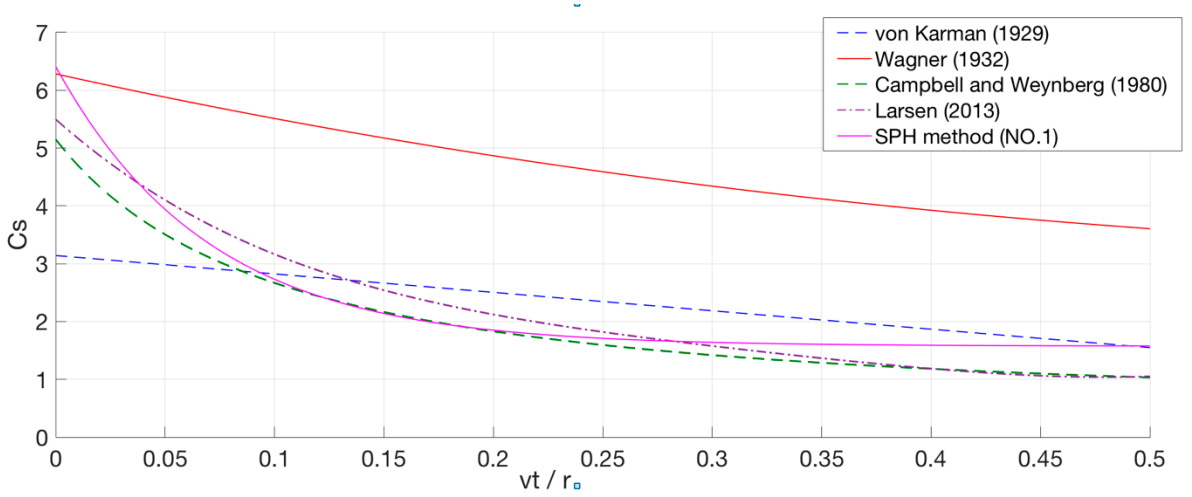

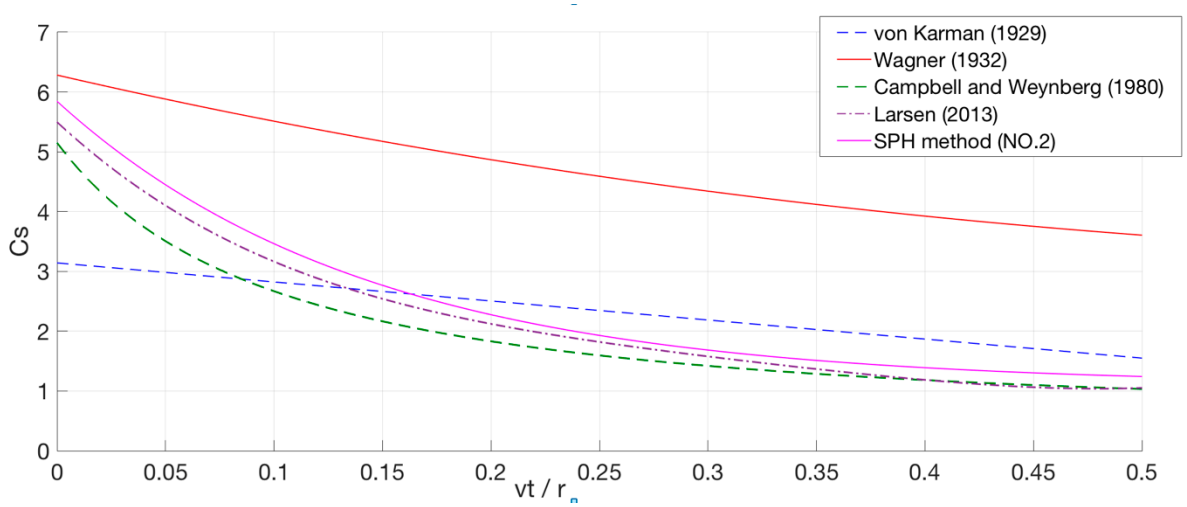

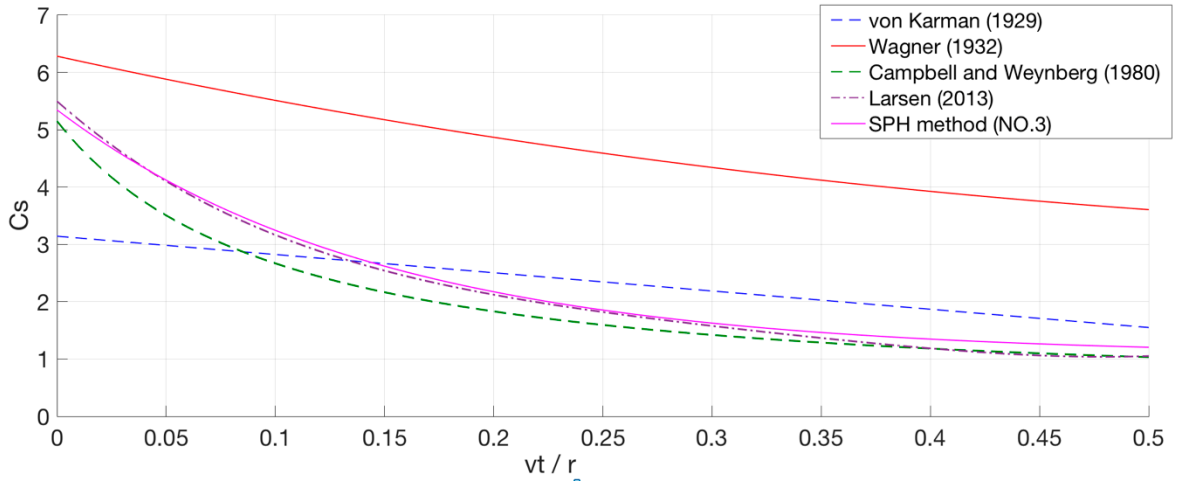

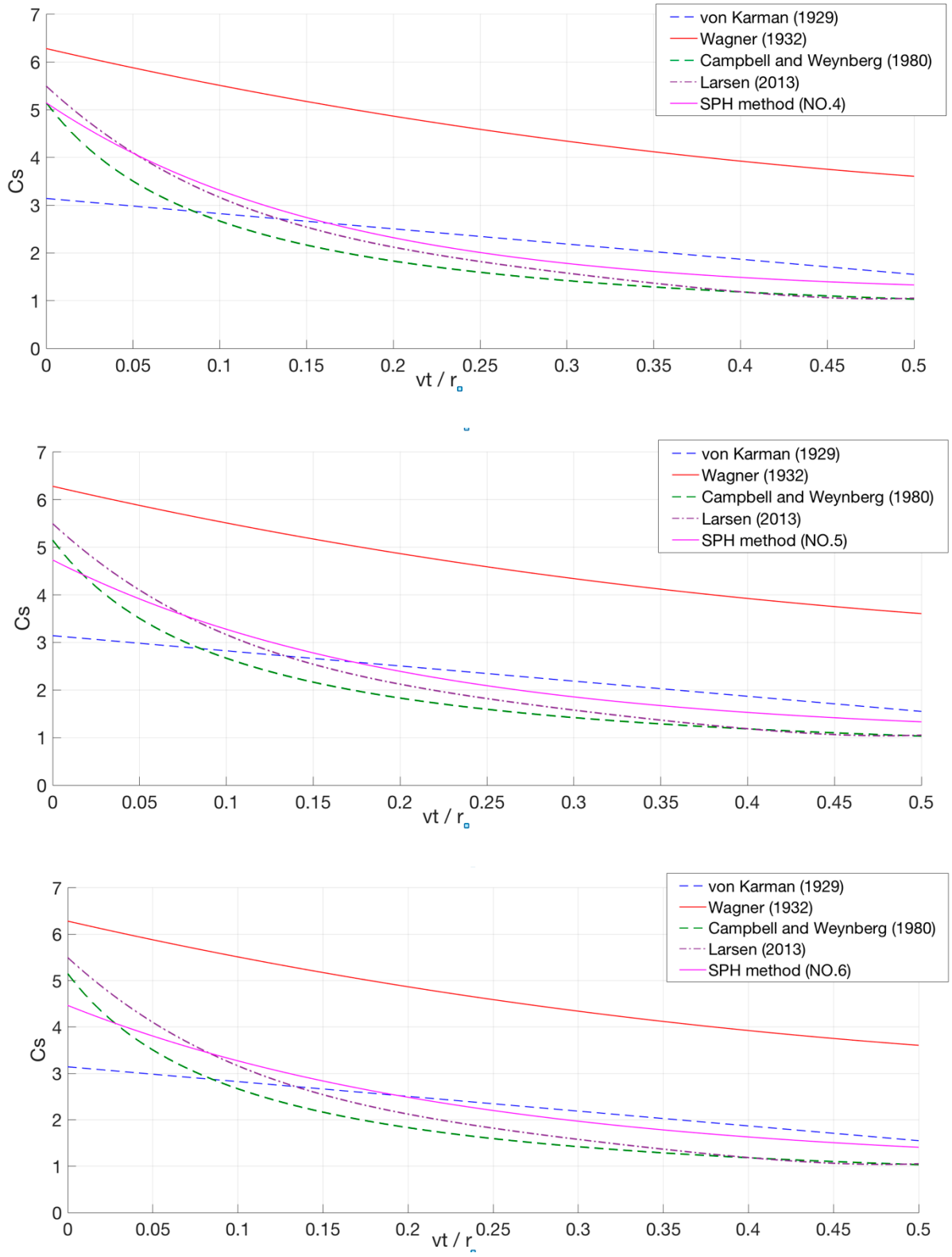

Figure 5-4 comparison of slamming coefficient with previous curve

5.1.3 Curve fitting method

As there is severe fluctuation in the original curves of the SPH method, the curve fitting method is necessary to create clear resulting curves. According to the previous theoretical analysis, two optional reference equations are applied here, the equation (2.4) by Campbell and Weynberg (1980) and equation (5.1) by Miao (1989),

$$C_S = 6.1e^{-\frac{6.2vt}{r}} + 0.4 \tag{5.1}$$

and take NO.3 for an instance, both the two fitting results are shown in figure 5-5.

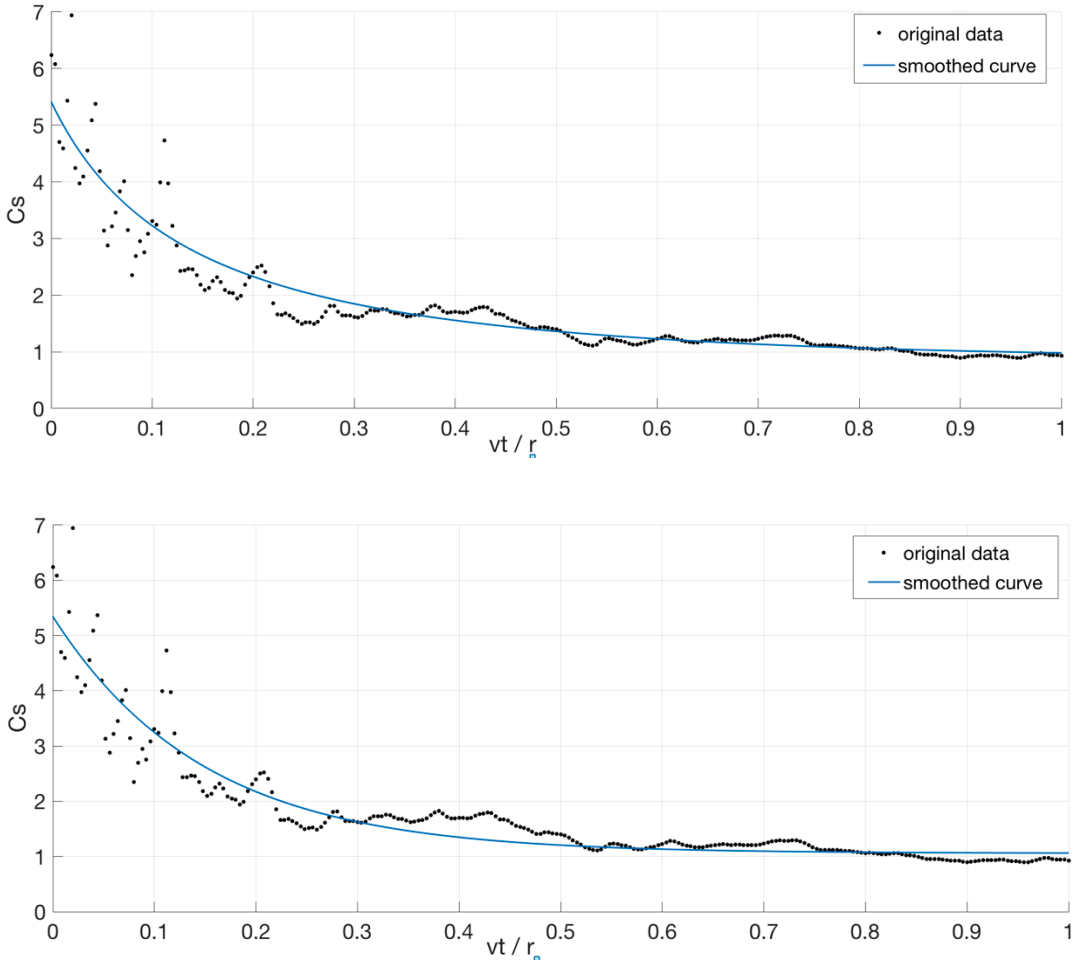

(a)

(b)

Figure 5-5 curve fitting methods (a) according to Campbell and Weynberg (1980); (b) according to Miao (1989)

There is no obvious difference between the two fitting methods, except that the values in figure 5-5 (b) are slightly smaller. Another difference not shown in the figures is that the smoothed curve will rise up with the increase of $\frac{vt}{r}$ values for the fitting method in figure 5-5 (a), which

is caused by the form of equation (2.4) and the influence of humps of the original curves. In this simulation, the fitting method in figure 5-5 (b) is applied for all the results.

5.1.4 Influence of slamming velocity

The numerical simulations of this section are made by varied non-dimensional Froude number as the main variable. According to Campbell and Weynberg (1980), the slamming coefficient is independent on the Froude numbers, and most of the other researches were also designed on the basis of different Froude numbers. Nevertheless, the study about the influence caused by varied penetrating velocities with the same Froude numbers is rare. As a result, in this section, three different penetrating velocities of the cylinder are tested and discussed. The other parameters, e.g. the domain size, particle distance, and the radius of the cylinder are under the same scale, as shown in table 5-3.

NO.	Velocity (m/s)	Radius (m)	Particle distance (m)	Domain size (m × m)	Scale of dimensions	Froude number
V1	5.0	0.025	0.000625	1.0 × 0.25	1	7.139
V2	10.0	0.1	0.0025	4.0 × 1.0	4	7.139
V3	20.0	0.4	0.01	16.0 × 4.0	16	7.139

Table 5-3 parameters for different velocities test

The initial position of cylinder is on the surface of the water, meaning that the slamming starts with the beginning of the simulation, which could affect the results of the simulation in some extent. However, according to the resulting curves in figure 5-6, the effects could be acceptable.

Generally, the levels of fluctuation for the three cases are similar, but the peak values are not the same. In curves of NO. V2 and NO. V3, the difference of peak values is small, large value occurs in No. V1, of which the dimensions and velocity are the smallest among the three. As the influence of domain size, particle distance and cylinder radius is eliminated, the reason could be the compressibility of the particles, or the error of DualSPHysics. For a general description, the tendency of all the three cases agrees well, meaning that in the condition of applying the same Froude number, different velocities make limited effects on the results.

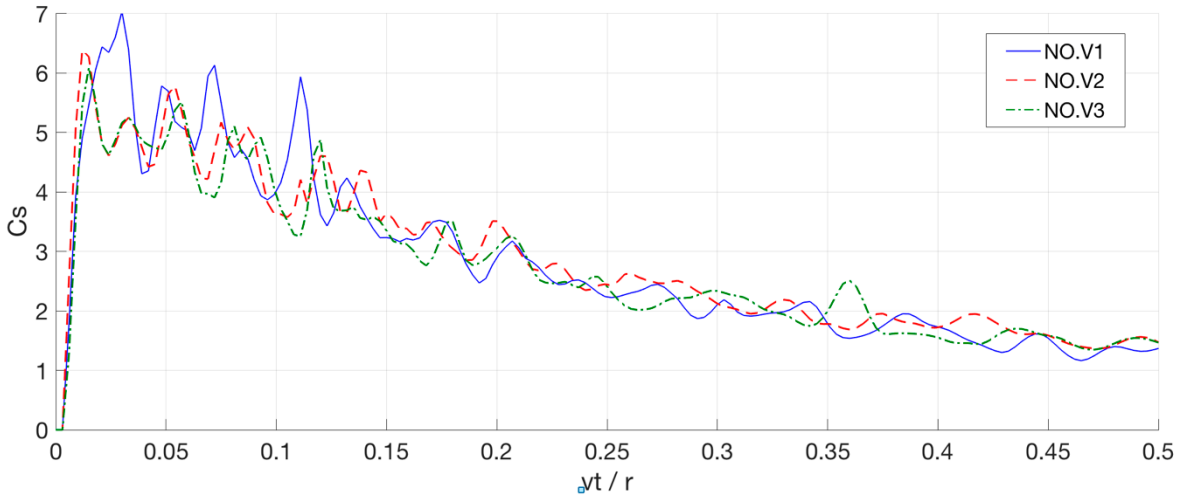

Figure 5-6 slamming coefficient curves of three different velocities

5.1.5 Summary

In this part, six different water entering simulations of the 2D horizontal cylinders are made based on varied Froude numbers, most of the results locate in the acceptable range predicted by previous theoretical researches and experiments. In the pro-processing, extreme values are omitted by the fitting methods. Furthermore, the simulating results with low Froude numbers are affected by the buoyancy, which are distinguished from the other results. In conclusion, the slamming coefficient can be possibly influenced by the Froude number in a limited extent, it is difficult to exclude all the errors of inaccuracy in DualSPHysics, so it needs more analyses and simulations in various cases to discuss this conclusion.

5.2 Free falling of 2D cylinder into calm water

In this part, the free falling of the half buoyant and neutrally buoyant cylinders are simulated. Half buoyant (HB) means that the density of the cylinder is a half of the water density, and neutrally buoyant (NB) represents that the density of cylinder equals the water density. Greenhow and Lin (1983) carried out the relevant experiments, and the pictures they took were good comparable objects cited in various papers. Larsen (2013) made the numerical simulation with CFD and obtained similar results to Greenhow and Lin. Here the simulation conducted by SPH method is presented and also compared with the previous works.

5.2.1 Parameters setting

According to the parameters in Greenhow and Lin (1983), the initial position between the center of the cylinder and the free surface is 0.5 m, the radius of the cylinder is 0.055 m, and the initial velocity of the cylinder is zero, so the slamming velocity when the bottom touches the water surface is about 2.95 m/s, and the slamming moment is $t = 0.301\ s$. The total simulation time is 0.5 s. For the parameters setting in DualSPHysics, the domain size is 4.0 m × 1.0 m, and the particle distance is 0.002 m, so the total particle number is about one million, which are all the same with the setting in last section.

In terms of the mass of the 2D cylinders, the results of the theoretical calculation are

$$m_{HB} = \rho_{HB} \cdot \pi r^2 = 4.75\ kg \tag{5.2}$$

$$m_{NB} = \rho_{NB} \cdot \pi r^2 = 9.50\ kg \tag{5.3}$$

However, in DualSPHysics, the cylinders are also constituted by particles, which can be imaged as a large amount of small rectangular particles. As a result, the total mass of these particles are more or less different from the theoretical value. If the quantity of the particles is large enough, the mass can be close to the theoretical value. In this simulation, the applied mass of the HB and NB cylinders are separately 5.122 kg and 10.244 kg, larger than the above numbers, this difference could have some effects on the results of simulation.

5.2.2 Results and discussion

The results are plotted in the form of penetration depth. Figure 5-7 shows the comparison of penetration depth on time variable with the experiment results by Greenhow and Lin (1983) and CFD simulating results by Larsen (2013). It can be obtained that the HB cylinder curve calculated in DualSPHysics agrees with the experiment result well, and both of the two curves

are under the result of CFD simulation. In terms of NB cylinder curves, all the three are obviously different, according to Larsen (2013), this could be due to the inaccurate experiment data by Greenhow and Lin (1983). Nevertheless, as mentioned before, the accuracy level of the DualSPHysics results depends on the particle distance setting. Although in this simulation, on the basis of the applied particle distance, the amount of the particles reaches a million, which is a relatively large number, the accuracy level could be still not good enough.

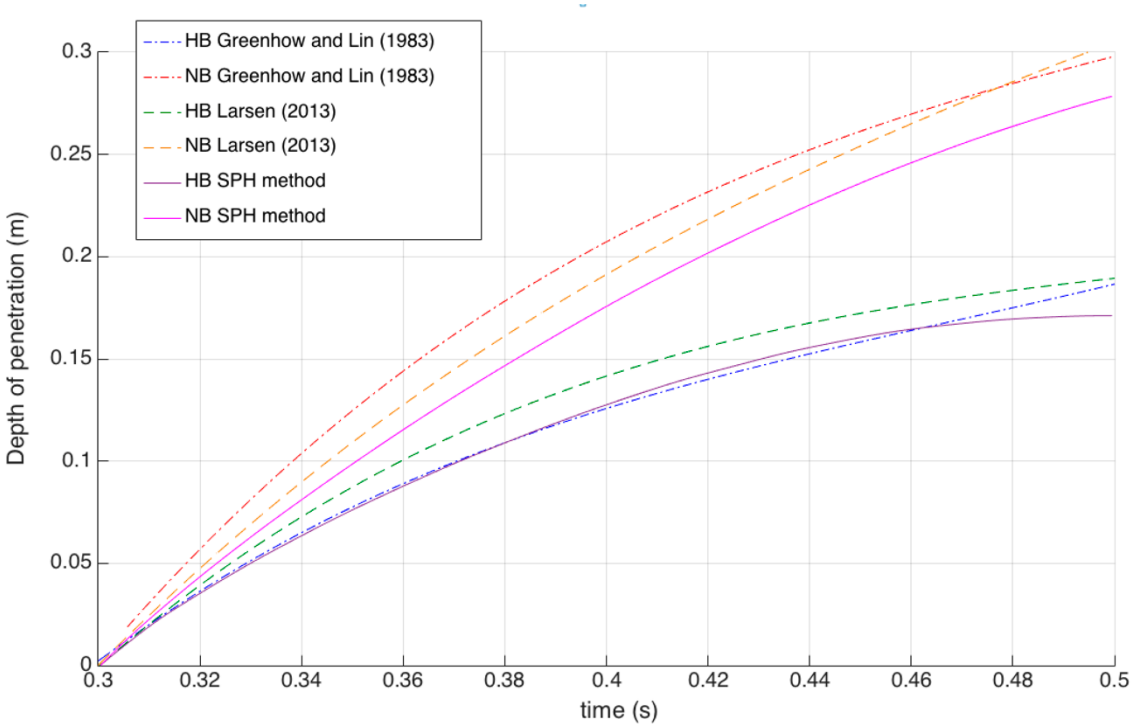

Figure 5-7 penetration depth curves compared with previous results

Besides, the penetration animations are in comparison with the pictures of the experiments by Greenhow and Lin (1983), which are widely considered as the accurate experimental records of the cylinder free falling research. For HB cylinder, the picture times are 0.305 s, 0.330 s, 0.385 s, 0.420 s, and the reference pictures are from Larsen (2013); for NB cylinder, the times are 0.315 s, 0.330 s, 0.410 s, 0.500 s, the pictures are from Faltinsen (1990). The difference between experiment data and numerical simulation data can also be obtained in the figures. See figure 5-8 and 5-9, different colors represent different particle velocities.

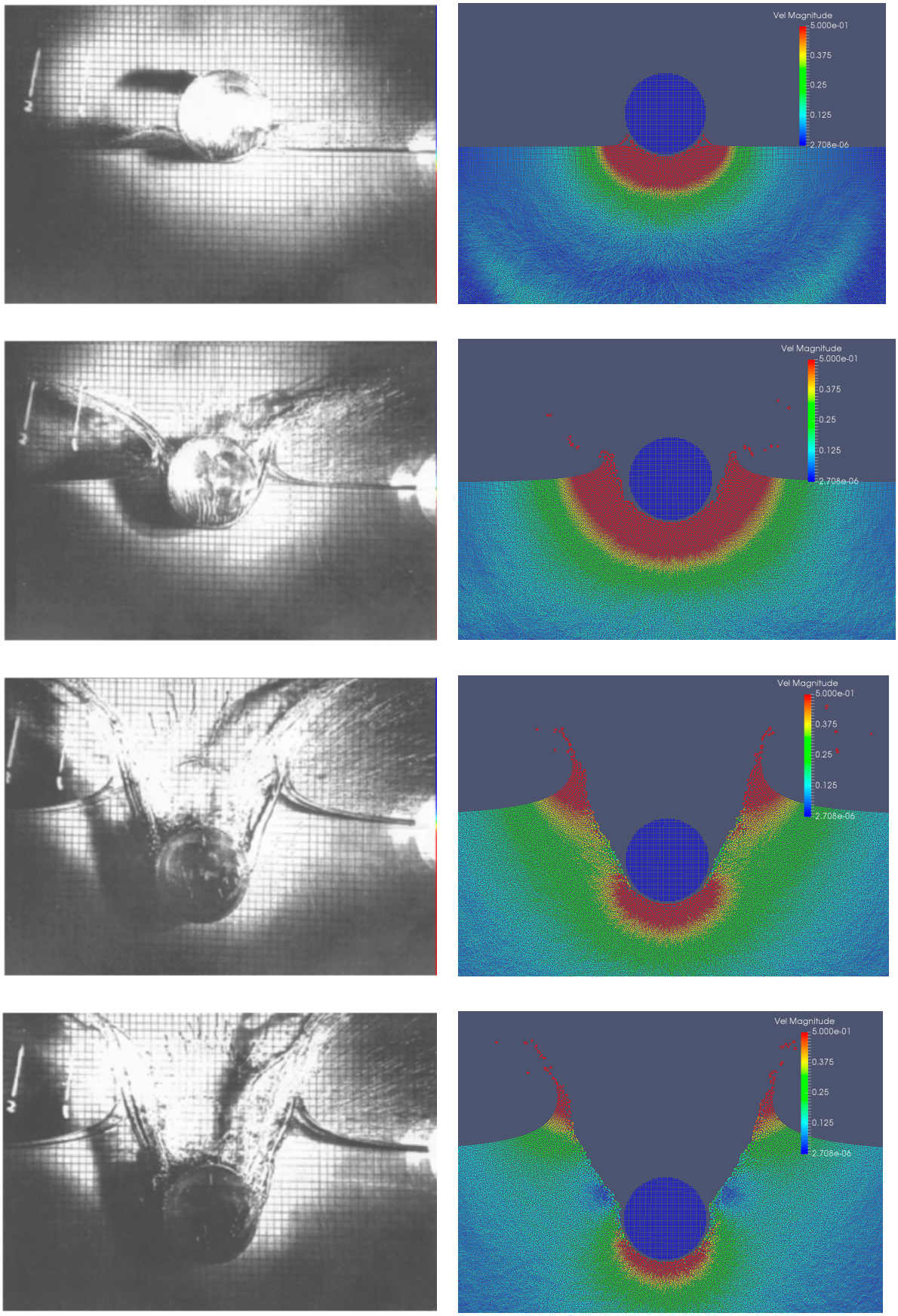

Figure 5-8 HB cylinder free falling comparison

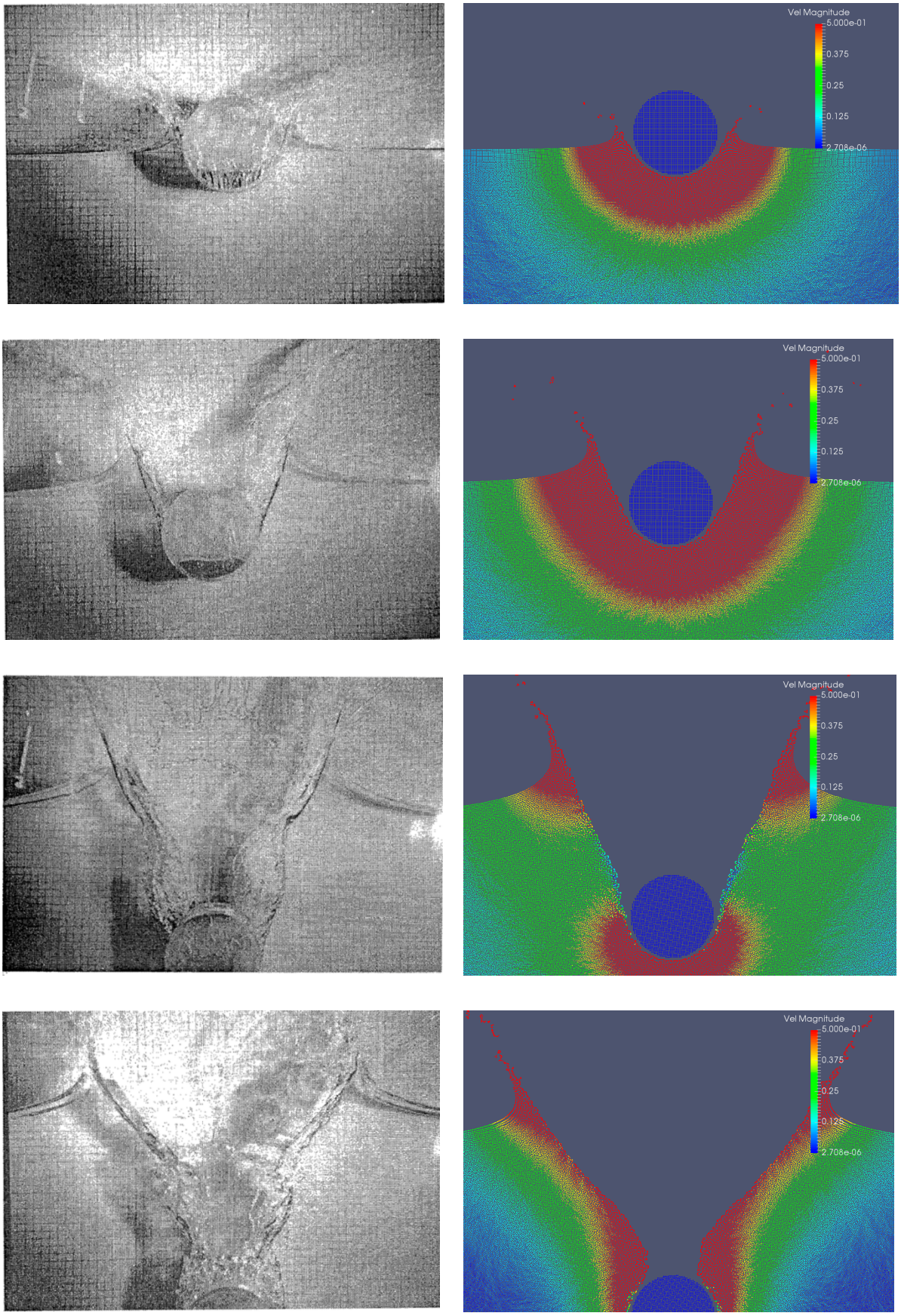

Figure 5-9 NB cylinder free falling comparison

5.2.3 Influence of particle distance

As mentioned above, the accuracy level of simulating results can be affected by the particle distance, i.e. the total quantity of the particles. In order to test the influence of the particle distance, a comparative free falling simulation of the NB cylinder is achieved with the same parameter setting except for the value of particle distance, see table 5-4. The NO. FF1 simulation is the same simulation in last section, NO. FF2 is the comparative simulation with a larger particle distance. The applied mass also changes due to the varied particle numbers which constitute the free falling cylinder.

NO.	Particle distance (m)	Particle numbers	Applied mass (kg)	Theoretical mass (kg)
FF1	0.002	1005362	10.244	9.50
FF2	0.0035	327939	10.645	9.50

Table 5-4 parameters setting of comparative simulation

The resulting curves are shown in figure 5-10, as expected, the curve of NO. FF2 is under NO. FF1, meaning that larger particle distance (also larger applied mass of the cylinder) causes lower accuracy level, which makes the penetration depth value smaller than the previous results. This could explain the curve of SPH method is under the curves of experiment and CFD method shown in figure 5-7.

5.2.4 Summary

In this part, both HB and NB cylinders are modeled and simulated in the free falling case, the parameters are selected according to the experiments by Greenhow and Lin (1983). And the results are also compared with their experiment results and numerical simulating results by Larsen (2013). For the HB cylinder, the curve of penetration depth with the time variable agrees well with the experiment curve. On the other side, the curve of NB cylinder result is under the other two curves. The difference is caused by the accuracy problem of parameter setting, which is approved by the comparative simulation with larger particle distance setting. Nevertheless, it is still difficult to improve the accuracy level in DualSPHysics, since large amount of particles requires huge power consumption of the computer.

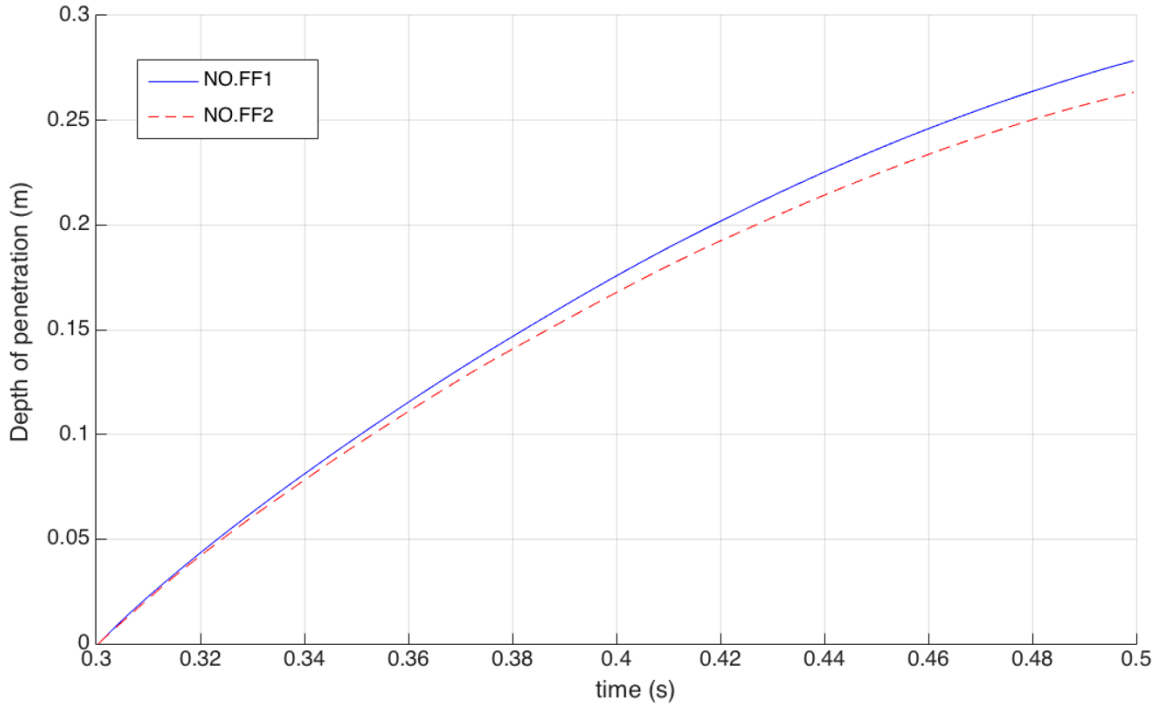

Figure 5-10 comparison of different particle distance

5.3 Vertical water entry of 2D wedge

For the study of slamming effects of vessels, especially the high speed ships, the water impact of wedges is the main studying object, which provides positive reference data to the research of structure strength in ship design. There are various aspects in the wedge slamming study, e.g. symmetric and asymmetric geometry, vertical and horizontal entry velocity, and pressures loading on various positions. In this part, the vertical forces and slamming coefficient are computed in DualSPHysics.

5.3.1 Parameters setting

In the simulation of wedge water entry, the main variable is the point angle of wedges. Due to the symmetric geometry, the height of the wedge is fixed at 0.1 m, and the main variables are defined by the deadrise angle β, which is the angle between the inclined edge and horizontal line. Consequently, the total width of the wedge B is varied according to the deadrise angles, as shown in figure 5-11. In terms of the parameter setting in DualSPHysics, most of the parameters are consistent with the settings in the cylinder simulation, e.g. total simulation time, time steps and the coefficient of sound speed. The forced constant velocity is 5 m/s, and the initial distance between the lower point and the free surface is 0.1 m.

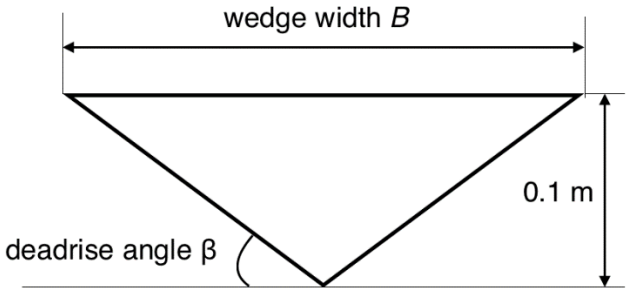

Figure 5-11 geometry of the wedge

5.3.2 Domain size test

Considering that the total width of the wedge varies in a large range, the maximum value could be more than 1.0 m according to the various deadrise angles, hence the domain size could be an important factor affected the simulating results. In this section, two different domain sizes are tested, the main relevant parameters are shown in table 5-5.

NO.	Domain size (m × m)	Particle distance (m)	Particle numbers	Deadrise angles (degree)
WD1	4.0 × 1.0	0.0035	331967	10
WD2	8.0 × 2.0	0.0035	1312661	10

Table 5-5 parameters of two domain sizes

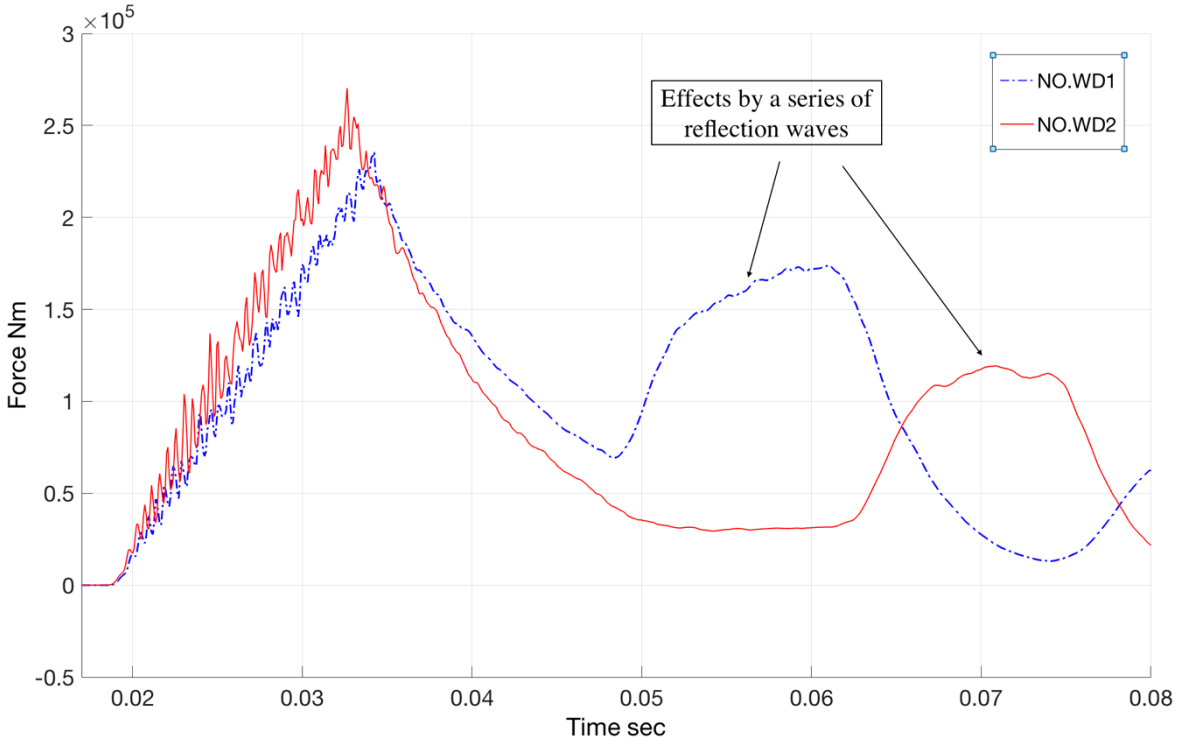

Figure 5-12 vertical force curves of two different domains

The vertical forces are plotted in figure 5-12, which are quite different from the curves of cylinders. The maximum value of NO. WD1 is larger than that of NO. WD2, which is caused by the initial effects of the domain size, as mentioned in chapter 4. High fluctuation level before the peak values can be obtained for both domains, in contrast, the curves decline smoothly after the maximum values. In terms of the marked interval in the plot, also similar to the water entry of the cylinders, the humps are caused by the reflection waves of the boundaries, so the moments when the values begin rising are different due to the domain sizes. Here it has to note that the reflection waves in the water entry of wedges are distinguished from the cylinders. The

slamming of the wedges makes a series of energy waves that are gradually increasing owing to the geometry, resulting a wide range of high values, and in small domain, the reflection waves have greater effects on the results, as shown in the plot. On the basis of this feature, relatively small domain size is not acceptable, and there is no doubt that larger domain is preferred in the wedge simulation, with which more accurate values can be obtained.

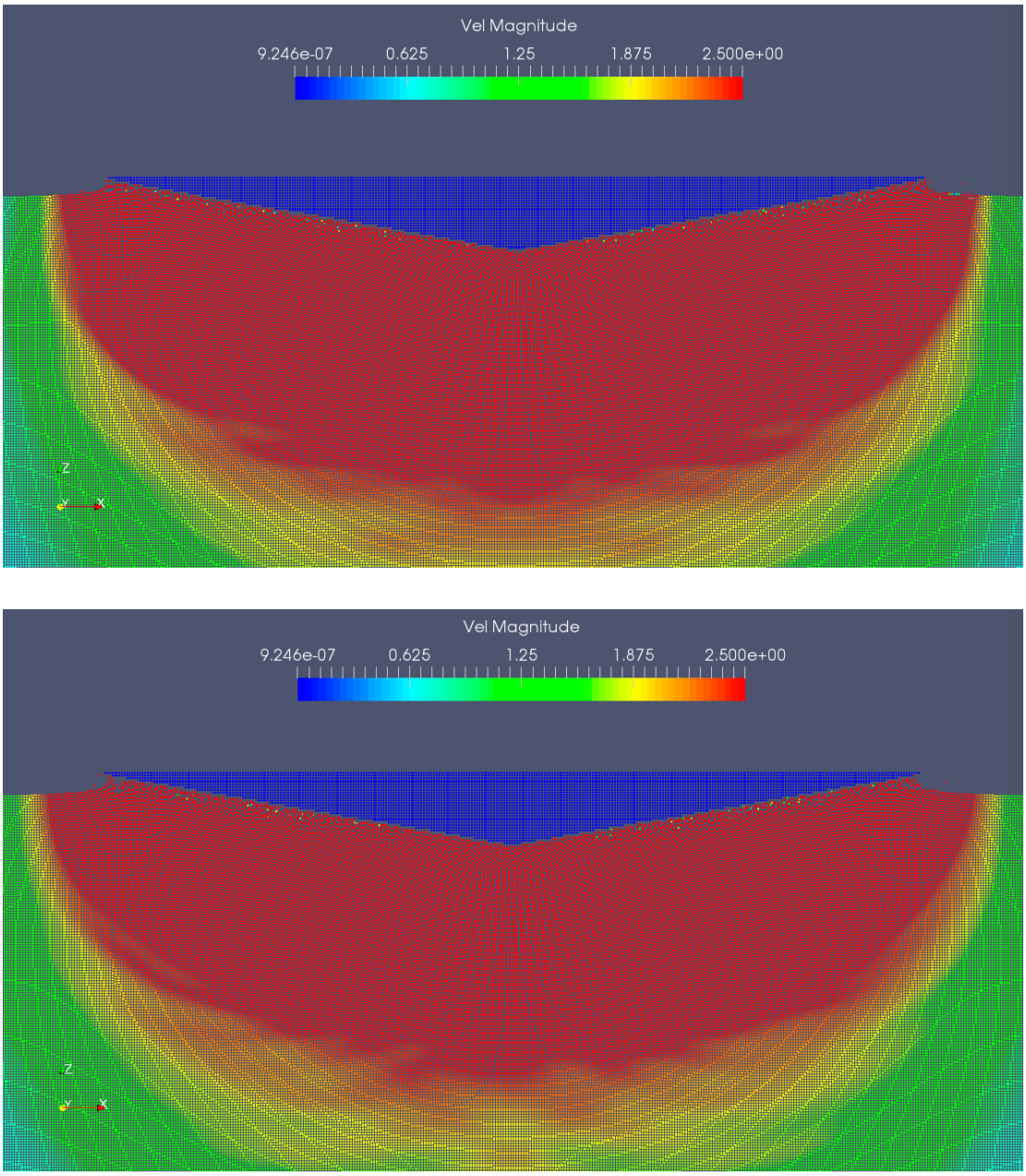

Figure 5-13 particles animation at the moments when the maximum force values appear

Figure 5-13 shows that the peak values for both the domains occur when the inclined edges are totally contained in the water pile-up region, instead of the fully submerged moment, which agrees with the theoretical model of Wagner (1932). The moments of figure 5-13 (a) for the NO. WD1 simulation and (b) for NO. WD2 are individually $t = 0.03424\ s$ and $t = 0.03264\ s$.

Another range of large vertical forces starts when the reflection waves reach the water surface. For instance shown in figure 5-14, while $t = 0.06712$ in NO. WD2 simulation, the force value rise to a high level under the effects of reflection waves.

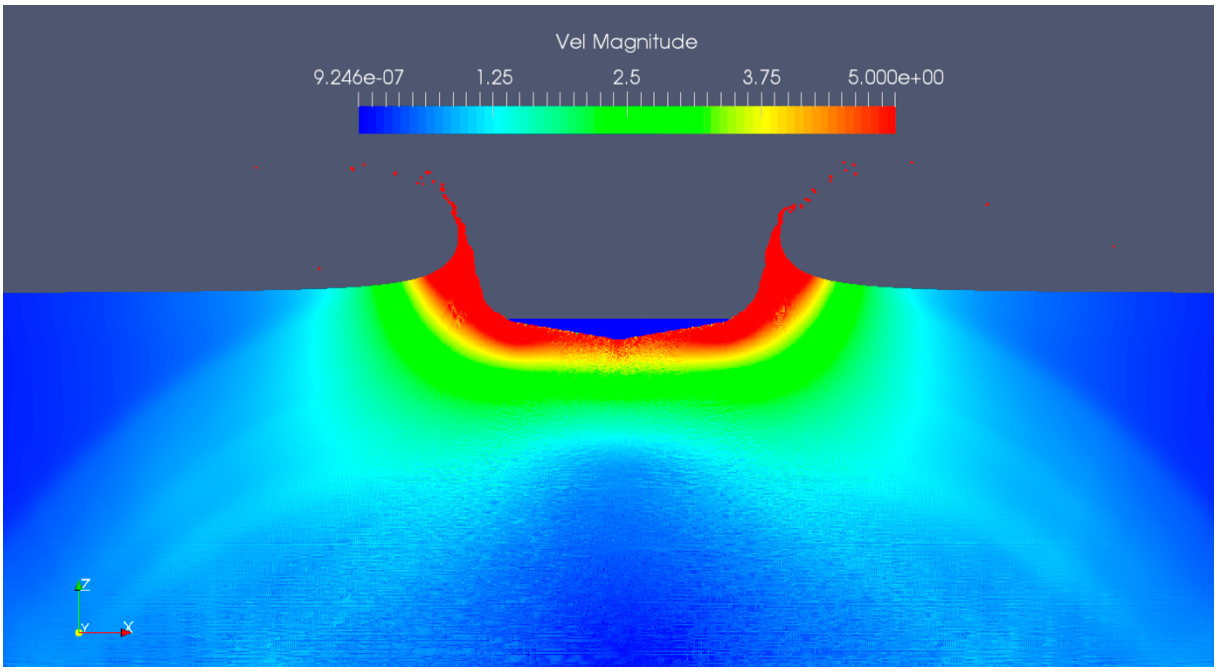

Figure 5-14 a series of reflection energy waves at t=0.06712

5.3.3 Results and discussion

In the water entry simulation, six wedges with different deadrise angles ranging from 10 to 60 degrees are modeled, the domain size in No. WD2 is selected, and the main parameters are shown in table 5-6. The resulting data are plotted in the form of slamming coefficient defined by equation (2.5), and then the comparison with results by previous works is made. Besides, the effects of reflection waves have been discussed in above section, hence in the simulating results the influence is omitted, meaning that the vertical force values after $t = 0.06\ s$ are not included in the analysis, and the main focus is on the slamming.

NO.	Deadrise angle (degrees)	Width (m)	Height (m)	Velocity (m/s)	Particle distance (m)
W1	60	0.1155	0.1	5.0	0.0035
W2	50	0.1678	0.1	5.0	0.0035
W3	40	0.2384	0.1	5.0	0.0035
W4	30	0.3464	0.1	5.0	0.0035
W5	20	0.5495	0.1	5.0	0.0035
W6	10	1.1343	0.1	5.0	0.0035

Table 5-6 parameters of wedges simulation

Due to the various deadrise angles, the width of the wedges changes in a large range, from 0.1155 m to 1.1343 m, meaning that the maximum value is ten times larger than the minimum. Therefore, the calculated vertical forces are also not in the same order of magnitude, the curves of vertical forces are shown in figure 5-15. For NO. W1, W2 and W3 simulations, severe fluctuations are found in the plots, which means that the behavior of wedges is easily influenced by the deadrise angles (or total width) under the condition of fixed height value. For the other three wedges, the vertical forces show similar changing tendencies, and for wedge with larger deadrise angle, the curve is more smooth.

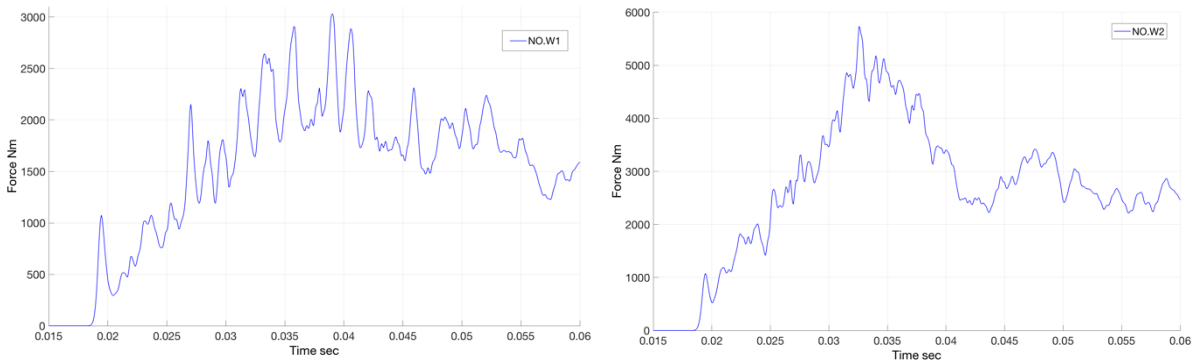

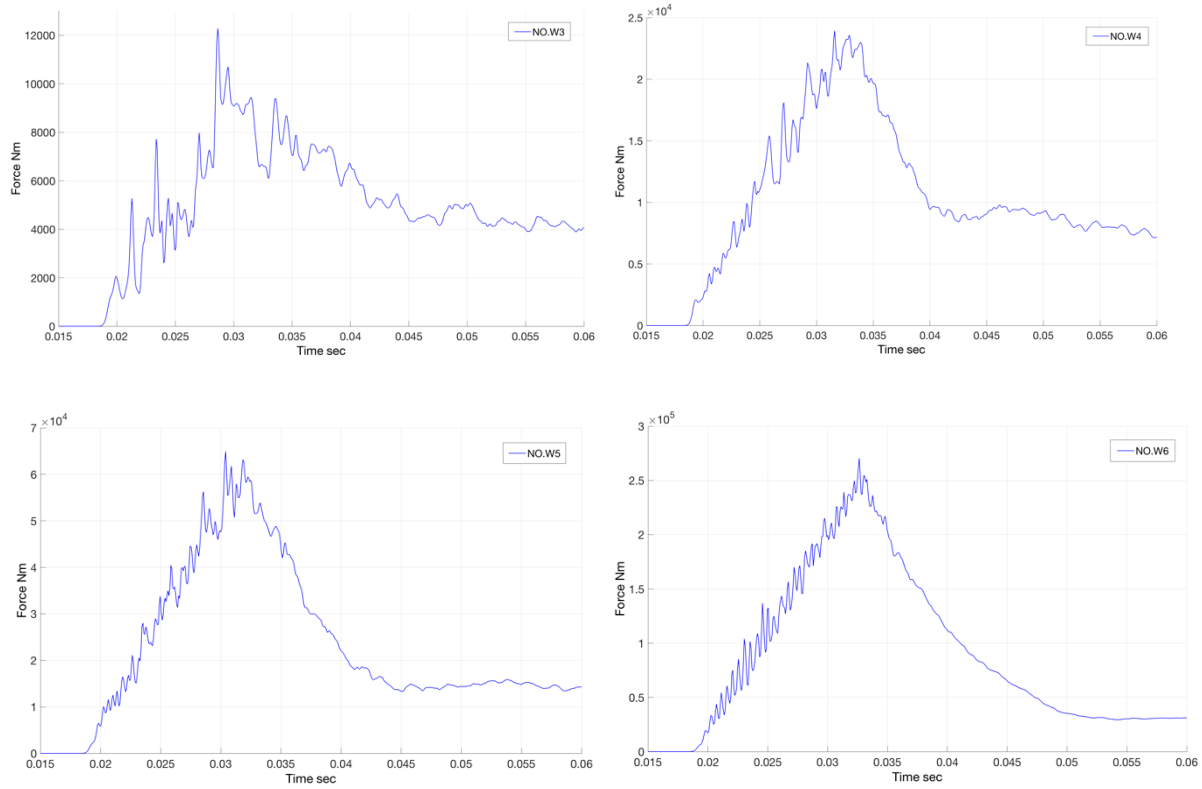

Figure 5-15 vertical force curves of simulations

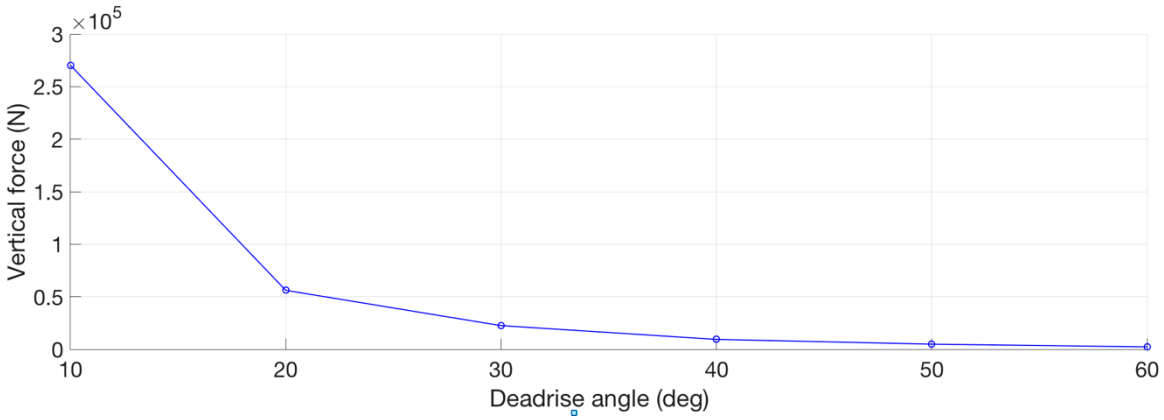

Figure 5-16 integrated curve of vertical forces

The peak vertical force values of all the six simulations is plotted in figure 5-16. For the original curves with high fluctuation level, the average peak values are utilized, so the extreme values are omitted. Based on the force curve, the slamming coefficient curve is plotted in figure 5-17 by the comparison with the previous curves in figure 2-6 by Faltinsen (2005).

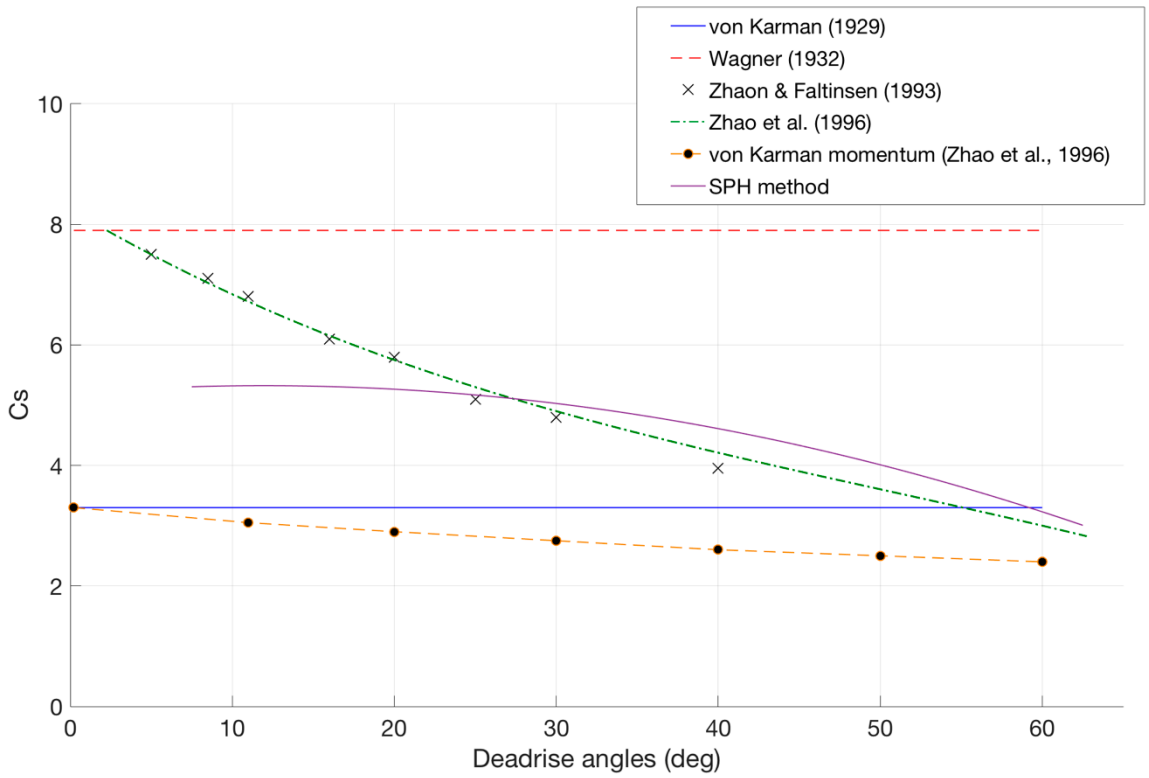

Figure 5-17 comparison of the slamming coefficients

The curve of the slamming coefficient computed with DualSPHysics is between the values of von Karman (1929) and Wagner (1932). Before 30 degrees, the smoothed curve keeps about 5.3 stably. After that, similar to the tendency of the data by Zhao and Faltinsen (1993) and Zhao et al. (1996), which decrease with the increasing of the deadrise angles. Generally speaking, the resulting curve agrees with the curve by Zhao et al. (1996), but for small deadrise angles, large gap could be obtained.

5.3.4 Summary

In this part, the water entry of varied wedges is simulated with a series of deadrise angles in DualSPHysics, and the main influence caused by the domain size is discussed. For small domain, the reflection energy waves make great effects on the computing results, and large domain is obviously preferred in this simulation. Due to the relatively high fluctuation level, the average values are applied in fitting the curves. In terms of the slamming coefficient, for large deadrise angles (larger than 30 degrees), the curve agrees with the previous result. On the other side, for small deadrise angles, the tendency is different but still in the range of theoretical analyses.

5.4 Water impact of 3D horizontal cylinder

In DualSPHysics, both two-dimensional (in X-Z axis system) and three-dimensional water entering models can be created and simulated. As the total amount of particles in three-dimensional simulation increases hugely, the applied particle distance and domain sizes are limited by the computation capability of the computer, especially the GPU power. In this part, the water impact of the horizontal cylinder is simulated in a three-dimensional environment, and the main parameters are as close as possible to the setting in two-dimensional simulation presented in section 5.1, in order to make comparison between the two results.

5.4.1 Parameters setting

To reduce the power consumption of the computer, a small-size domain is selected, and an appropriate length value of the cylinder is defined according to the domain size. In X-Z plane, all the dimensions of the cylinder and the domain are consistent with in simulation NO. D1. Along the Y axis, the length of the cylinder is 0.5 m, which is five times of the radius, and the length of the domain is 2.5 m. The initial position of the cylinder is shown in figure 5-18.

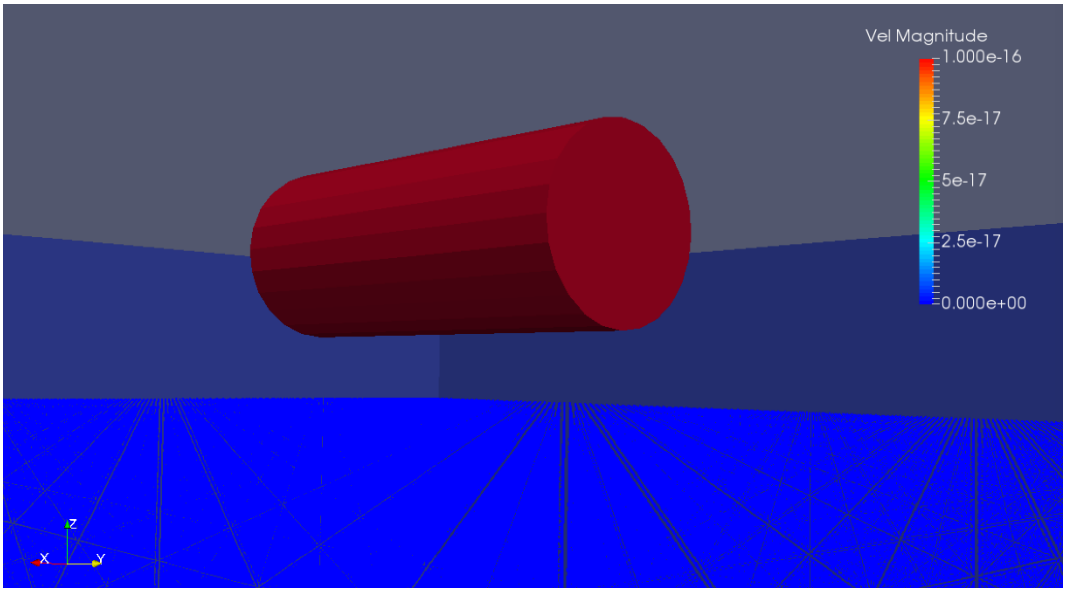

Figure 5-18 initial position of the 3D animation

5.4.2 Particle distance test

The particle numbers are greatly limited by the computation capability of the computer, so the particle distance applied in the three-dimensional simulation is relatively large. As discussed in chapter 4, the particle distance parameter has influences on the simulating results. In order to

test the influence level in three-dimensional environment, a comparing simulation is made with larger particle distance setting, the details are shown in table 5-7.

NO.	Particle distance (m)	Particle numbers	Domain size (XYZ) (m × m × m)
TPD1	0.015	783346	2.0 × 2.5 × 0.5
TPD2	0.020	337452	2.0 × 2.5 × 0.5

Table 5-7 parameters of 3D simulations

The particle distance of NO. TPD2 is only one third larger than NO. TPD2. However, the particle numbers become smaller than one half of the latter one, meaning that in three-dimensional environment, even small particle distance changes could cause great variation of the total amount of the particles.

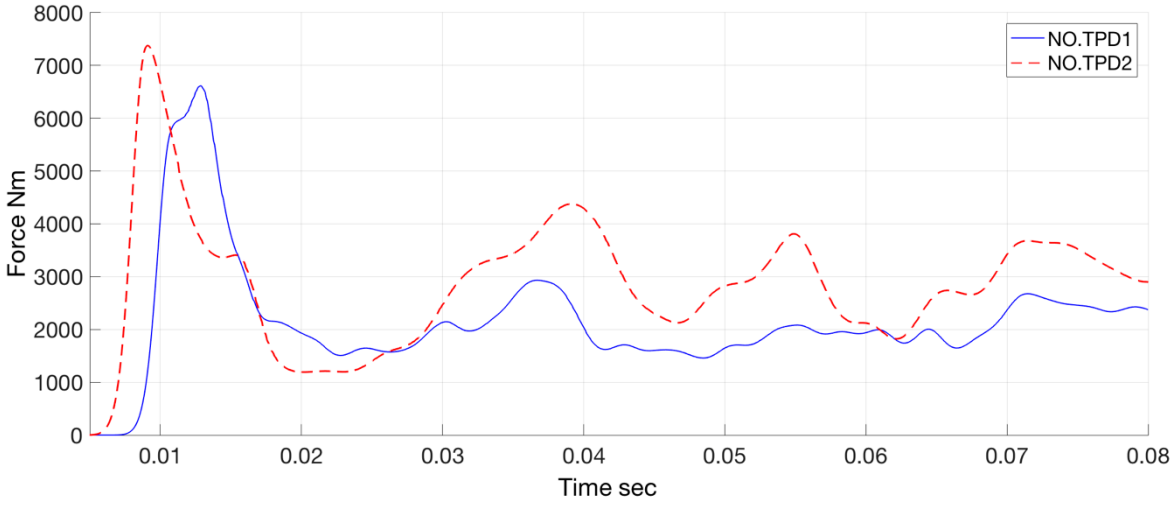

Figure 5-19 comparison of forces with different particle distances

Figure 5-19 presents the vertical force curves of the two simulating results. In general, the average value of NO. TPD2 is larger than the other one, because larger particle distance means greater smoothing length in calculation. Therefore, though the same amounts of particles are involved within the relevant ranges, greater smoothing length causes larger interaction radius and interaction forces. Besides, the peak values of the two curves obviously exist in different moments, and both of them are earlier than the theoretical slamming moment 0.02 s. This error is also caused by the particle interaction ranges, compared with the setting in two-dimensional

simulation, the three-dimensional particle distance is capable to affect the geometry of the cylinder in a large extent. Under this premise, smaller particle distance setting is preferred for higher accurate level.

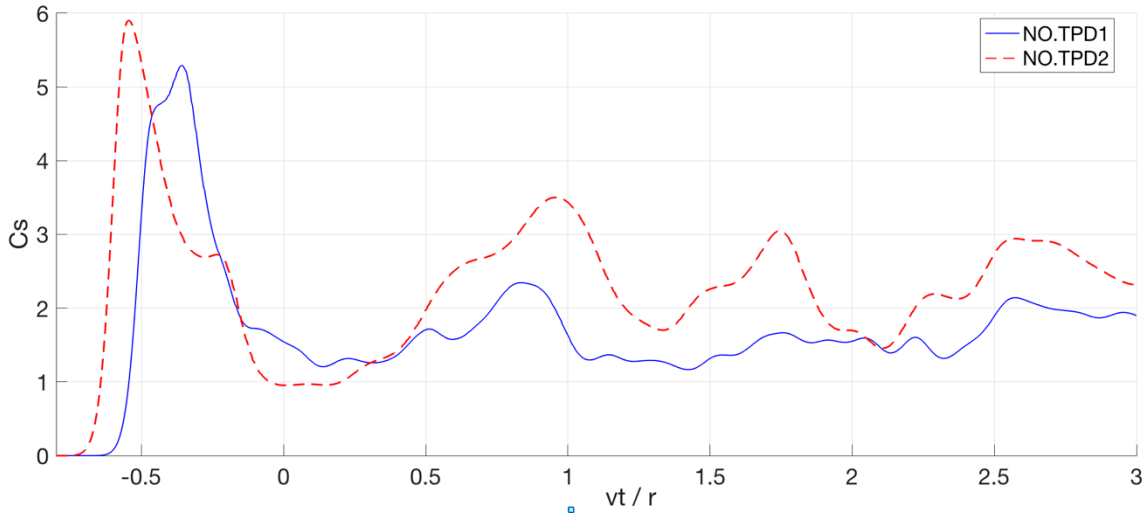

Figure 5-20 comparison of slamming coefficients with different particle distances

The same tendency can be obtained in slamming coefficient curves shown in figure 5-20, since the fluctuation of the curves is not as severe as in two-dimensional simulation, the peak values can be trusted. Here the formula of the slamming coefficient C_s is different from the definition in equation (2.2), so in three-dimensional environment,

$$C_S = \frac{F_3^{(3D)}}{\rho v^2 r \cdot L} \tag{5.4}$$

where L is the length of the cylinder along Y axis.

5.4.3 Comparison of 2D and 3D simulating results

The slamming coefficient curve of NO. TPD1 is compared with that of NO. D1, in X-Z plane, the parameters settings are the same except for the particle distances. Figure 5-21 shows the original curves of these two simulations. Compared with the curve of the two-dimensional simulation, three-dimensional curve is much more smooth, meaning that less noisy points exist in the results. For instance, in the peak value interval of NO. D1 simulation, there are only two points with extreme values higher than 5.0, which are omitted with applying the average value by fitting method. This situation cannot be found in the three-dimensional curve with a low fluctuation level, meaning that the results are not disturbed by the noisy points much.

Although the slamming moments of the two curves are quite different, as mentioned in above section, which is caused by the particle distance setting, the second humps occur almost in the same period, as marked by the dash rectangle in figure 5-21. As the the setting of sound speed coefficient, the reflection waves move with the same velocity in the water, which is not influenced by the particle distance. Besides, the hump caused by reflection waves is also smooth in three-dimensional environment, and this result is reasonable because the three-dimensional simulation is more similar to the real world where the energy waves propagate and decline continuously.

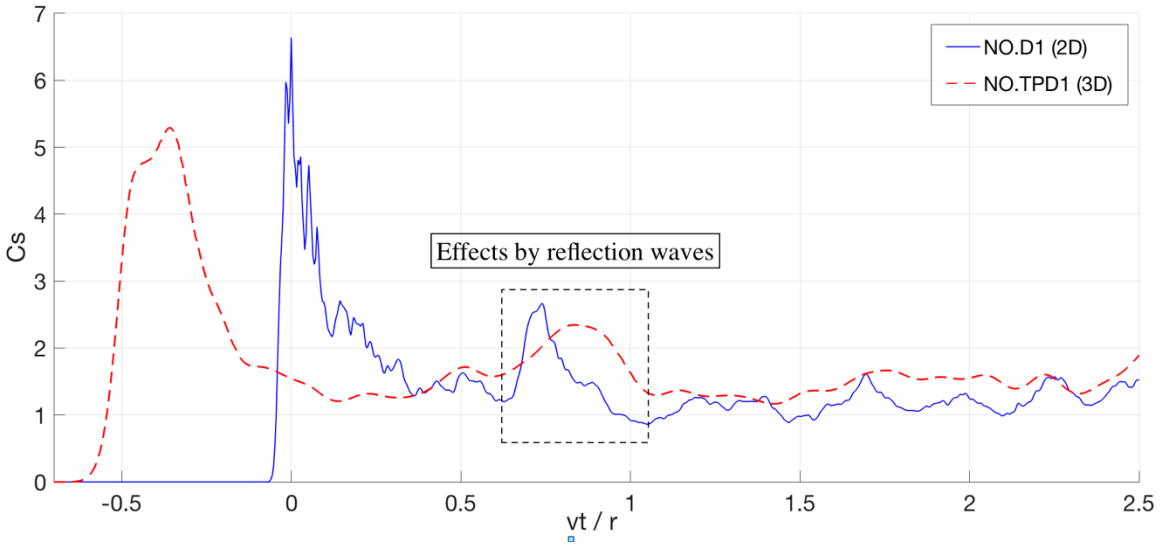

Figure 5-21 original curves of 2D and 3D simulations

Both the curves are smoothed with the fitting method according to equation (5.1). Besides, because the slamming moment of NO. TPD1 is much earlier than NO. D1, the non-dimensional time variable $\frac{vt}{r}$ is adjusted to keep in accordance with the theoretical moment, during the process, the C_S values will not change.

As shown in figure 5-22, the slamming coefficients at the slamming moment for both two-dimensional and three-dimensional simulations are very close, actually the two curves agree with each other well before about $\frac{vt}{r} = 0.15$, meaning that only limited effects on the slamming coefficient can be caused by different dimensions, i.e. no matter in two or three dimensions, the results are almost the same. However, after 0.15, the difference gradually becomes obvious, and when the tendency of the curves is in a stable period, the curve of NO. TPD1 stays above

the other one. Combined with the comparison in the previous section, it is caused by the particle distance setting, in other words, the accuracy level of NO. D1 is better than NO. TPD1.

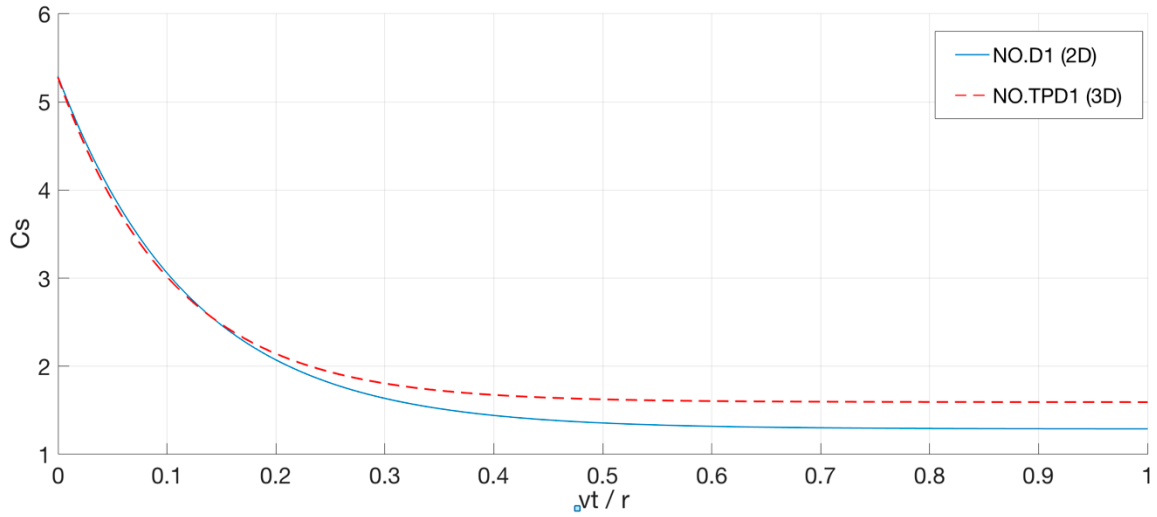

Figure 5-22 smoothed curves of 2D and 3D simulations

The animations of the two simulations at $t = 0.0363\ s$ are shown in figure 5-23, and it is obtained that in three-dimensional animation, the interaction range is larger than the actual volume of the cylinder, so the gap between the cylinder and the fluid is quite obvious. Besides, the particles that constitute the cylinder can be observed clearly, including the large particle distance between them.

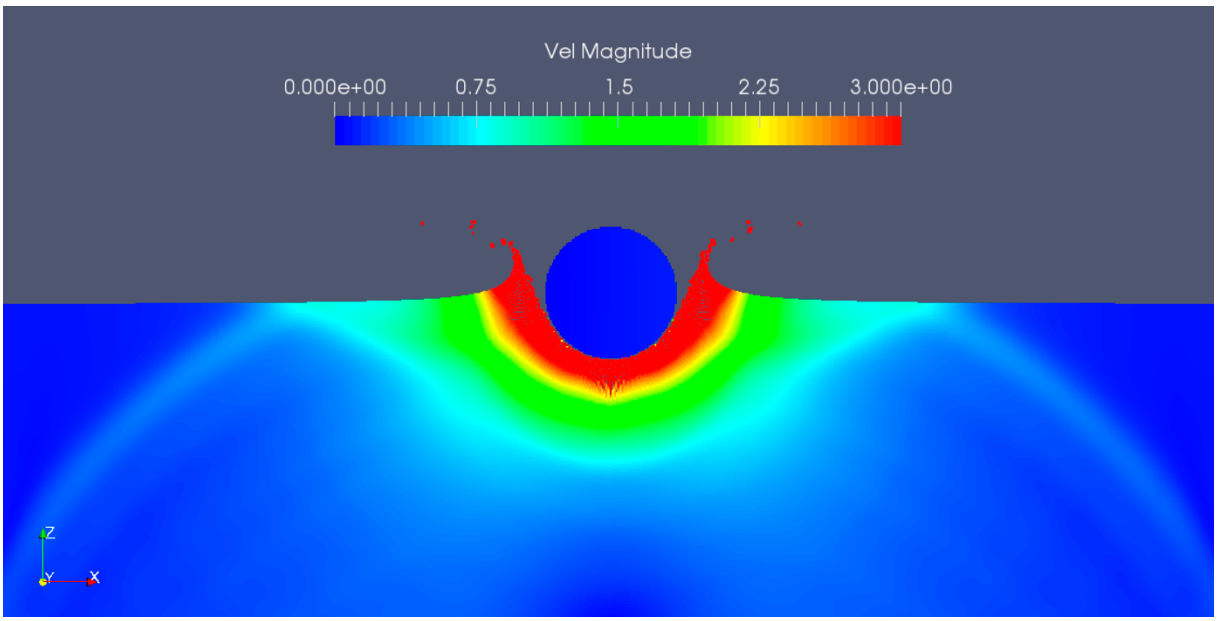

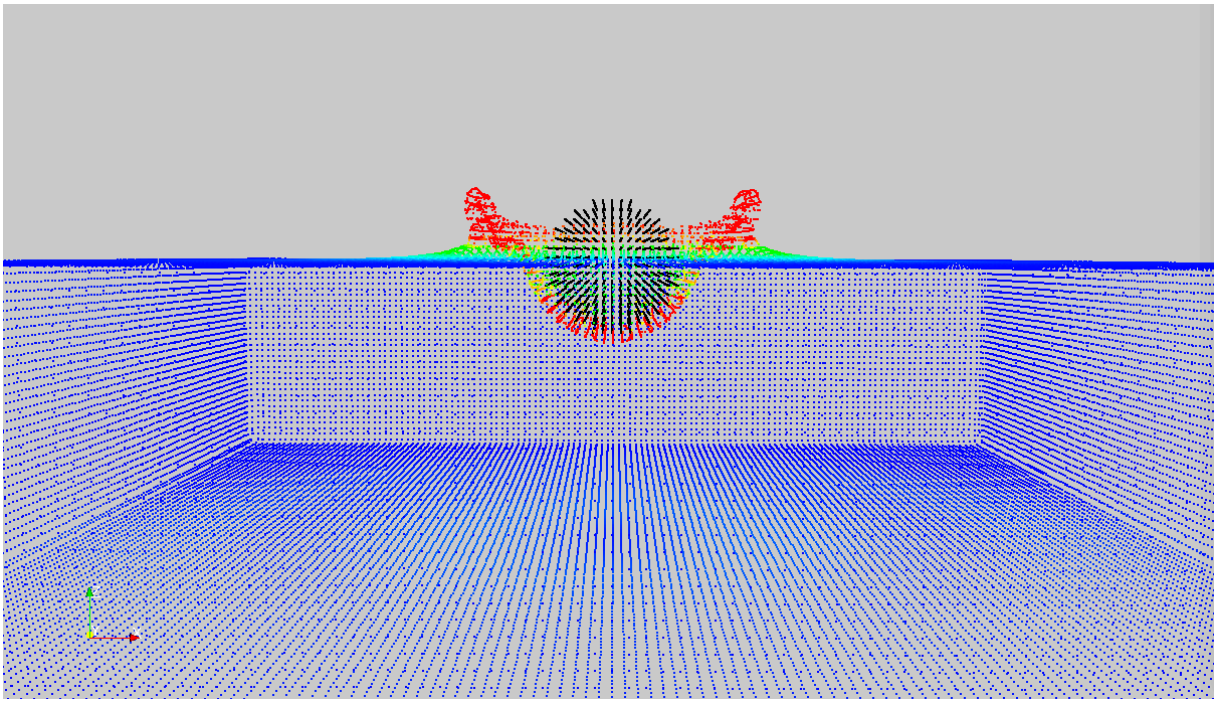

Figure 5-23 animations of 2D and 3D slamming moment

5.4.4 Summary

In this part, water impact of the three-dimensional cylinder is simulated with the same parameters setting with that in two-dimensional cylinder simulation in section 5.1, except for the particle distance, which is limited by the computing capability of the computer. In three-dimensional simulation, the particle distance parameter affects the results in a relatively large extent, and with smaller particle distance setting, larger vertical forces and slamming coefficients are obtained. The result of the three-dimensional simulation is close to the real world situation theoretically, with smooth curve and low fluctuation level. In the comparison of two- and three- dimensional smoothed curves, the difference is very small and satisfied.

6 Conclusion and future work

In the thesis, four different cases are simulated in DualSPHysics that is a numerical computing program applying SPH method. The cases include the water impact of both two-dimensional and three-dimensional horizontal cylinder, free falling of the HB and NB cylinders, water entry of wedges with various deadrise angles. For all the cases, the main analyzed results are vertical forces and slamming coefficients in slamming process.

The parameter settings are discussed in details for the simulations, which demonstrates that the computing results can be influenced by the parameters, e.g. domain size, particle distance, time steps, slamming velocities, and coefficient of sound speed. Although DualSPHysics is a powerful program that is capable to simulate various cases of fluid hydrodynamics study, the accuracy level is still limited by the parameters selection. As discussed in the thesis, noises and unstable results caused by the variation of parameter settings are obtained during the simulations. The possible method to improve the accuracy level is to increase the domain size and the quantity of the particles, which also leads to large power consumption of the computer. Therefore, the developing of computer technology could bring large benefits to the numerical computation with SPH method.

In terms of the computing results, most of them are acceptable, the numerical results with SPH method can agree with the previous theoretical analyses, experiments and numerical simulations in a satisfied extent. Due to the errors of numerical simulations, the appropriate fitting method is necessary, and during the fitting process, some extreme values and severe fluctuations are omitted. Under most of the situations, the average values are applied, which also seems to be a common method in previous studies.

In the water impact of two-dimensional horizontal cylinder simulation, the obtained results are different from the widely acceptable theory by Campbell and Weynberg (1980), i.e. the slamming coefficient could be affected by the variation of Froude numbers in a limited range. This could be caused by the errors of DualSPHysics, because the program is very sensitive to the parameter setting. To make further discussion on the conclusion, more accurate simulations are needed, meaning that more powerful computer with high CPU and GPU performance could be utilized. In the three-dimensional simulation, the requirement of computing power is much higher for the same parameter setting compared with in two-dimensional simulation.

As the CFD and SPH are two approaches with different methods, the simulating procedures and results can be compared in the same cases. Generally speaking, each method has its own

advantages and disadvantages, and there are also various commercial programs with varied particularities based on the two methods, more simulations could be made in these programs. In this thesis, most of the models are built in DualSPHysics 3.2 version, but the simulations finally run in DualSPHysics 4.0 version, new functions are added in the new version, including wave generation and force calculation, which offer great convenience to users. In future, more functions can be expected, as well as the improvement of the computing accuracy. Besides, the animation output is an important feature of numerical simulations, and the characteristics of SPH method provide powerful visualizing capability to simulate the fluid flow behavior. Compared with the traditional experiments, numerical simulation also possesses the advantages of high repeatability and reproducibility. It is believed that with the improvement of the computing accuracy, the SPH method can be much more widely applied in the fluid hydrodynamics studies.

Reference

Bašić, J., Degiuli, N. and Werner, A. (2014). Simulation of water entry and exit of a circular cylinder using the ISPH method. Transactions of FAMENA XXXVIII-1.

Campbell, I.M.C., Wellicome, J.F. and Weynberg, P.A. (1977). An investigation into wave slamming loads on cylinders. Wolfson Marine Craft Unit Report No. 317.

Campbell, I.M.C. and Weynberg, P.A. (1980). Measurement of Parameters Affecting Slamming. Wolfson Unit for Marine Technology Report No. 440. University of Southampton.

Cossins, P.J. (2010). Smoothed Particle Hydrodynamics, University of Leicester. PhD. Thesis.

DNV (2014). Modelling and Analysis of Marine Operations. DNV-RP-H103.

DualSPHysics (2013). User Guide for DualSPHysics code.

Fabula, A.G. and Ruggles, I.D. (1955). Vertical broadside water impact of circular cylinder: growing circular - arc approximation. NAVORD Report No.4947.

Faltinsen, O., Kjærland, O., Nøttveit, A. and Vinje, T. (1977). Water impact loads and dynamic response of horzontal circular cylinders in offshore structures. Houston, Offshore Technology Conference, No. 2741.

Faltinsen, O. (1990). Sea Loads on Ships and Offshore Structures. the Press Syndicate of the University of Cambridge.

Faltinsen, O. (2005). Hydrodynamics of High-Speed Marine Vehicles. New York, Cambridge University Press.

Ghadimi, P., Dashtimanesh, A. and Djeddi, S.R. (2012). Study of Water Entry of Circular Cylinder by Using Analytical and Numerical Solutions. Braz. Soc. of Mech. Sci. & Eng XXXIV(3): 225-232.

Greenhow, M. and Lin, W. (1983). Nonlinear - Free Surface Effects: Experiments and Theory. Report No. 83-19. Department of Ocean Engineering, MIT.

Gu, H.B., Qian, L., Causon, D.M., Mingham, C.G. and Lin, P. (2013). Numerical simulation of water impact of solid bodies with vertical and oblique entries. Ocean Engineering.

Larsen, E. (2013). Impact loads on circular cylinders, Norweigian University of Science and Technology. Master Thesis.

Liu, G.R. and Liu, M.B. (2003). Smoothed Particle Hydrodynamics - a meshfree particle methods. Singapore, World Scientific Publishing Co. pte. Ltd.

Miao, G. (1989). Hydrodynamic Forces and Dynamic Responses of Circular Cylinders in Wave Zones. Department of Marine Hydrodynamics, NTH, Trondheim, Norway. PhD. Thesis.

Miller, B.L. (1977). Wave slamming loads on horizontal circular elements of offshore structures. Journal of the Royal Institute of Naval Architects, RINA Paper No.5: 169–175.

Oger, G., Doring, M., Alessandrini B. and Ferrant, P. (2005). Two-dimensional SPH simulations of wedge water entries. Computational Physics, **213**(2006): 803–822.

Sollied, A. (1976). Student project, Division of ship hydrodynamics. NTH, Trondheim.

SPHysics (2010). User Guide for the SPHysics code.

Von Karman, T. (1929). The impact on seaplane floats during landing. N.A.C.A. Technical Note NO. 321.

Wagner, H. (1932). Über Stoß - und Gleitvorgänge an der Oberfläche von Flüssigkeiten. Zamm - zeitschrift Fur Angewandte Mathematik Und Mechanik **12**(4): 193-215.

Zhao, R., Faltinsen, O. and Aarsnes, J. (1996). Water entry of arbitrary two - dimensional sections with and without separation. In Proc. Twenty-first Symp. on Naval Hydrodynamics: 408-423.

Zhao, R. and Faltinsen, O. (1993). Water entry of two- dimensional bodies. Fluid Mech. **246**: 593–612.

Appendix (Draft)

SPH simulation of cylinder and wedge water entries

Abstract

Smoothed particle hydrodynamics (SPH) is a numerical approach applied meshless Lagrangian method in the fluid study. With the support of the fast developing computer technology, the numerical approaches are playing a more and more important role nowadays. In this paper, the water impact simulations are made in the DualSPHysics, which is a numerical program based on the SPH method. Four cases are simulated: water entries of both two- and three-dimensional horizontal cylinders with the constant velocities, free falling of two- dimensional cylinders, and water entries of two-dimensional wedges with various deadrise angles. The results of simulations in DualSPHysics are estimated through the comparison with previous works.

Key words: SPH, DualSPHysics, water impact, slamming coefficient, cylinder, wedge.

Introduction

The water impact problem has been paid great attentions on the field of fluid mechanics research. Various aspects have been studied in the water impact process, e.g. vertical hydrodynamic forces and slamming coefficients, and the deformation of the free surface. The paper by von Karman (1929) was considered as the beginning of the research of water impact problems. After that, theoretical analyses and experiments were made by various researchers. Among these researches, the impact on calm water of rigid cylinders and wedges was widely studied, since they were close to the practical situations. The results of researches contained the slamming coefficient in the function of non-dimensional time variables and vertical forces.

SPH method was utilized to deal with astrophysical problems in 1970s, and with the development of computer technology, it has been widely used in many fields. In spite of being questioned to be less accurate than CFD method on simulation of fluid flow, SPH approach is still an appropriate method for certain numerical simulation study, especially for calculation in large scale simulation.

Theory

Kernel function

In SPH method, particles are thought as basic elements which form the fluid, each single particle is influenced by its neighbor one, and the interaction between particles decreased with

the distance increasing, therefore, according to Cossins (2010), the kernel function W can be written as

$$\lim_{l\to 0} W(z,l) = \delta(z)$$

where z refers to the position of the particle in fluid, l is the smoothing length that describes the distance of interaction of the particles, hence it can be considered that no effect between particles can be found if their distance is beyond l, $\delta(z)$ here is called Dirac delta function (Cossins, 2010).

Fluid equations

The main fluid equations are transformed to the SPH form, in which the smoothing kernel function is applied as the basic expressions utilized in SPH calculation and simulation. There are three standard equations used to describe the fluid behavior as follows.

- Continuity equation:

$$\frac{d\rho_j}{dt} = \sum_i m_i(v_j - v_i)\nabla_j W(z_j - z_i, l)$$

- Momentum equation:

$$\frac{dv_j}{dt} = -\sum_i m_i(\frac{P_j}{\rho_j^2} + \frac{P_i}{\rho_i^2})\nabla_j W(z_j - z_i, l)$$

- Energy equation:

$$\frac{du_j}{dt} = \frac{P_j}{\rho_j^2}\sum_i m_i(v_j - v_i)\nabla_i W(z_j - z_i, l)$$

where ρ is the fluid density, v is the velocity and u is the specific internal energy, P represents the fluid pressure.

Sensitivity analysis

In this chapter, the initial simulating parameters are discussed separately, since in numerical simulation, the selection of parameters could have positive or negative impacts on the final results in various extents. The main parameters contain domain size, particle distance and time steps; and system parameters which are specialized variables in SPH method, including the coefficient of sound speed, smoothing length. During the analysis, the case of the water entry of a two-dimensional horizontal cylinder with a constant velocity (Case.1) is selected for testing.

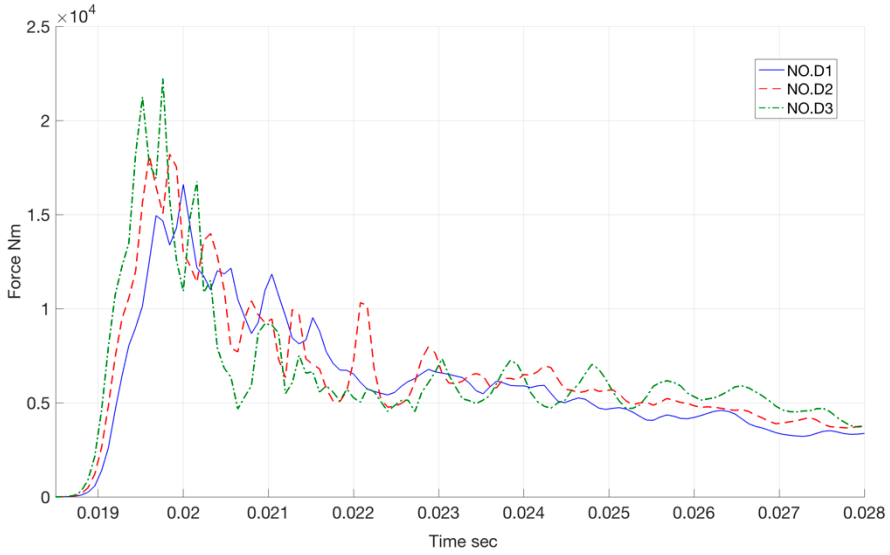

Figure-1 curves of various domain sizes test

Figure-1 shows the peak vertical forces calculated individually in these three domains. With the increase of the domain size, the slamming force rises substantially. It is difficult to explain why the slamming force that happens in a very short time is influenced by the domain size, i.e. higher slamming forces could be obtained in larger domain, this could be due to the error of numerical method in DualSPHysics. It is noted that larger force values do not equal better accuracy level, since more extreme values are also found in the curve of NO. D3, which is the largest domain. However, in smaller domain the results are easily influenced by the reflection energy waves, i.e. the fluctuation level of the resulting curve is higher.

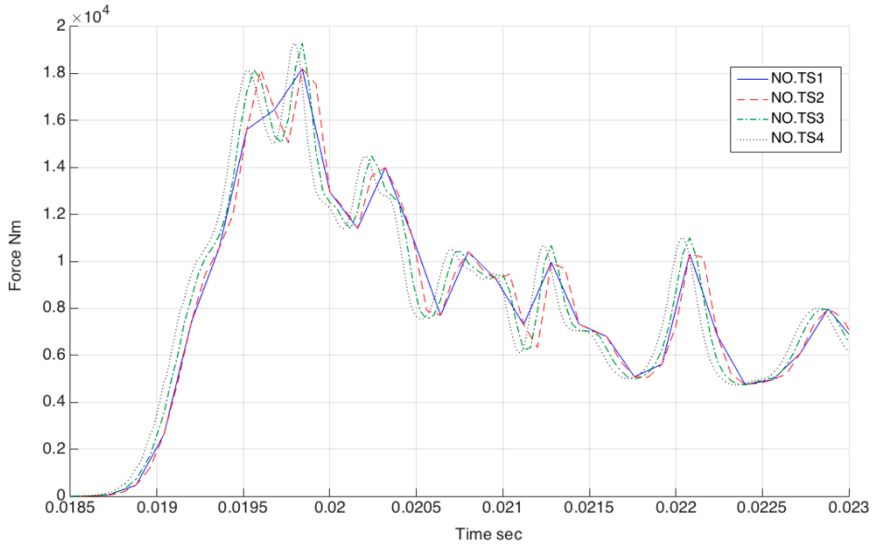

Figure-2 curves of various time steps test

The vertical force curves of various time steps are shown in figure-2, the NO. TS1 simulation with the smallest time step value 500 is not accurate enough for missing some peak values, and the other three have the same level of accuracy. Therefore, considering that larger time step setting could increase the computing time consumption, NO. TS2 simulation with 1000 time steps are considered to be a better optimized scenario for the simulations.

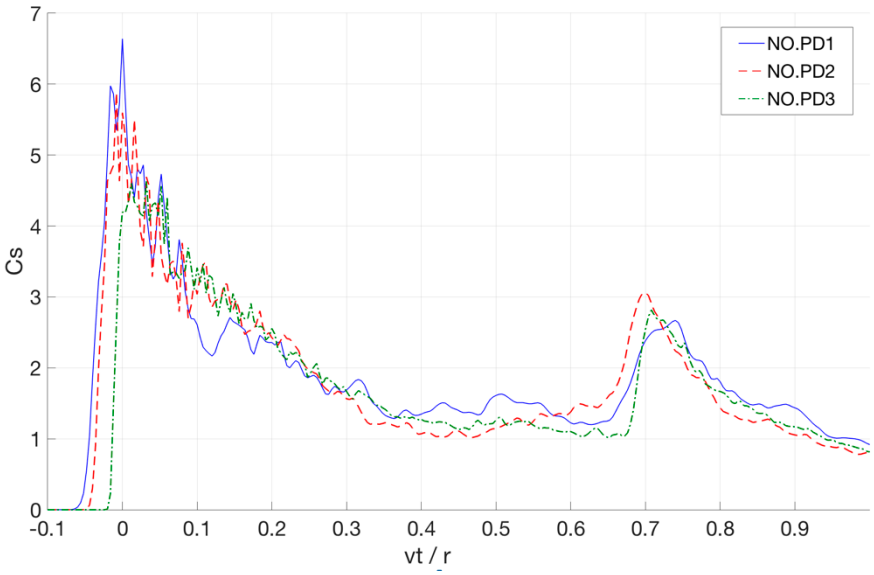

Figure-3 curves of various particle distances test

In figure-3, the difference of the peak values of the slamming coefficient can be obtained substantially, and it is noted that the slamming moments are related to the particle distances, i.e. larger particle distance makes the slamming occur much earlier than the theoretical value. For NO. PD1 simulation with the largest particle distance setting, the noises of the resulting values are more than the other two, which make the curve relatively unstable.

In figure-4, the fluctuation level of the dash curve with the smaller smoothing length setting is much higher than the solid curve, which proves that the relevant fluid is less viscous and easy to be influenced in the slamming process. Besides, more extreme values can be obtained in the dash curve, because the constrains of the particles become weak under the condition that less particles involved in the interaction. In this comparison plot, the result of dash curve is unacceptable due to the fluctuation level and extreme values, in contrary, the result of the default setting $coef$ = 1.2 is satisfied.

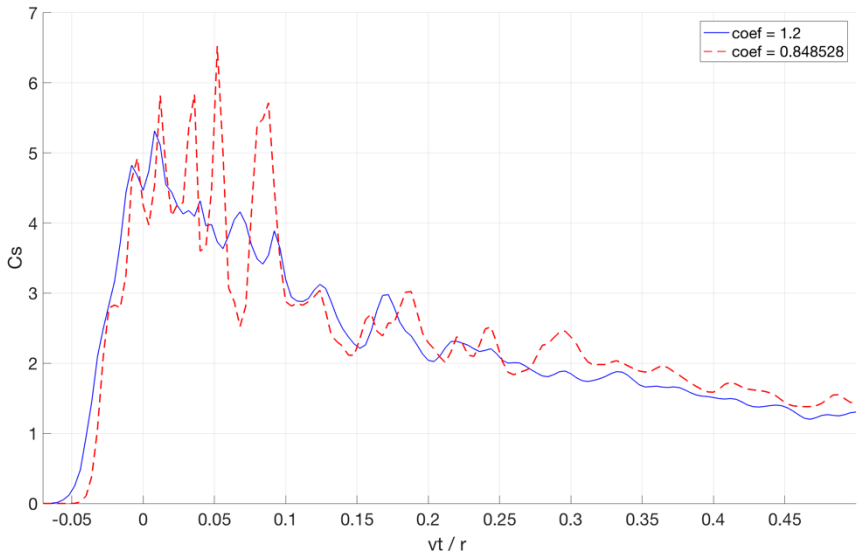

Figure-4 curves of two smoothing length coefficients

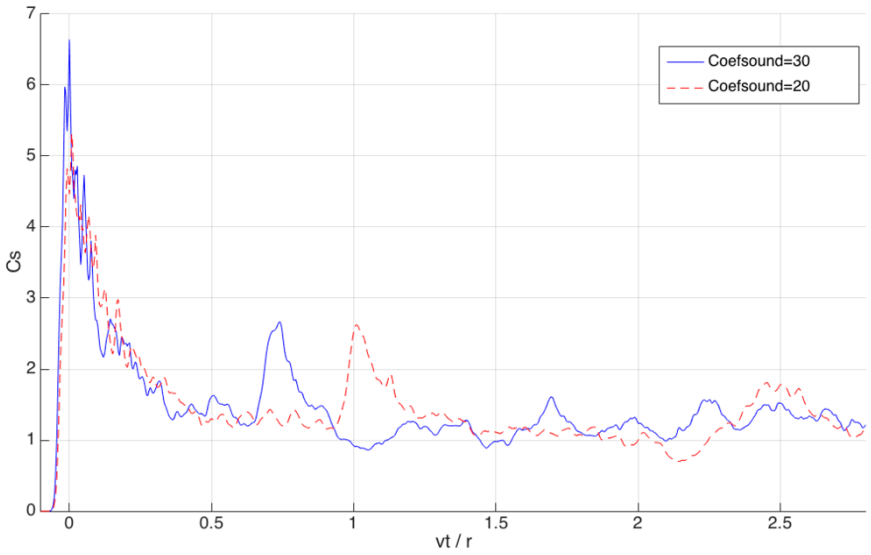

Figure-5 curves of two sound speed coefficients

The most obvious difference of the curves is the occurrence moment of the humps, because the reflection waves moves at the sound speed, meaning that higher Coefsound value could cause the humps to exist earlier and more frequently, which could be obtained in figure-5 that the fluctuation of the solid curve is much severer than the dash curve, and the first hump also occurs earlier due to larger sound speed. The comparison proves that Coefsound = 20 is more suitable for the water impact simulation.

Results

Case.1 Water impact of 2D horizontal cylinder

The initial position of the center of the cylinder is 0.2 m above the free surface, and the radius of the cylinder is 0.1 m as the default radius in the simulation. Therefore, the gap between the bottom of the cylinder and the free surface was 0.1 m according to the applied radius of the cylinder. Six different Froude numbers are applied in the range from 1.428 to 7.139. The parameters are shown in table-1.

NO.	1	2	3	4	5	6
Froude number	1.428	2.856	3.570	4.284	5.711	7.139

Table-1 Froude number parameters of Case.1

In figure-6, the resulting slamming coefficient at the beginning moment varies substantially. Most of the values are in an acceptable range, and the peak value drops down with the increase of Froude number. The conclusion is in contradiction with the Campbell and Weynberg's theory, which is that the slamming coefficient is independent of Froude numbers, the results of the simulations present changeable slamming coefficient according to various Froude numbers. Considering the empirical formula has been widely accepted and applied in practice, e.g. in DNV (2014), the possibility of errors in DualSPHysics cannot be excluded, as discussed in previous chapter, different parameters setting can make results fluctuate in some extent.

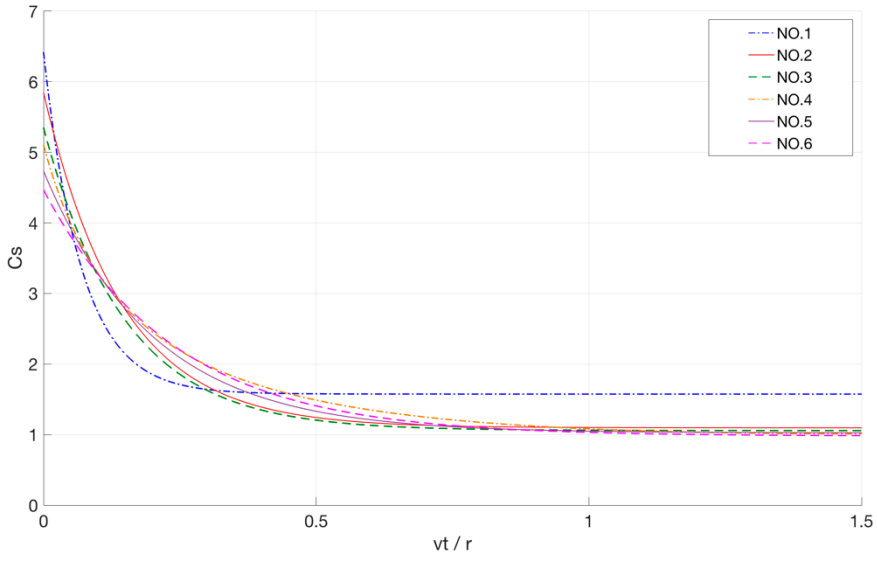

Figure-6 smoothed curves of slamming coefficient

The smoothed curve of the NO.3 simulations is compared with the results of previous works, see figure-7. As the calculation parameters are the same as Larsen (2013) with CFD method, the curves are also plotted based on the comparison figure of his thesis. The curve agrees with Larsen's curves best as shown in the figure, both of which are made by numerical simulations, SPH and CFD methods, and the tendency of the two curves are the same with the curve of Campbell and Weynberg (1980).

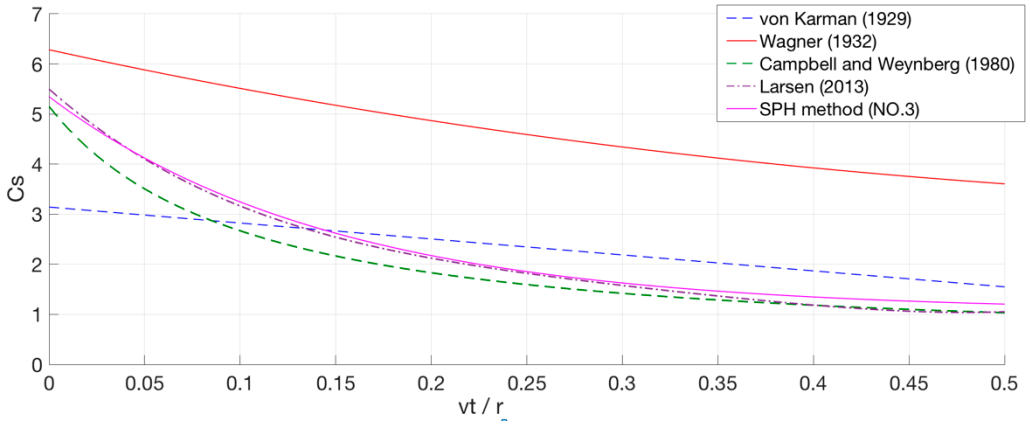

Figure-7 comparison of slamming coefficient with previous works

Case.2 Free falling of 2D cylinder into calm water

According to the parameters in Greenhow and Lin (1983), the initial position between the center of the cylinder and the free surface is 0.5 m, the radius of the cylinder is 0.055 m, and the initial velocity of the cylinder is zero, so the slamming velocity when the bottom touches the water surface is about 2.95 m/s, and the slamming moment is $t = 0.301\ s$. Both half buoyant (HB) and neutrally buoyant (NB) cylinders are simulated.

In DualSPHysics, the cylinders are also constituted by particles, which can be imaged as a large amount of small rectangular particles, as a result, the total mass of these particles are more or less different from the theoretical value. If the quantity of the particles is large enough, the mass can be close to the theoretical value. In this simulation, the applied mass of the HB and NB cylinders are separately 5.122 kg and 10.244 kg, larger than the theoretical numbers, this difference could have some effects on the results of simulation.

Figure-8 shows the comparison of penetration depth on time variable with the experiment results by Greenhow and Lin (1983) and CFD simulating results by Larsen (2013). It can be obtained that the HB cylinder curve calculated in DualSPHysics agrees with the experiment result well, and both of the two curves are under the result of CFD simulation. In terms of NB

cylinder curves, all the three are obviously different, according to Larsen (2013), this could be due to the inaccurate experiment data by Greenhow and Lin (1983). Anyway, as mentioned before, the accuracy level of the DualSPHysics results depends on the particle distance setting. Although in this simulation, on the basis of the applied particle distance, the amount of the particles reaches a million, which is a relatively large number, the accuracy level could be still not good enough.

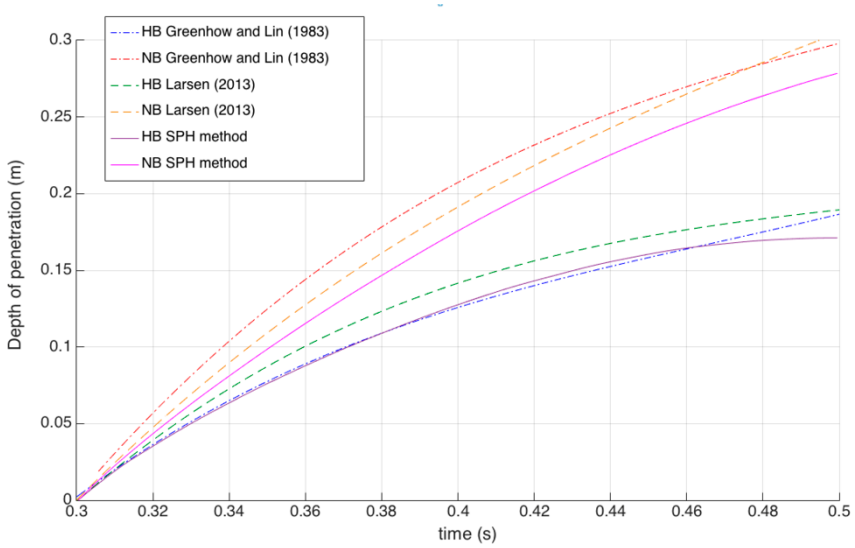

Figure-8 penetration depth curves compared with previous works

Case.3 Vertical water entry of 2D wedge

Six wedges with different deadrise angles ranging from 10 to 60 degrees are modeled. Most of the parameter settings are similar with that in Case.1. Here the height of the wedges is 0.1 m, and the slamming velocity is 5 m/s. The resulting data are plotted in the form of slamming coefficient, and then the comparison with results by previous works is made. The main parameters are shown in table-2.

NO.	W1	W2	W3	W4	W5	W6
Deadrise angle	60	50	40	30	20	10
Width	0.1155	0.1678	0.2384	0.3464	0.5495	1.1343

Table-2 parameters of wedges

As shown in figure-9, The curve of the slamming coefficient computed with DualSPHysics is between the values of von Karman (1929) and Wagner (1932). Before 30 degrees, the smoothed

curve keeps about 5.3 stably, after that, similar to the tendency of the data by Zhao and Faltinsen (1993) and Zhao et al. (1996), which decrease with the increasing of the deadrise angles. Generally speaking, the resulting curve agrees with the curve by Zhao et al. (1996), but for small deadrise angles, large gap could be obtained.

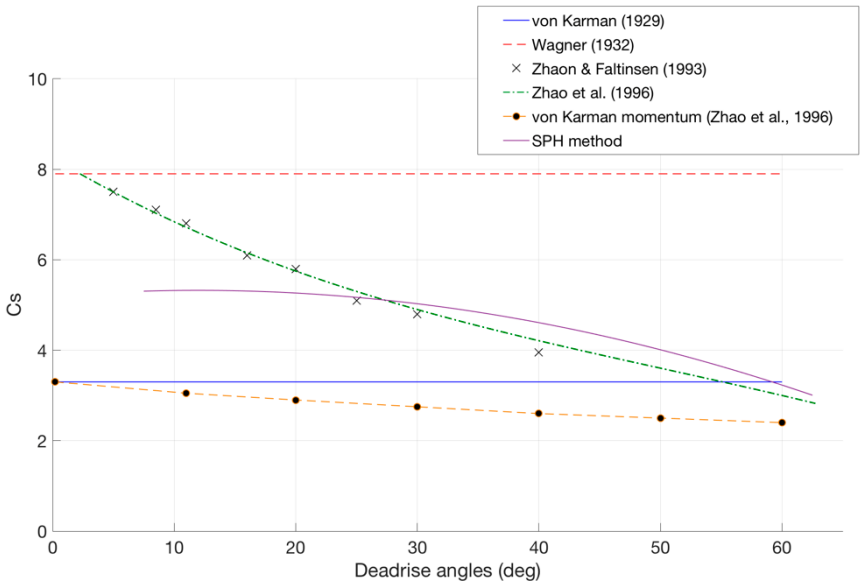

Figure-9 comparison of slamming coefficient

Case.4 Water impact of 3D horizontal cylinder

In DualSPHysics, both two-dimensional (in X-Z axis system) and three-dimensional models can be created. In this part, the water impact of the horizontal cylinder is simulated in a three-dimensional environment. In order to make comparison between the two- and three-dimensional simulations, all the dimensions of the cylinder and the domain are consistent with the settings in Case.1. Along the Y axis, the length of the cylinder is 0.5 m, which is five times of the radius, and the length of the domain is 2.5 m. As the total amount of particles in three-dimensional simulation increases hugely, the applied particle distance setting is limited by the computation capability of the computer, which is much larger than in Case.1.

As shown in figure-10, the slamming coefficients at the slamming moment for both two-dimensional and three-dimensional simulations are very close, actually the two curves agree with each other well before about $\frac{vt}{r} = 0.15$, meaning that only limited effects on the slamming coefficient can be caused by different dimensions, i.e. no matter in two or three dimensions, the results are almost the same. However, after 0.15, the difference gradually becomes obvious, and when the tendency of the curves is in a stable period, the curve of three-dimensional

simulation stays above the other one. This is caused by the particle distance setting, in other words, the accuracy level of two-dimensional simulation is better than the three-dimensional.

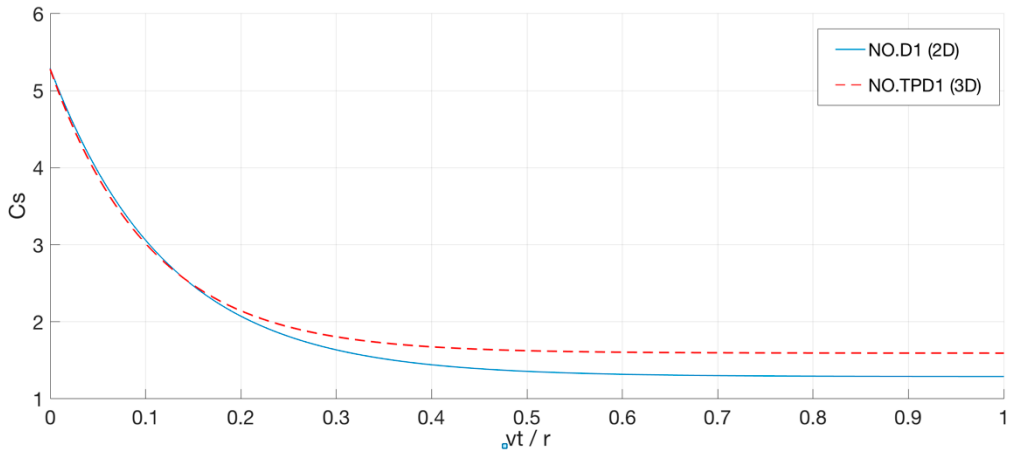

Figure-10 smoothed curves of 2D and 3D simulations

Conclusion

The parameter settings are discussed in details for the simulations, which demonstrates that the computing results can be influenced by the parameters. Although DualSPHysics is a powerful program that is capable to simulate various cases of fluid hydrodynamics study, the accuracy level is still limited by the parameters selection. As discussed in the paper, noises and unstable results caused by the variation of parameter settings are obtained during the simulations. The possible method to improve the accuracy level is to increase the domain size and the quantity of the particles, which also leads to large power consumption of the computer. Therefore, the developing of computer technology could bring large benefits to the numerical computation with SPH method.

In terms of the computing results, most of them are acceptable, the numerical results with SPH method can agree with the previous works in a satisfied extent. Due to the errors of numerical simulations, the appropriate fitting method is necessary. Under most of the situations, some extreme values and severe fluctuations are omitted, and the average values are applied, which also seems to be a common method in previous studies. In the water impact of two-dimensional horizontal cylinder simulation, the obtained results are different from the widely acceptable theory by Campbell and Weynberg (1980), i.e. the slamming coefficient could be affected by the variation of Froude numbers in a limited range. This could be caused by the errors of DualSPHysics, because the program is very sensitive to the parameter setting. To make further discussion on the conclusion, more accurate simulations are needed.